personal buildup for

Force Motors Ltd.

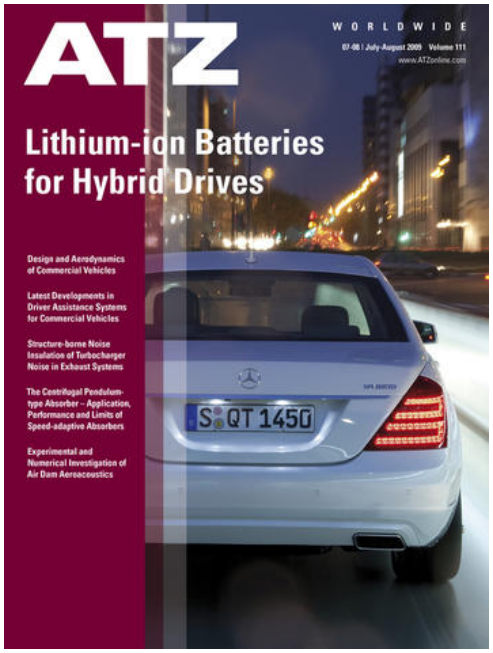

ATZ .worldwide 8/2009, as epaper released on 25.06.2009
http://www.atz-worldwide.com

content:

ATZ

WORLDWIDE

07-08 | July-August 2009 Volume 111

www.ATZonline.com

Lithium-ion Batteries for Hybrid Drives

personal buildup for Force Motors Ltd.

Design and Aerodynamics of Commercial Vehicles

Latest Developments in Driver Assistance Systems for Commercial Vehicles

Structure-borne Noise Insulation of Turbocharger Noise in Exhaust Systems

The Centrifugal Pendulum-type Absorber – Application, Performance and Limits of Speed-adaptive Absorbers

Experimental and Numerical Investigation of Air Dam Aeroacoustics

For more information visit:
www.ATZonline.com

COVER STORY

Lithium-ion Batteries for Hybrid Drives

4
ATZ shows how Daimler made it possible to develop to maturity the **Lithium-ion Technology** hitherto used in consumer products for the use in vehicle batteries in the Mercedes-Benz S 400 Hybrid. This is accompanied by an article from Behr to cool down these batteries optimally.

COVER STORY

DEVELOPMENT

RESEARCH

RUBRICS

Something to be Proud of

Dear Reader,

If you have children of your own, you will be familiar with that special kind of pride that you experience when your child scores the most goals in a football tournament or plays the main role in the school musical. The editorial team at ATZ felt the same pride recently for its new magazine "Automotive Agenda".

At the end of May, Automotive Agenda was awarded the accolade of "Business Medium of the Year 2009" by the Association of German Business Media — for us specialist journalists in Germany, that means as much as an Oscar for an American actor. When presenting the award, the jury justified its choice as follows: "This magazine extends far beyond the market that otherwise addresses car manufacturers, service providers and top decision-makers from the automotive industry. It avoids monotonous news reporting, focusing instead on monothematic differentiation and a refreshing change in the way issues are presented and in its journalistic text types. With clear reader guidance, skilful presentation, a high level of comprehensibility without simplification, an almost artistic layout and differentiated imagery."

Automotive Agenda has been published by our publishing house since the end of last year, and ATZ played a key role in bringing it to life. In contrast to the technical depth that is the responsibility of ATZ, every issue of Automotive Agenda examines the strategic aspects of a topical issue. For example, the next issue, which will be published on the occasion of the International Motor Show in Frankfurt, will discuss the question "Premium – quo vadis?"

If you would like to find out more about this new magazine, you can order a trial issue now at www.automotive-agenda.de.

Johannes Winterhagen
Wiesbaden, 8 June 2009

Johannes Winterhagen
Editor-in-Chief

personal buildup for Force Motors Ltd.

ATZ WORLDWIDE
07-08|2009

Organ of the VDI-Gesellschaft Fahrzeug- und Verkehrstechnik (FVT)

Organ of the Forschungsvereinigung Automobiltechnik e. V. (FAT) and of the Normenausschuss Kraftfahrzeuge (FAKRA) in the DIN Deutsches Institut für Normung e. V.

Organ of the Wissenschaftliche Gesellschaft für Kraftfahrzeug- und Motorentechnik e. V. (WKM)

Lithium-ion Battery
First Series Application in S 400 Hybrid

In the summer of 2009, Mercedes-Benz will launch the first production passenger car to be fitted with a lithium-ion battery. The aim of the development was to replace the lead battery in the engine compartment with an high-voltage battery generating an output of 25 kW, equivalent to a power density of 2000 W/l for the entire system. At present, only lithium-ion technology is capable of meeting this requirement. Within a period of three years, Daimler made it possible to develop to maturity the technology hitherto used in consumer products for use in vehicles. The focus of development was on safety technology, service life issues, material developments and the set-up of production facilities.

1 Introduction

The Mercedes-Benz S 400 Hybrid is the first hybrid series production vehicle by Mercedes-Benz, and the first series production passenger car to be equipped with lithium-ion (Li-ion) battery technology. The vehicle will be launched in the key markets for the S-Class starting in the summer of 2009.

The most important objective for the vehicle was to fulfill without restriction all of the expectations that customers have of an S-Class and furthermore to cut fuel consumption and CO_2 emissions to an all-time low in the premium class. In addition to retaining the agility and the familiar level of comfort, particular attention was devoted during the designing of the vehicle to ensure that there was no restriction of the effective load space and the load capacity available to the customer compared with the base vehicle. Since the high-voltage battery used in hybrid vehicles is the component that requires the most installation space, a solution had to be found to house the battery in an existing space, preferably that provided for the conventional starter battery.

2 The Lithium-ion Battery System in the S 400 Hybrid

The high-voltage battery technology currently used in series production in the automobile industry is based on nickel metal hydride (NiMH) cells [1]. The objective in developing the first Mercedes hybrid vehicle was to replace the NiMH technology with the superior lithium-ion technology that had previously only been used in the consumer electronics sector (laptops, cell phones, tools, etc.). Only in this way is it possible to install the high-voltage battery in place of the conventional starter battery, as the new technology is clearly superior to conventional nickel metal hydride technology in terms of energy content and power density.

2.1 Lithium-ion Technology

The electrodes of the round lithium-ion cells used are made of aluminum foils coated with graphite (anodes) and copper foils coated with lithium metal oxide (cathodes). The anodes and cathodes are separated by the plastic separator. The wound electrode is soaked with an organic electrolyte, which enables the transfer of lithium ions in the first place.

During the charging process, lithium ions are released from the metal oxide and move through the separator to the graphite electrode where lithium carbide forms, **Figure 1**. The energy stored in the process can be released again by the inverse chemical reaction that occurs during the discharge process. Metallic lithium is not present. Depending on the ma-

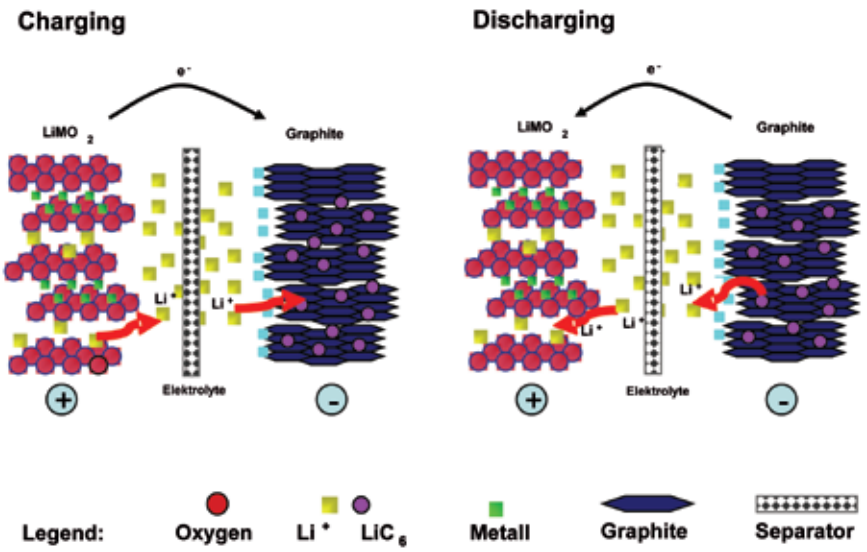

Figure 1: The reaction mechanism in a lithium-ion cell

The Authors

Dr.-Ing. Arnold Lamm is Senior Manager High Voltage Storage Development at Daimler AG in Kirchheim unter Teck (Germany).

Dr. rer. nat. Wolfgang Warthmann is Manager Electrochemical and Overall System at Daimler AG in Kirchheim unter Teck (Germany).

Dr. rer. nat. Thomas Soczka-Guth is Manager Electrochemistry at Daimler AG in Kirchheim unter Teck (Germany).

Dr. rer. nat. Rainer Kaufmann is Manager Mechanical Engineering and Cooling Design of High Voltage Storage Development at Daimler AG in Kirchheim unter Teck (Germany).

Dr. rer. nat. Bernd Spier is Manager Battery Management System Hardware/Software and High Voltage Electric/Electronic at Daimler AG in Kirchheim unter Teck (Germany).

Dr. rer. nat. Peter Friebe is Manager Battery Testing and Validation at Daimler AG in Kirchheim unter Teck (Germany).

Dipl.-Ing. (FH) Heiko Stuis is responsible for Test Data Analysis of High Voltage Storage Systems at Daimler AG in Kirchheim unter Teck (Germany).

Dr. rer. nat. Christian Mohrdieck is Senior Manager Fuel Cell and Battery Drive Development at Daimler AG in Kirchheim unter Teck (Germany).

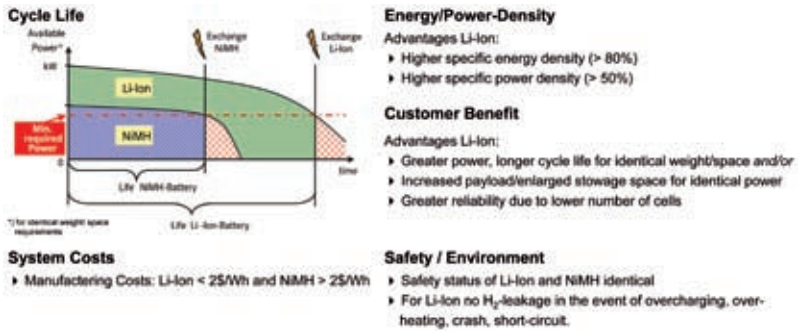

Figure 2: Comparison of Lithium-ion and nickel metal hydride technology

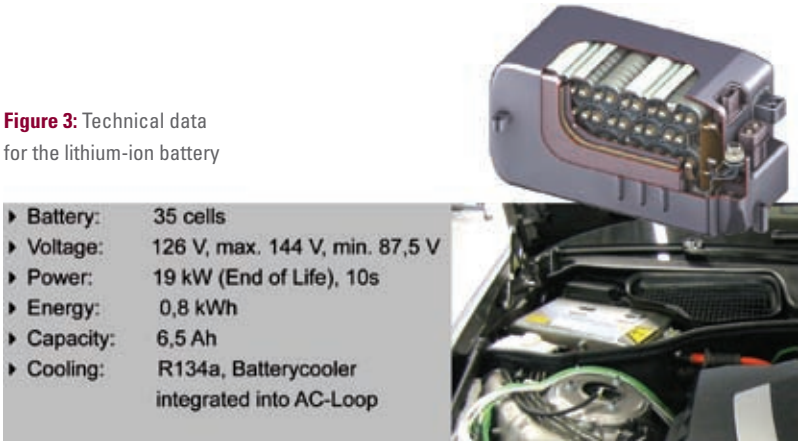

Figure 3: Technical data for the lithium-ion battery

terials used, these charging/discharging cycles can be repeated in a lithium-ion battery for several thousand cycles until the electrode is finally exhausted. In the cell used in the S 400 Hybrid, this is equivalent to more than 400,000 cycles (for a typical charge/discharge depth < 5 %).

The advantages of lithium-ion technology are shown in **Figure 2**. Without doubt worthy of particular mention are the high energy density and power density that are accompanied by the technology's exceptional safety standard and the high recharge efficiency and improved cold start performance, especially at temperatures below 10 °C. Naturally, long-term experience of using the technology under the harsh conditions in the vehicle over a period of more than ten years is not yet available. To ensure a long service life, it is therefore essential that the thermal balance of the battery be monitored.

2.2 Design of the Battery

The use of lithium-ion technology enables an energy content of 0.8 kWh and a minimum capacity of 6.5 Ah to be achieved in the space taken up by a 90 Ah starter battery. This allows the required electrical end of life system performance of 19 kW. **Figure 3** provides an overview of the battery's technical data.

The battery consists of a welded sheet metal housing containing a pack of cells comprising 35 round cells along with an integrated aluminum cooler that connects directly to the vehicle air conditioning system. In order to secure the cells mechanically in the pack while at the same time optimizing the cooling through thermal conduction, the entire block is fitted with a plastic lining. The electronic cell voltage monitoring system along with the battery management system and the two main contactors and fuse are still also accommodated in the battery housing. All connections such as the high-voltage plug, the connection to the DC/DC converter, the on-board power supply and the air conditioning system are arranged at the front end. The total weight of the battery is 24.5 kg. The mechanical strength and fatigue durability of the selected design were verified in complex FEM calculations. Likewise, the demonstration of crash safety that is standard in the automobile industry was conducted in real-life vehicle tests.

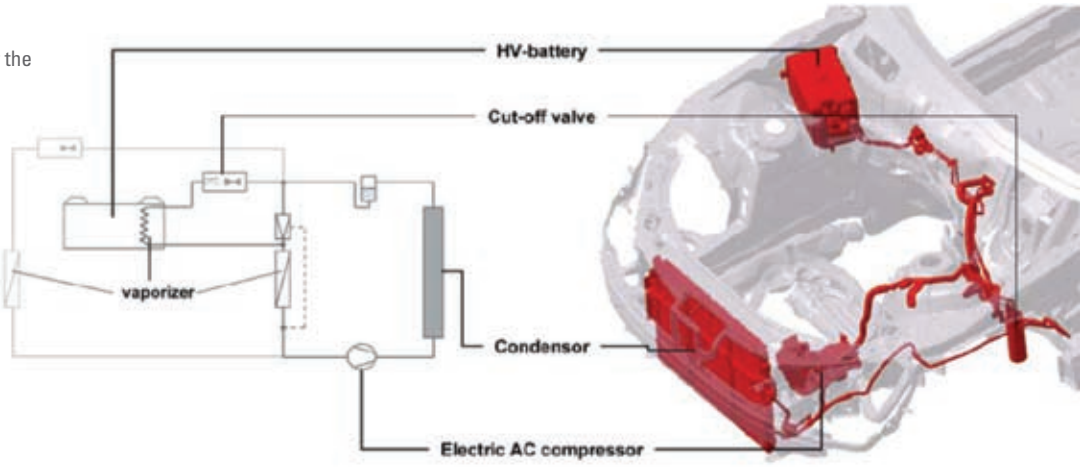

Figure 4: Radiator system for the S 400 Hybrid battery

2.3 Battery Cooling

As a result of its installation in the engine compartment, the battery is exposed to substantial ambient temperatures. Since its service life is essentially dictated by the temperature profile throughout its lifespan, it is imperative to provide a cooling system. To prevent the battery cooling from impairing the control of the air conditioning in the vehicle interior, cut-off valves are integrated into the system that allow the customer to switch off the air conditioning without interrupting the battery cooling, **Figure 4**. When the engine is not running, the electrical A/C compressor not only provides the air conditioning but also guarantees that the battery's operating temperature limit of 50 °C is not exceeded in this state either.

The design of the cooling system was based on the thermal description of the connection between the cells and the cooler supported by simulations. The calculations for typical driving cycles in reality show the efficiency of the chosen cooling design.

Measurements taken in the field indicate a thermal output of between 4 and 6 W per cell during real-life operation. Coolant inlet temperatures are generally between 10 and 15 °C. Accordingly, the maximum cell temperatures are around 30 °C, which corresponds with measurements taken in the vehicle (Chapter 5).

3 Material Development

As already described in Chapter 2.1, the lithium ions within the cells used provide the charge equalization and therefore the flow of current. In reality, however, it is the metal oxide and the carbon in the electrodes that are the active materials. For lithium-ion batteries, there is a variety of active materials that can be used to create electrodes in which lithium ions can be inserted or with which lithium reacts, **Figure 5**, [2].

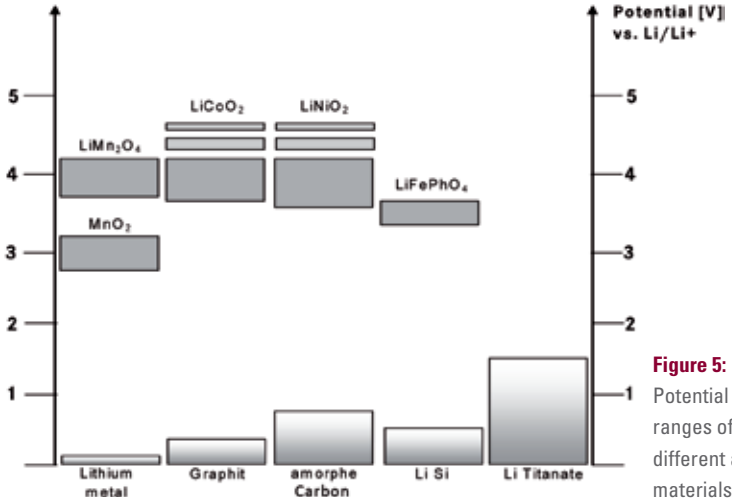

Figure 5: Potential ranges of different active materials [2]

Although a high energy content is not the primary design criterion for our application, sufficient cell capacity does nevertheless constitute an important reference point – given the direct link between the depth of the typical charge and discharge cycle (as a function of the cell's capacity) and the service life of the cell. In our case, this resulted in an optimum nominal capacity of between 6 and 7 Ah. Other design points are derived from the required battery output at the end of the minimum service life and the state of charge of the HV network.

Various materials (such as iron phosphate cathodes or lithium titanate anodes) were excluded due to the unfavorable potential layer, the resultant low cell voltage and the consequential need for a greater number of cells to achieve the desired system voltage in the available installation space. Due to the decomposition voltage for the electrolytes in common use today, voltages above 4.2 V cannot be achieved, Figure 5.

3.1 Characterization of Anode Materials

Table 1 provides a comparison of the different materials used for the anode. In addition to the potential range (with a target value approaching zero volts), the decisive factor in terms of evaluating the specific energy is the capacity for storing lithium ions expressed in mAh/g. This comparison currently indicates that the graphite anode is the optimum choice in terms of energy, safety, stability and cost. For this reason, graphite is the standard anode material in the latest cells. For safety reasons relating to the available cell and battery designs, the use of metallic lithium is not an option. Lithium titanate systems, which are being used to an increasing degree

Table 1: Characterization of anode materials

	Lithium metal	Armorph. carbon	Graphite	Lithium alloys	Lithium oxides	Lithium titanate
Potential range in mV vs. Li/Li+	0	100–700	50–300	50–600	50–600	1400–1600
Capacity in mAh/g	3860	approx. 200	372	3990 (Si), 1000 (Sn)	1500	150
Safety	–	+	+	o	+	++
Stability	–	+	+	–	–	++
Cost	+	o	+	++	–	–

Table 2: Characterization of cathode materials

	$LiCoO_2$	$LiNiCoAlO_2$	$LiMn_2O_4$	$Li[Ni_xCo_xMn_x]O_2$	$LiFePhO_4$
Mean voltage in mV vs. Li/Li+	3.80	3.9	4.0	3.8–4.0	3.3
Capacity in mAh/g	150	170	120	130–160	170
Safety	–	0	+	+	+
Cycle stability	+	+	0	+	++
Cold starting	+	++	0	+	–
Temperature stability	+	++	–	+	0
Price	– –	0	++	0	++

by cell manufacturers, do offer advantages in the areas of safety and stability, but the capacity is half that achievable using graphite. In addition, the total voltages in the cell as a result of the high potential range of 1400 to 1600 mV are too low to achieve attractive energy densities.

3.2 Characterization of Cathode Materials

Table 2 contains a list of the most common cathode materials along with their generic characteristic profile. The capacities for all materials are within a narrow window ranging from 150 to 170 mAh/g, and are thus significantly below the capacities of available anode materials.

The lithium iron phosphate cells available up to now offer significant development potential because of their high cycle strength, their relative safety and the fact that they do not need costly metals such as nickel or cobalt. However, the cold-start and high-temperature aging characteristics of iron phosphate cells have yet to reach the favorable levels that would justify their use in hybrid and electric vehicles.

Manganese spinel cathodes have failed to make significant inroads despite the cost advantage and the excellent safety offered by these systems. Ultimately, the thermal stability of the cathode material during all tests proved insufficient: small quantities of manganese released from the cathode corrode the anode, particularly at high temperatures, and lead to undesirable reactions there. Combinations with more resilient carbon materials also failed to offset these reactions sufficiently. The nickel cobalt manganese or NCM system with the molecular formula $Li[Ni_xCo_xMn_x]O_2$ represents an optimum solution with regard to energy, safety, cycle stability, cold starting, calendrical service life and price.

The NCA system, which consists of nickel, cobalt and aluminum, behaves similarly to the NCM material referred to above, and combines excellent cycle strength and cold-start characteristics with high cycle stability and high capacity.

3.3 Separators and Electrolytes

The separator is the electrically insulating, mechanically stable protective layer between the electrodes. Short-circuits must be prevented at all times. Separators are made of electrically insulating materials such as highly porous plastic films of polyethylene or polypropylene. High porosity and good wettability of the separator enables absorption of the electrolyte and ensures a high level of ionic conductivity between the electrodes. The thickness of the polymer film is approximately 20 µm in order to minimize the internal resistance. In future, we are likely to see more widespread use of ceramic separators aimed at improving safety standards. The electrolyte is composed of various components – the liquid component (mixture of solvents), the conducting salt that contains the lithium ions, and further liquid additives.

3.4 Material Selection for the Battery in the S 400 Hybrid

Due to outstanding cycle stability, cold-start characteristics and calendrical service lives, development of the battery was based on a nickel cobalt aluminum cathode (NiCoAl or NCA, see Table 2). The anode is based on a graphite material.

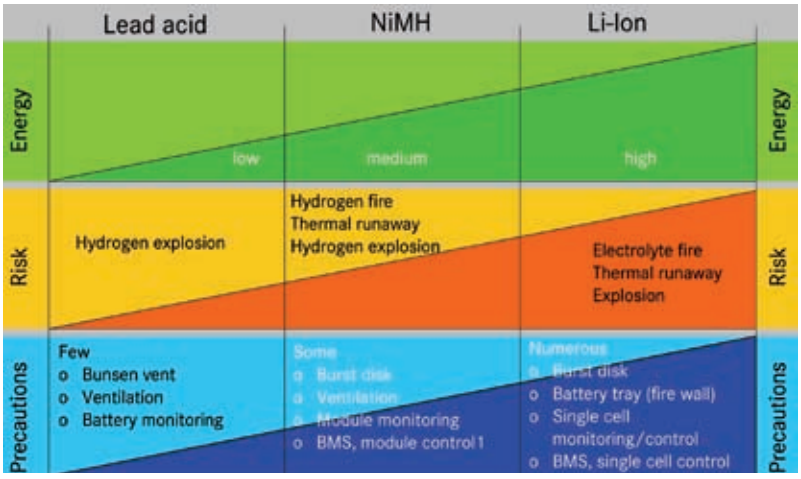

Figure 6: Different safety requirements pertaining to battery technologies

4 Safety Technology

The rising storage capacity and reactivity of the active materials are accompanied by increasing safety requirements pertaining to the cell and battery technology, **Figure 6**. For this reason, particular attention was devoted to the issue of safety. Among other things, the development process took into account the many years of experience accumulated by the Daimler research departments. The challenge in this case did not only lie in complying with all the worldwide statutory and in-house crash test requirements, but also in ensuring the greatest possible safety of the electrical components. This safety focus already applied in production, includes workshop personnel during servicing and maintenance, and also takes into account the emergency services recovering passengers following an accident.

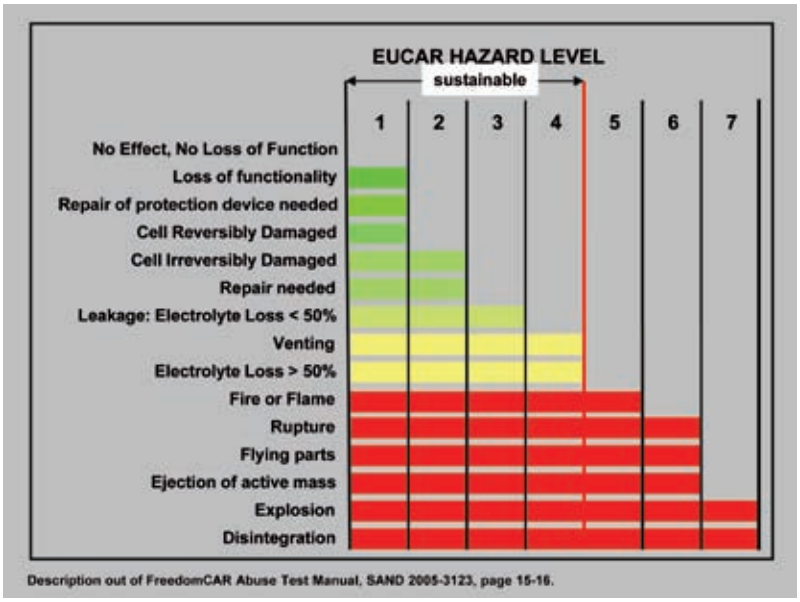

Figure 7: EUCAR test description

4.1 Elements of the Safety Concept

In addition to the Mercedes-Benz standard, the hybrid technology in the S 400 Hybrid is equipped with a comprehensive, seven-stage safety concept, with the battery as the central component. The safety concept comprises the following elements:

1. In the first stage, all cables are unambiguously color-coded and marked with the relevant safety instructions. This prevents accidental assembly errors on the production line and makes the regular service checks easier to carry out.
2. The second stage provides seamless contact protection for the entire system by means of generously sized insulation and newly developed special-purpose connectors.
3. As the third stage, the world's first lithium-ion battery to be used in a series-production model has been given a whole package of carefully coordinated safety measures. This innovative battery is accommodated in a high-strength steel housing, and additionally secured in place. Bedding the battery cells in a special gel dampens any jolts and knocks effectively. There is also a blow-off vent with a bursting disk and a separate cooling circuit. An internal electronic controller continuously monitors the safety requirements and immediately signals any malfunctions.
4. The fourth stage of the safety concept entails separation of the battery terminals, individual safety wiring for all high-voltage components and continuous monitoring by multiple interlock switches.
5. This means that all high-voltage components are connected by an electric loop. In the event of a malfunction, the battery management system automatically shuts down the high-voltage system.
6. Active discharging of the high-voltage system as soon as the ignition is switched to „Off", or in the event of a malfunction, is part of the fifth stage.
7. During an accident, the high-voltage system is completely switched off within fractions of a second (stage six).
8. As the seventh and last stage, the battery management system continuously monitors the system for short circuits.

4.2 Validation at Cell Level

As part of the US-american Freedom CAR and the European EUCAR support programs, proposals were developed for safety tests and for evaluation criteria at the cell and battery level, **Figure 7**. Overcharging, puncturing the cell with a nail, deep discharging, shock, external short circuit and deformation of a cell are designated as forms of abuse. In Europe, these results were transferred to safety levels by EUCAR (European Council for Automotive R&D). At the lowest safety level (EUCAR Hazard Level 7), the cells explode when subjected to the described abuse tests. At the highest safety level, these tests do not lead to any impairment of cell function.

In accordance with the voluntary commitment by the automotive manufacturers, only cells that fulfill level 4 are used, in order to ensure compliance with the high standards of safety insisted upon. Extensive test runs confirm the safety requirements of the cells used with positive results. These include, for example, a rigid design of the battery housing in stainless steel, and a sealed pack in the battery interior to inhibit the supply of oxygen in the event of the battery being damaged.

5 Validation at Vehicle Level

The process of securing the validation results at cell and battery level in the vehicle as well poses another challenge. Traditionally, summer and winter tests are conducted for validation purposes. During summer testing, the main focus is on ensuring the provision of adequate cooling and on testing the behavior of the battery temperatures should the vehicle's cooling system fail. During winter testing, attention focuses on the cold-

start characteristics of the battery and on its ability to level out at an operating temperature above freezing point via corresponding load cycles.

In addition to winter and summer testing, validation is also ensured by means of vehicle endurance tests using different driving profiles, such as urban endurance tests, motorway endurance tests or rough-road endurance tests. In these cases, the focus is primarily on safeguarding the correct functioning of the specified component service lives. The various endurance test profiles are designed to simulate a compressed service life that would apply during customer operation and therefore deliberately incorporate higher stress levels specific to each type of endurance test. However, the validation process for the high-voltage accumulator only involves a slightly higher load, since although all mechanical and electronic components are subjected to time-compression here, the extent to which a change in the cell chemistry can be represented or understood is currently limited.

In addition to validating the service life of the mechanical and electrical subcomponents of the battery, the objective of endurance testing is also to determine the various factors that influence cell aging. A service life model is used to validate the specified service life. This involves offsetting data (determined at the cell and battery level, such as cycle lives and calendrical service lives) against the recorded test data. The results of the model calculation are checked with regular inspections on the test stand, where the capacity and the internal resistance are determined in order to create a standardized comparable basis. The simulated calendar life is determined based on the battery's operating temperature profiles during the endurance test (averaging 30 °C, **Figure 8**, and the temperature profiles when the vehicle is stationary (for instance USABC hot profile). The state-of-charge (SOC) profiles during the test determine the influence on the cycle life. A combined total service life statement in the model is determined from the two service life statements. A comparison is then carried out between the modeled result and the inspection findings. After around 100,000 kilometers of testing have been conducted using a large number of endurance test vehicles, a validated model for predicting the service life is available.

6 Battery Management System

The battery management system (BMS) is a control unit whose role is to guarantee the battery's functional reliability at the maximum level of availability. It consists of the central control unit with the interface to the vehicle, the shunt for measuring the battery current, measurement equipment for the intermediate circuit voltage and cooling system temperatures, and the cell monitoring modules (CSC) for measuring the cell voltages, selected cell temperatures, and switches for passive charge equalization, **Figure 9**. In addition, the system includes insulation monitoring for the high-voltage circuits inside and outside the battery. The BMS checks the main contactors in the positive and negative branch of the battery and the precharge circuit for charging the intermediate circuit capacitor in the vehicle. The expansion valve is activated by the BMS to regulate the cooling capacity at the battery.

The interaction of energy management (EMM) in the components coordinator (AGK) and the BMS can be clearly tracked based on the operating states: start, driving, switching off and park mode.During the start-up procedure, the EMM sends a request to the BMS to close the contactors. When the BMS wakes up, the SOC counter is set to the current state of charge. The BMS then initiates charging of the intermediate circuit and permits the flow of energy by closing the

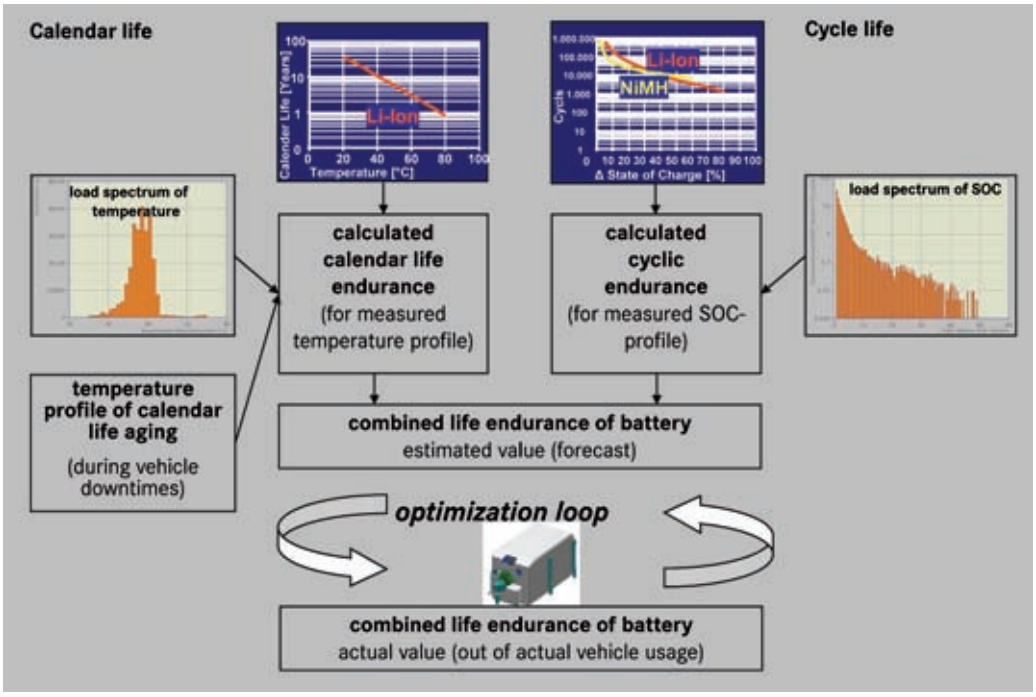

Figure 8: Determining the service life of a high-voltage battery

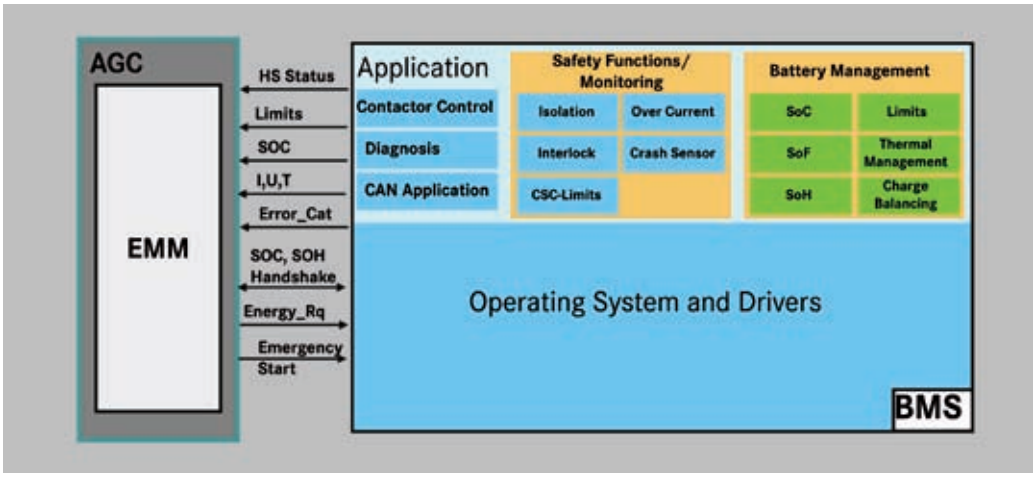

Figure 9: Battery management system and energy management interface

main contactors, provided that the SOC, battery temperature and cell voltages are within the operating range.

Once in operation, the BMS continually calculates the SOC and determines currents, battery temperatures and the voltages in the individual cells. The permissible current and voltage limits are also calculated. If the limits of the charging state, battery temperatures or cell voltages are approached, the system adjusts the current limits for charging and discharging in order to avoid critical battery states such as overheating, deep discharging or overloading. Battery cooling is regulated in accordance with the battery temperature through control of the expansion valve. The BMS uses the SOC to signal to the EMM whether the battery needs to be charged or whether additional scope for energy recovery (regeneration) should be created by discharging the battery to a greater extent. In addition to the SOC, the battery sends the EMM the prevailing battery current, the voltage and the battery temperature. Likewise, the current and voltage limits are transmitted via the CAN bus in order to calculate the battery's current possible output. SOC integration errors that occur in driving mode are reset by means of a hand shake between the EMM and the BMS. Following the occurrence of battery states that block continuous battery operation, the "emergency start signal" can be used to force a vehicle start. The battery is then not used until the states are normalized. The process of switching off the battery is also initiated by the EMM. The BMS now opens the main contactors, saves the current status data and enters sleep mode.

When the vehicle is in park mode, the BMS is regularly woken by a real-time clock in order to determine the states of charge in the individual cells as well as the charge state of the battery as a whole. Based on the results, charge equalization is now performed on the cells until the cell voltages are within the tolerance range. Cells whose charge state is too high are differentially discharged with the aid of connected resistors. In order to minimize the closed-circuit consumption, the CSCs operate without being monitored by the central control unit.

The use of high voltages in the vehicle calls for additional measures to comply with safety standards. When the vehicle is in operation, the insulation state of the high-voltage circuits in the battery and in the vehicle are continuously monitored; insulation malfunctions are signaled and the high-voltage system is shut down. Likewise, the interlock loop of the high-voltage system is operated and checked by the BMS. If the loop is opened, the high-voltage components are deactivated immediately for safety reasons. The current high-voltage safety and fault status is continuously sent to the EMM to ensure that the vehicle's energy management system is always informed of the battery state and is able to react.

An additional processor-independent path provides redundant possibilities for forcing the battery to switch off without BMS processor control in the event of excess current, excess temperature or overvoltage. However, these shut-down conditions are not reached during normal operation, as cut-off strategies for the current, voltage and temperature take effect beforehand. In accordance with the U. S. Federal Motor Vehicle Safety Standard FMVSS 305, the high-voltage battery is automatically switched off during a crash by the opening of the main contactors.

7 Summary

In introducing lithium-ion technology in the Mercedes-Benz S 400 Hybrid, the process of developing the battery revolved around the safety technology, material development, the design of the cooling system and service life testing. These results must now be applied to other applications such as electric vehicles. However, the cells used for these types of applications differ significantly from those of the power-driven hybrid application due to the substantially higher specific energy content.

References

[1] Konstantin Ledjeff: Energie für Elektroautos, (in German only) Verlag C.F. Müller Karlsruhe, 1993
[2] Andreas Jossen, Wolfgang Weydanz: Moderne Akkumulatoren richtig einsetzen, (in German only) U Books on demand, January 2006

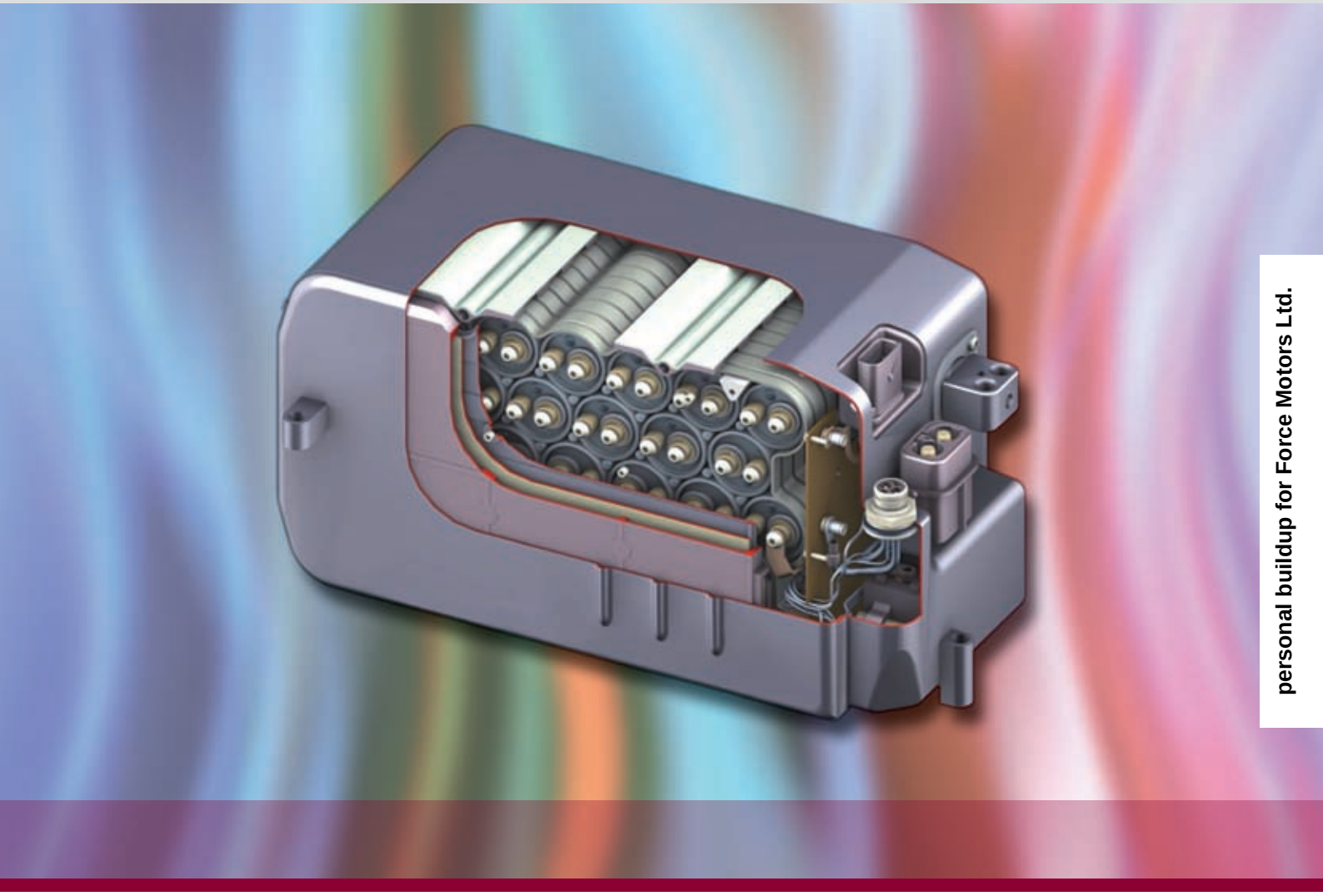

Thermomanagement of Li-ion Batteries

With the increasing electrification of vehicle power trains, the electrical energy storage unit is assuming an ever stronger role as a key technology in the drive concept. While today's series-produced hybrid vehicles still use nickel metal-hydrid batteries, ever-greater demands are necessitating a change in technology to the lithium-ion battery. The first series-produced hybrid passenger car in Europe with the newest energy storage system is the Mercedes-Benz S 400 Hybrid. Behr describes the cooling of the battery. The supplier also presents the nature of the thermal management of battery cells in general terms to ensure full efficiency and the lifetime required.

1 Introduction

Compared to the nickel metalhydrid (NiMH) battery used today, the lithium-ion (Li-ion) battery is characterized by a significantly higher volumetric and gravimetric energy density and also permits a greater number of charging and discharging cycles. However, the electrochemistry of the Li-ion battery is much more sensitive to higher temperatures. Cell temperatures even above 45 °C accelerate the aging processes to such an extent that the required lifetime of more than ten years is difficult to achieve.

The Li-ion electrochemistry tolerance of temperature gradients within the cell, and differences in temperature between the different cells in the battery module, is likewise only a few Kelvin. Accordingly, for its own protection, the battery must be switched off every time it reaches a critical thermal state. For a hybrid vehicle, this would mean that the hybrid operating mode, that means in particular the electric boost on start-up and the fuel-saving recuperation of braking energy, would not be available.

In a fully electric vehicle, the situation would be even worse; in this case, it would not be possible to switch off the batteries temporarily, since this would cause the vehicle to come to a standstill. This demonstrates how fundamentally important it is to keep the Li-ion battery in a non-critical thermal state under all operating conditions, and this requires efficient thermal management.

2 Cell Cooling Concept

The essential requirement is an effective cooling concept at the level of the cell. How this is designed depends on the type of cell, its external dimensions, its internal structure, and the level of the heat flow to be dissipated, **Figure 1** shows the cell types that are currently to be found on the market. In the case of the round cell and prismatic cell, the active material, consisting of electrodes and separators, is generally rolled up into a coil and placed in a robust aluminum housing. In the case of the pouch cell, the individual layers of the active material are stacked or folded, and packaged in a flexible aluminum composite film. From a cooling perspective, the round cell has geometric drawbacks compared with the prismatic and pouch cells. The relatively low surface-to-volume ratio compromises the transfer of heat away from the cell interior to the surface, so that considerable radial temperature gradients develop inside the cell. In addition, the curved outer surface makes it difficult to achieve optimal thermal contact of heat conducting elements, by means of which the cell's waste heat can be dissipated to a heat sink. Since, however, the choice of a suitable cell type is influenced not just by cooling factors, but also by criteria such as availability, production maturity, safety, service life, and, not least, cost, the round cell is now used relatively frequently.

All three cell types have in common a very good heat conduction along the electrodes (20 W/m/K < $\lambda_{\parallel}$ < 50 W/m/K), **Figure 2** (a). This is a result of the physical phenomenon whereby good electrical conduction also results in good heat conduction. In contrast, perpendicular to the layers, the heat conduction is reduced by one to two orders of magnitude (0.5 W/m/K < $\lambda_{\perp}$ < 2 W/m/K). The spectrum of the specified heat conduction is, on the one hand, the result of the different active materials that different cell manufacturers use. On the other hand, the cell's electrical power requirement plays a role. Cells for electric vehicles therefore have a somewhat different internal structure, and, accordingly, they also have different thermal properties than do cells for hybrid applications.

The principal cell cooling concepts are shown schematically in Figure 2b to 2e [1]. In air cooling, Figure 2b, cooling air flows around the cell, cooling the freely accessible surfaces. Since this cooling type does not require any direct thermal contact with the cell, the interface to the cooling system takes a relatively simple form, and for practical reasons it is therefore often

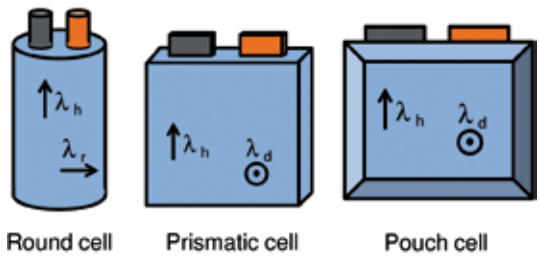

Figure 1: Currently used cell types of Li-ion batteries

The Authors

Dr. Achim Wiebelt is Head Heat Transfer, Technology and Methods Center, at Behr GmbH & Co KG in Stuttgart (Germany).

Tobias Isermeyer is Team Leader Pre-Development at Behr GmbH & Co KG in Stuttgart (Germany).

Thomas Siebrecht is Team Leader Serial Development at Behr Industry in Stuttgart (Germany).

Dr. Thomas Heckenberger is Head of the Technology and Methods Center at Behr GmbH & Co KG in Stuttgart (Germany).

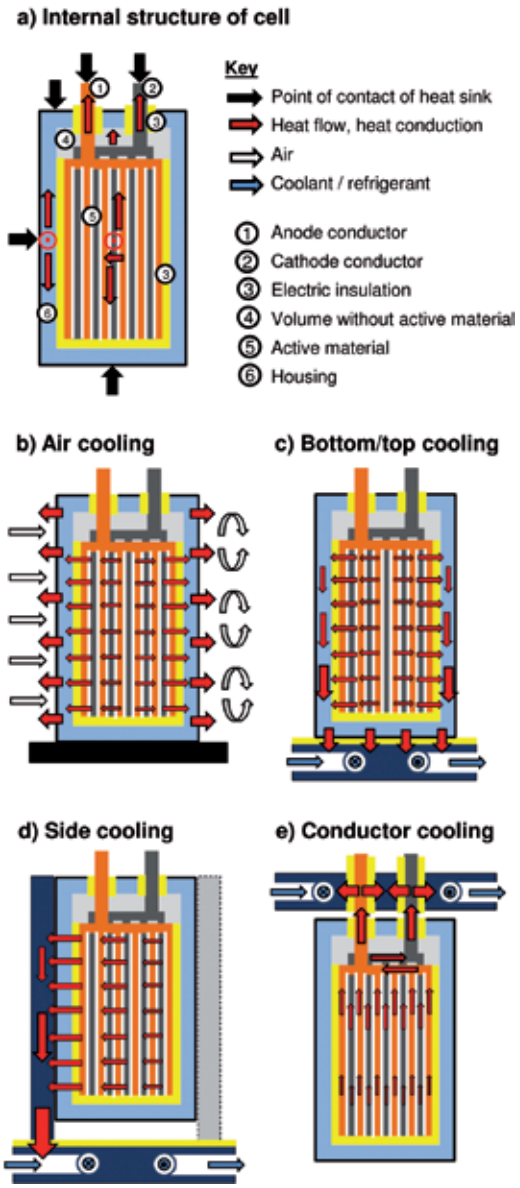

Figure 2: Structure of the cell and cell cooling methods a) to e)

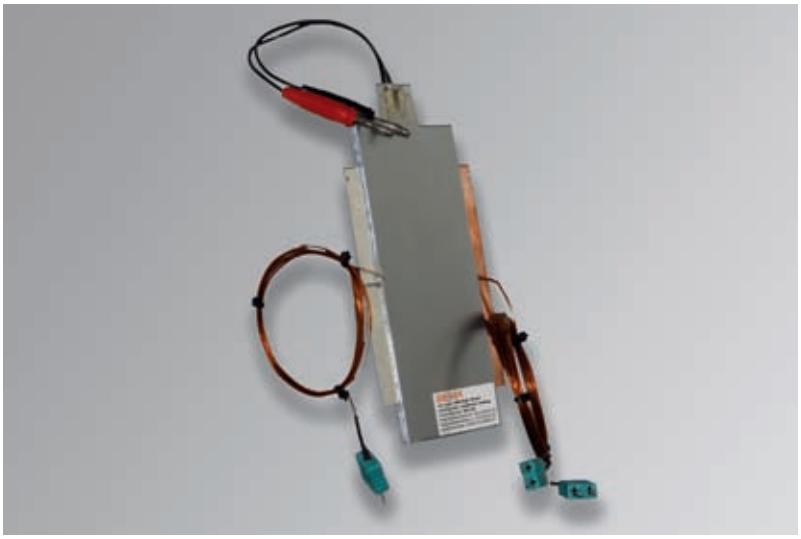

Figure 3: Cell dummy for a pouch cell

the first choice. However, the package space for the cooling air channels between the cells, the feed and outlet channels for the battery module, and the small HVAC unit for air conditioning is considerable. The cooling efficiency, too, in particular the homogeneity of the cell cooling, is often unsatisfactory.

In contrast, the cooling types that involve thermal contact with the cell and that dissipate the heat through heat conduction are clearly superior in terms of package space and cooling efficiency. However, the thermal contacting poses new challenges, and the interface with the cooling system is more complex, because the cooling device is in direct contact with the electrical components of the battery. In the case of cells of lesser height and with sufficiently thick cell walls, it is sufficient to simply contact the bottom or top of the cell, Figure 2c. If this is not sufficient, heat conducting elements must be provided between the cells, Figure 2d.

Conductor cooling represents a particularly efficient type of cooling, Figure 2e. This involves cooling the inside of the cell directly via the electrodes. Pouch cells in particular are suited to this type of cooling. In all cases, the heat lost from the cells is transported to a cooling plate. There, either cooling water or an evaporating refrigerant absorbs the heat and discharges it into the atmosphere via the vehicle's cooling or air conditioning system.

3 Thermal Validation

In the battery, at the interface between electrochemistry and cooling, the battery's own significant thermal requirements clash with the requirements of the power train and the performance capabilities of the cooling or refrigerant circuit system [2]. This interface is correspondingly complex. Conventional numerical design tools are therefore not sufficient for the thermal design of the battery cooling system. At both component and system level, experimental tests are essential.

At the component level, Behr uses cell dummies, **Figure 3**, with which realistic thermal tests can be undertaken without having to use real cells. This is particularly useful when real cells are not yet available. The dummies are constructed in

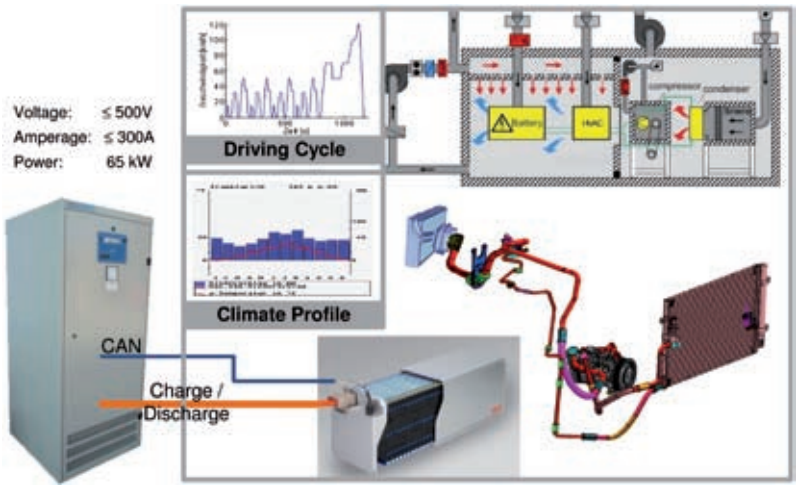

Figure 4: Schematic build-up of the climate battery system test bench at Behr

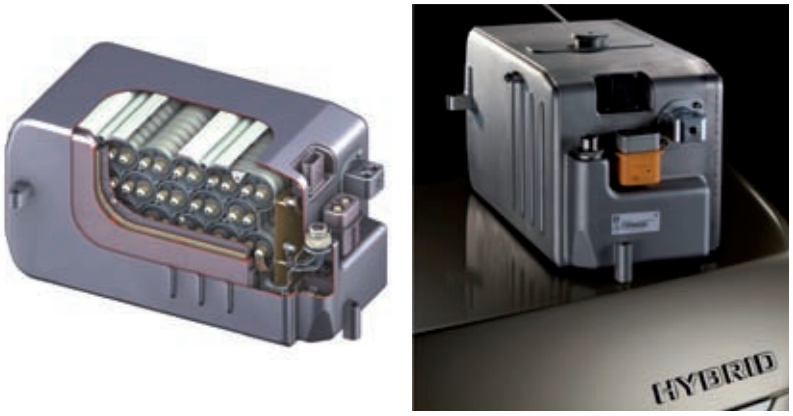

Figure 5: Lithium-ion battery for the Mercedes-Benz S 400 Hybrid (source: Daimler AG)

such a way that they replicate the thermal properties of a real cell, that means first and foremost the anisotropic heat conduction, and the heat capacity. The dissipated energy is represented by heating foils. These, in turn, are dependent on the temperature, state of charge (SOC), and charging or discharging rates from the internal resistances of the cell.

Behr has a unique test facility in the climate battery system test bench, **Figure 4**, that makes it possible to operate a real battery under real-life operating conditions. While the battery is charged and discharged according to a predetermined operational cycle, the battery cooling is integrated into a real cooling or refrigerant circuit system. Thanks to the two separate climate chambers, the thermal conditions of the cooling system that are actually encountered in the vehicle cabin and in the vehicle environment can be demonstrated.

4 Battery Cooling System for the Mercedes-Benz S 400 Hybrid

The Li-ion battery of the Mercedes-Benz S 400 Hybrid contains 35 round cells [3] that are tightly packed together so as not to exceed the specified space envelope of a standard lead battery, **Figure 5**. The cooling device thus also needed a very compact design. It is not only responsible for the cooling of the cells, but also serves as the container for holding the cells. As a battery evaporator, the cooling unit is directly integrated into the vehicle's refrigerant circuit.

The cooling device is made up of an evaporator plate, a container, and numerous heat conducting elements that are connected to the evaporator plate. In the peripheral area of the evaporator plate, several screw points are provided, with which the cooling unit is attached to the battery housing. All the cooling unit parts are firmly brazed together to form a single unit. A special manufacturing process ensures that the individual components have the necessary positional tolerances and dimensional stability even after the brazing operation.

The cooling elements provide cooling of the inside of the battery by supporting the dissipation of the heat lost from the cells to the evaporator plate. The container also plays a part in the dissipation of the heat. In the evaporator plate, channels are provided, in which the refrigerant evaporates and thus absorbs the heat lost from the cells. The channels are arranged so as to produce a very homogeneous distribution of temperature over the entire evaporator plate. This homogeneity and the uniform heat conduction in the cooling elements and in the container wall work in harmony with one another to ensure that the entire cell area is subjected to the consistent cooling required.

5 Summary

The electrochemistry of the Lithium-ion battery places considerable demands on its thermal state. Efficient thermal management is therefore essential to meet the high service life requirements. The nature of the cooling of the individual cells depends on type, geometry, and application profile.

Behr has a climate battery system test facility that makes it possible to test the interaction between the real battery and real cooling system under real operating conditions. The cooling device for the Li-ion battery of the Mercedes-Benz S 400 Hybrid is a contemporary example of efficient battery cooling.

References

[1] Heckenberger, Th.: Cooling of Li-Ion-Batteries in Hybrid and Electric Vehicles. 1st International CTI Forum „Alternative and Hybrid Drive Trains", Berlin, Germany, 4th/5th December 2008

[2] Brotz, F.; Isermeyer, T.; Pfender, C.; Heckenberger, Th.: Kühlung von Hochleistungsbatterien für Hybridfahrzeuge. In: ATZ 109 (2007), Nr. 12, S. 1156-1162

[3] Luy, J.-F.; et al.: Quality of HV Li-Ion-Batteries. Symposium „Kraftwerk Batterie – Lösungen für Automobil und Energieversorgung", Haus der Technik, Essen, 20./21. Januar 2009

The Design and Aerodynamics of Commercial Vehicles

Improving transport efficiency is an ongoing challenge for bus and truck manufacturers. Especially aerodynamics offer a high potential in terms of reducing fuel consumption and emissions of trucks and buses. MAN reaches with a aerodynamic-optimised semitrailer tractor a c_W value of 0.30.

1 The Initial Situation

For decades, OEMs and suppliers have been contributing to the development of energy-efficient vehicles - focusing on the customers' requirements. Trucks or buses whose fuel consumption was too high and whose CO_2 balances were correspondingly poor simply stayed on the shelf. Success is there for all to see: since the end of the sixties, the consumption of a forty-tonne articulated truck has been reduced by around a third, **Figure 1**. Since the beginning of the nineties, however, fuel consumption has remained at a relatively constant level. The reason: the emission limits have become stricter, phase by phase, and this inherently results in increased consumption, which in turn has to be compensated for by complex measures designed to increase efficiency.

Great potential for further reductions in the vehicles' fuel consumption can be found in aerodynamics. However, as opposed to buses and passenger vehicles, where the manufacturer is responsible for the form of the entire vehicle, when it comes to trucks, the customers and the planned utilisation contribute decisively to their aerodynamic form. And so the customers have to decide whether they will take the following aerodynamic influences into consideration for their vehicles:

- use of and correct settings for roof spoilers
- use of side panels on tractor and trailer
- correct positioning and covering of the load
- optimum aerodynamic combination of driver's cab type and trailer type.

And because the customer often ignores these parameters, the observer's impression is that: „There's no money in aerodynamics for commercial vehicles." This is clearly underestimating the influence of aerodynamics on fuel consumption. If we look at the energy expenditure of a 40-t semitrailer tractor travelling horizontally at 85 km/h, we see that rolling and air resistance are the decisive factors, **Figure 2**.

2 Design and Aerodynamics – History

Applying aerodynamics to the construction of commercial vehicle was only thought of for the first time in the thirties, when the motorways were built. Buses and trucks were originally no more than elongated passenger vehicles. When it became important to reduce the air resistance of commercial vehicles, the first measures to be applied were those that were already known from passenger vehicles. These were based on forms designed by the pioneers of aerodynamics, Jaray and Kamm.

It was only with Gaubschat's „trambus" (1935), which was constructed on a chassis from Büssing – today MAN – that the bus took on a style different to that of the passenger car.

The VW Transporter, developed in 1949 and known around the world by its nickname „Bully", was a milestone of aerodynamics in commercial vehicles. Thanks to the Transporter's rounded front, its c_W value was reduced to only half that of the preliminary design, which had a squared front. The VW Transporter became the prime example of commercial-vehicle aerodynamics. As one of Volkswagen's most successful vehicles ever, the Transporter is an impressive repudiation of the general opinion prevailing even today: „Aerodynamics don't sell." [1]

As the historic pictures clearly show, the aerodynamics are almost exclusively defined by the form of the vehicle. However, for the vehicle designer this is of great importance. Any proposed changes to the form of the vehicle put forward by the aerodynamicists can only have an effect on the vehicle's development if they are accepted by the designer. The more

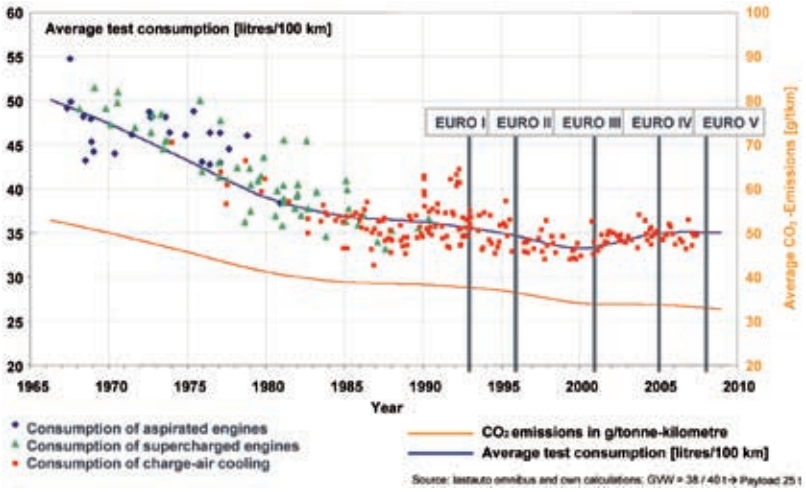

Figure 1: Average consumption of 40-t semitrailer tractors (1965 to 2008)

The Authors

Stephan Kopp
is Head of Body/Cabin/Aerodynamics at MAN in Munich (Germany).

Stephan Schönherr
is Head of Bus Design at MAN in Munich (Germany).

Holger Koos
is Head of Truck Design at MAN in Munich (Germany).

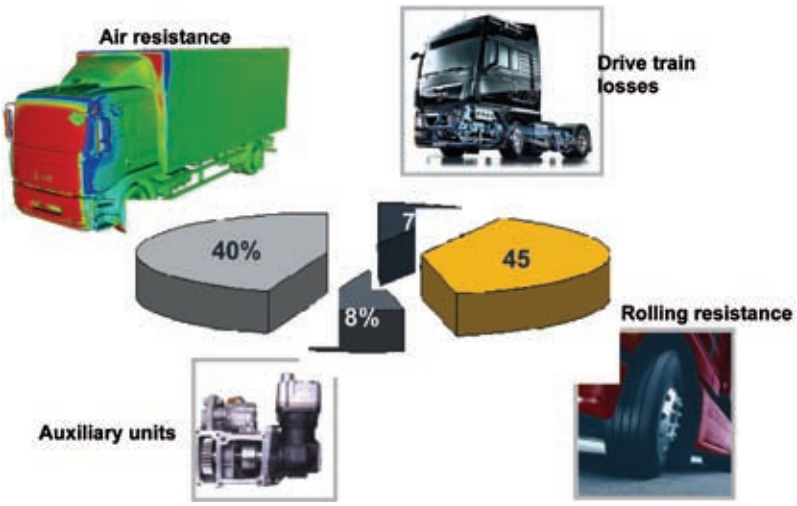

Figure 2: The percentages of energy expended by a 40-t semitrailer tractor on a level stretch at a constant 85 km/h

the aerodynamicist can empathise with the designer, the more likely it is that the two will reach a win-win situation.

3 Design and Aerodynamics – Trucks

The development of design and aerodynamics in commercial vehicles is narrowly restricted. In the case of trucks, primarily the lengths and heights prescribed by law have to be utilised, as a rule to their full extent, in order to realise the maximum loading space. Moreover, in the overwhelming majority of cases, the truck manufacturer is only responsible for the development of the vehicle's chassis, drive train and driver's cab, while the bodies, trailers and semitrailers required for the various different branches are designed by independent firms. The situation that has arisen out of statutory requirements and the traditional division of labour between vehicle and body manufacturers has led to the European truck market becoming dominated by the so-called forward control type of truck, which offers only a restricted amount of space for aerodynamic design. In this restricted space – a length of approximately 2.30 m – an attractively designed cab with sufficient space for two drivers to work and live in has to be harmonised with the aerodynamics. What is more, increasing demands with regards to engine cooling, interior air-conditioning, the soiling of the vehicle and aero-acoustics also have to be taken into consideration. This balancing act is performed by optimising many of the details of individual components, most of which remain invisible to the untrained eye, **Figure 3**.

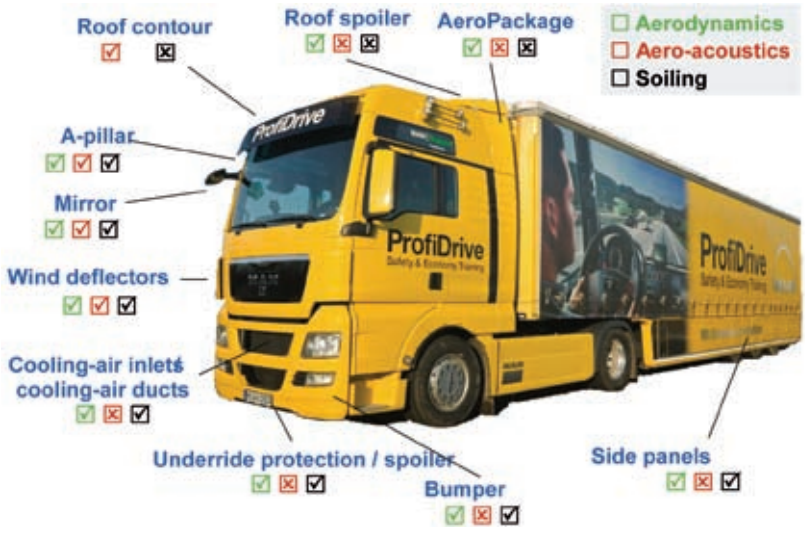

Figure 3: The aerodynamically relevant parts of a long-haul semitrailer tractor

4 Design and Aerodynamics – Buses

The situation with regard to buses is somewhat easier: here, designers and aerodynamicists are able to create the complete vehicle, the front, the sides and the rear, as a single form-fitting unit. The only factors mitigating against the aerodynamic optimum are the customer's desire for as many seats as possible, together with the corresponding amount of space for baggage, and the requirements laid down in the technical vehicle specifications.

The greater scope for design when it comes to buses is impressively exemplified by the Neoplan Starliner and Cityliner coaches, whose air-resistance coefficients of c_W 0.36 and 0.35 respectively have already reached passenger vehicle level. The considerably larger radii of the corners and the pronounced angle of the roofs of these luxury coaches very largely prevent flow separation and the area of dynamic pressure in the front. The flow remains attached for a long period and thus decisively reduces the air resistance, **Figure 4**.

The designers were able to achieve an additional reduction in air resistance by means of an aerodynamic, stylish tail. Tapering reduces the area of the wake and thus the air resistance. The undesired but largely unavoidable soiling at the back of the Starliner shown in **Figure 5** indirectly demonstrates the efficacy of the tail's tapered design. The flow remains attached to the roof and the upper side wall right up to the separation edge, which reduces the area of sub-pressure at the rear. A pleasant side-effect: those parts of the body where the flow remains attached show no evidence of soiling.

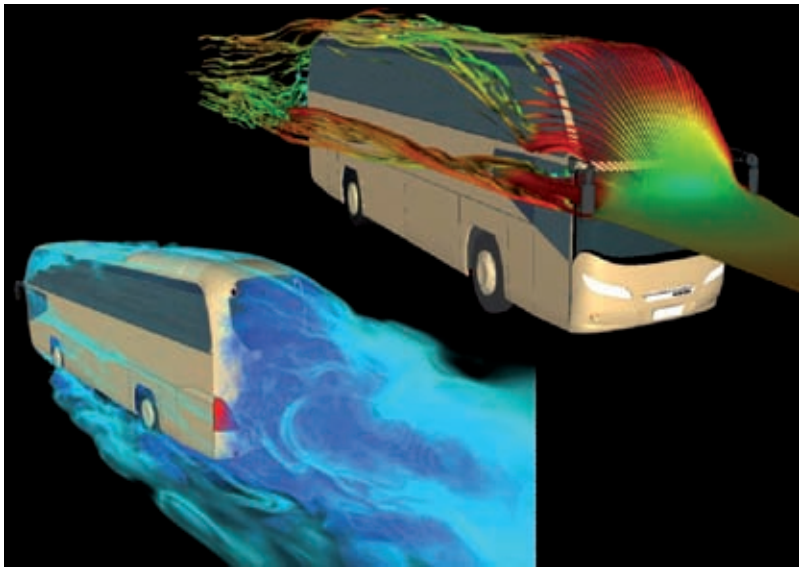

Figure 4: Visualisation of the Neoplan Cityliner flow

5 Design and Aerodynamics Development Process

The example of the two new heavy truck series introduced in 2007 – the TGS and the TGX – serves to demonstrate how the close interaction between design and aerodynamics in the early phases of development can achieve a noticeable reduction in air resistance (always bearing in mind that this can only be within the narrow limits described above). By contrast with its predecessor model, the TGA, it was possible to reduce the c_w value by 4 %, even though the basic structure of vehicle and cab was not changed. Taking the Cityliner as an example, thanks to the above-mentioned greater latitude allowed by the law it was possible to realise even greater potentials. The c_w value was reduced by 15 %.

The development of the TGS and TGX began in 2004 with the so-called definition phase and the requirement specification. Amongst other aspects, this contained definitions of consumption, efficiency and comfort objectives relevant to the aerodynamics. In this early phase, which is distinguished by a wide range of different design concepts and scale models, close cooperation with the Design Department is of major concern to aerodynamics.

In this creative phase, it is particularly important to help the designers find the right form or to test the flow optimisation of their design ideas early on by quickly performing aerodynamic studies. The cooperation between design and aerodynamics opens up possibilities for helping the designer substantiate the selected forms: the design that is most favourable from the point of view of the flow is also the right one because of its more favourable c_w value and it should be preferred.

CFD (Computational Fluid Dynamics) simulation is used here as a fast development tool. It provides swift results on the air-resistance coefficients and volume flow rates of cooling air that the design models being tested can be expected to deliver and visualises specific flow topologies which give the aerodynamicist solid pointers to optimisation potentials. These in turn can then be put through specific tests in the wind tunnel and be presented graphically to the designer.

In this phase, the designer and the aerodynamicist must not only see to it that the vehicle is aerodynamic and pleasing to look at, but also that crucial vehicle functions are ensured, the cooling of the engine and the electrical components of the hybrid bus, for example.

Amongst other aspects, the design of the roof of the newest generation of MAN hybrid buses, **Figure 6**, came to be decisively influenced by the flow topology. Following the definition phase comes the concept phase, which is distinguished primarily by measurements in the model wind tunnel. At MAN the models used are generally on a scale of 1:4. The models are subjected to wind speeds of 290 km/h, which corresponds to a flow of 72 km/h in reality. In order to optimise the aerodynamic qualities of a model, the geometry of the components is

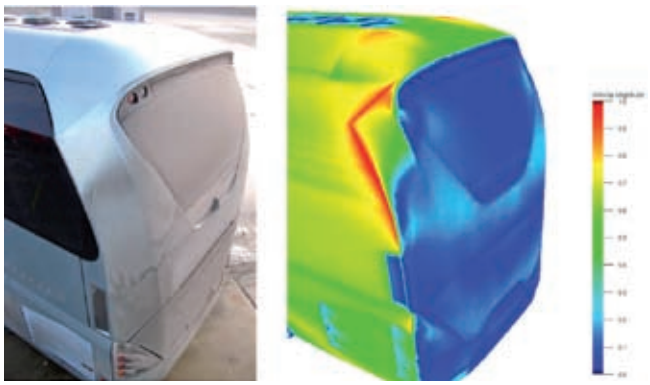

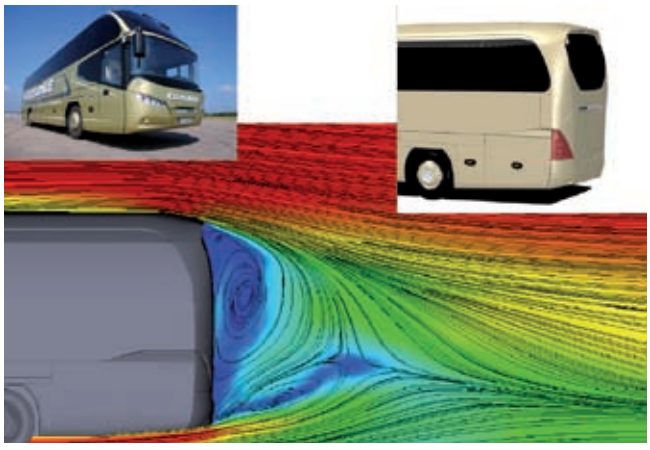

Figure 5: Visualisation of the flow around the rear ends of the Neoplan Starliner & Cityliner

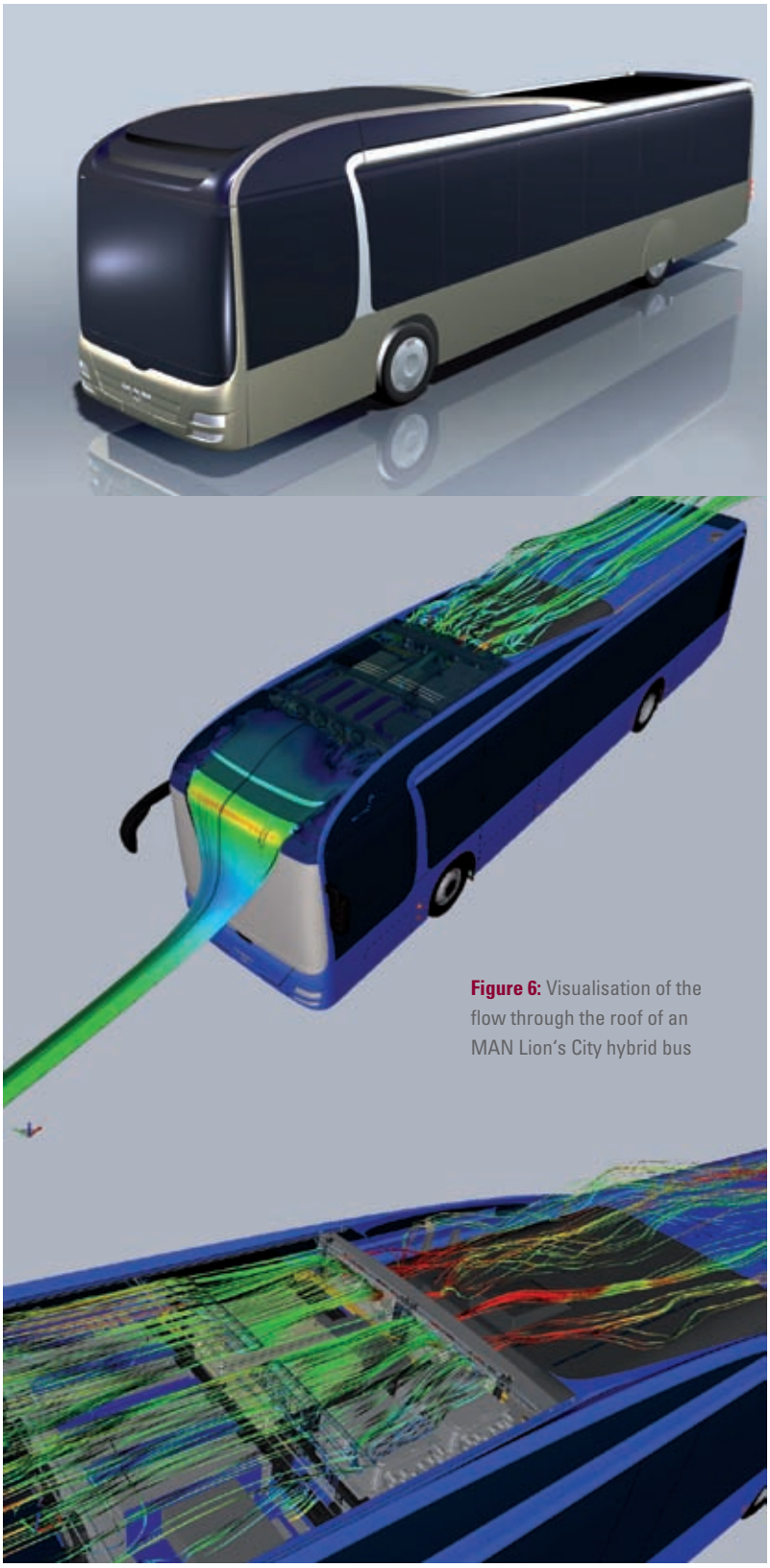

Figure 6: Visualisation of the flow through the roof of an MAN Lion's City hybrid bus

changed one step at a time and the c_w values of each configuration ascertained. On average, 30 configurations go through model wind tunnel testing every day: the end result is the aerodynamically most favourable form of the tested components. The responsible designers are usually part of the teams for these wind tunnel test, which enables them to make the fullest and most efficient use of the design possibilities.

With the commencement of the third phase, the preparation for series production, a styling freeze is imposed on the basic form of the driver's cab. The first aerodynamic prototypes are constructed from glass-fibre reinforced plastic shells and the optimisation of body component details now takes place in the full-sized wind tunnel. Not only aerodynamic improvements to body parts are measured here, but also details that could only be modelled with difficulty or not at all, primarily the cooling-air ducts, the aeroacoustics and the self-soiling characteristics. MAN carries out these full-scale aerodynamic measurements in Europe's biggest wind tunnels, the DNW (German-Dutch Wind Tunnels) in Amsterdam and the RTA (Rail Tec Arsenal) in Vienna. Air-resistance and aero-acoustic measurements are the main focus of tests in the DNW, while in the RTA the focus is on soiling, climatic and engine-cooling issues.

In order to ensure continual development, MAN's wind tunnel tests always examine the current sample: A-samples, made of hand-formed parts, for example; B-samples, produced with prototype tools, and C-samples, produced by series tools. Validation then follows, with series parts. The final check of whether all the measures that have been developed have had the desired effect is carried out on the part in series production status as delivered to the customer.

Special attention is paid to the design of the two exterior mirrors. The reason for this is that because the basic shape of the truck is rectangular, a shape which is unfavourable for air flow, the mirrors can take over an air-guiding function. Correspondingly-shaped mirror casings can guide the air in a controlled manner along the side of the cab and thus contribute to a reduction in air resistance. Some of the air that flows past the vehicle is now guided by the newly-designed external mirror casings along the side windows. The mirror wake has been correspondingly shortened. In addition, water management has been integrated in order to minimise the water splashing

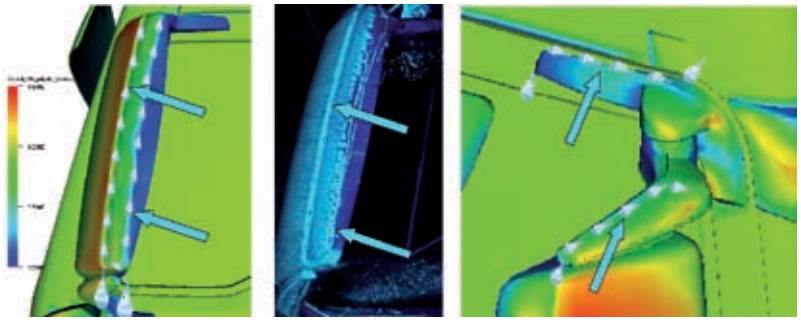

Figure 7: Harmonious integration of aerodynamic features in the overall appearance of the TGX&TGS side mirrors

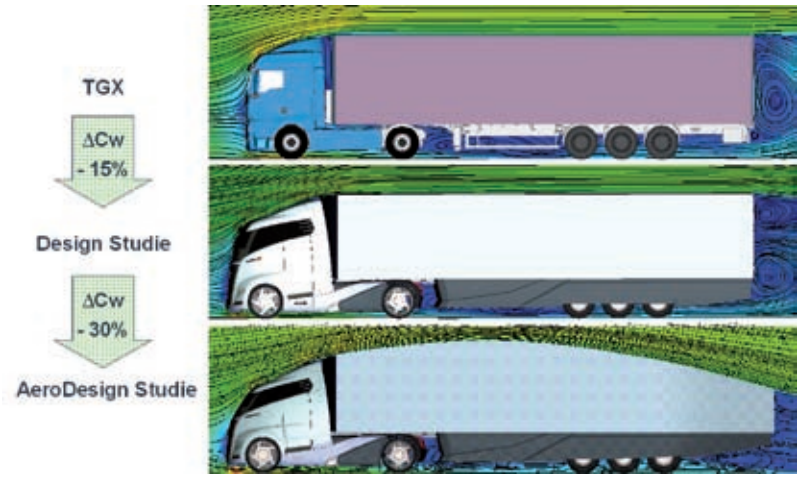

Figure 8: The creation of a future-oriented vehicle concept

annoyingly against the side windows and the glass of the mirror, **Figure 7**. The designers have integrated these measures harmoniously into the overall appearance so that the customer won't even be aware of these purely technology-driven features as such. This interplay between attractive design and aerodynamic efficiency is realised not only in the design details of the series vehicles but also in the creation of future-oriented vehicle concepts.

This is how the Design Department gives form to its visions, which are subsequently examined in the usual way from the aerodynamic point of view, **Figure 8**. In the course of the continuous interplay of development, a new vehicle concept evolves, visually appealing and aerodynamically at the very highest level. Thanks solely to current laws, unfortunately still outside the realm of what can be realised.

6 Visions of the Future

The current conventional forward control trucks are at a level of aerodynamics that can hardly be improved any more under the given conditions. Major improvements in reducing air resistance will only be possible when the restrictions on maximum dimensions permitted by law are loosened or replaced by alternative regulations. In the U.S.A., for instance, the length of the vehicle itself is not limited, only the size of its usable cargo bay. At last year's IAA Commercial Vehicles, MAN presented a semitrailer tractor that had been aerodynamically optimised: its flow topology was based on that of a dolphin. The tractor had been lengthened by 80 cm, while the semitrailer had been raised by 20 cm and tapered. Tractor and semitrailer together achieved the sensationally low c_W value of 0.30. For buses there still is a high potential, too, **Figure 9**. In this way it would be possible to improve the CO_2 balance of the road haulage sector significantly in a short space of time – if the lawmakers go along with it.

References

[1] Hucho, W.-H.: Aerodynamik des Automobils, 5. Auflage, GWV Fachverlage, Wiesbaden 2008
[2] Hoepke, E. ; Breuer, S. : Nutzfahrzeugtechnik, 5. Auflage, GWV Fachverlage, Wiesbaden 2008

Figure 9: Neoplan vision

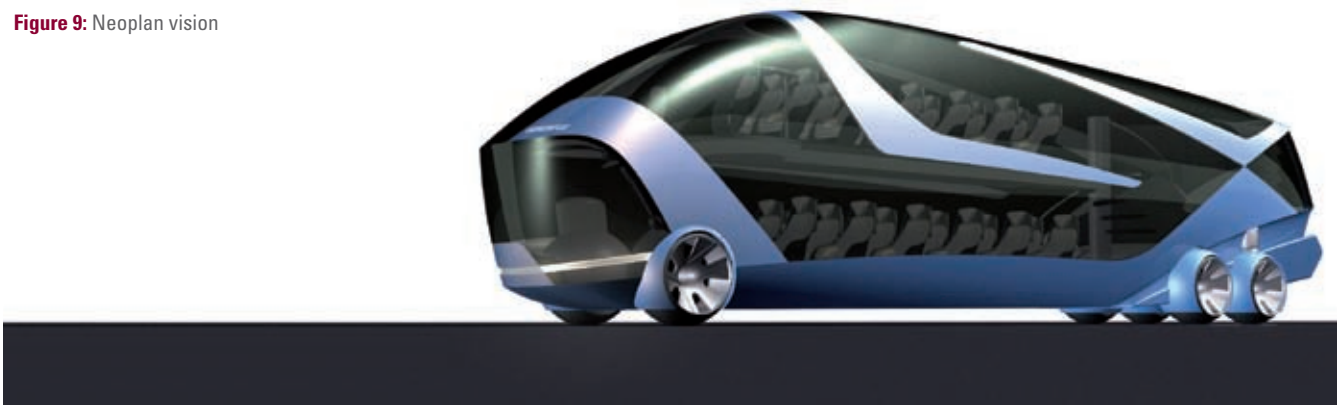

personal buildup for Force Motors Ltd.

Latest Developments in Driver Assistance Systems for Commercial Vehicles

Driver Assistance Systems (DAS) can support drivers in avoiding collisions or mitigating their effects. This article provides an overview of the evolution of advanced safety systems for commercial vehicles as well as an outlook for developments. It features the latest technology breakthrough, Wabco's "OnGuardMax", which is an autonomous emergency braking system that reacts to both moving or stopped vehicles and can bring the vehicle to a complete stop.

1 Introduction

The European Commission's White Paper on European Transport Policy for 2010 includes an ambitious goal to halve the number of fatalities in road traffic in the European Union (EU) between 2001 and 2010 [1]. In 2001, the number of fatalities in road traffic totaled around 50,000 in the 15 member states of the EU. In 2007, 42,300 fatalities were recorded in 26 EU member states [2]. Despite the enlargement of the EU, such fatalities have declined over the past years. Nonetheless, this trend shows that the EU's goal of 25,000 fatalities by 2010 is, indeed, ambitious.

For commercial vehicles, the most frequent accidents are rear-end collisions, lane departure accidents and collisions with oncoming traffic. According to findings of researchers at DEKRA, a German institute for safe and efficient mobility, these three types of accidents together account for 45 % of all accidents involving commercial vehicles [3]. It is estimated that related accident costs total EUR 370 million annually in the European economy [4].

To reach its goal of halving the number of fatalities, the European Commission strongly recommends the introduction and use of intelligent active safety systems in vehicles, supplemented by education and training of drivers as well as an intelligent infrastructure such as adaptive traffic control systems or incident detection on highways [5]. There are a number of initiatives within the EU to make active safety systems mandatory: for example from November 2011, electronic stability control will become mandatory for first type approval commercial vehicles and from November 2014 also for first national registrations. Furthermore, it is mandated that first type approvals from November 2013 and first national registrations from November 2015 in the EU must be equipped with advanced emergency braking systems and lane departure warning systems.

2 Improving Road Safety with Advanced Safety Technology

In addition to driver education and training as well as intelligent infrastructure, vehicle safety systems can help improve road safety, particularly during the pre-crash phase when an accident can still be avoided or at least its effects mitigated. This means advanced driver assistance systems contribute to saving lives and reducing costs by minimizing damage and downtime due to accidents.

Studies by the Technical University in Munich, Allianz Insurance and MAN Nutzfahrzeuge AG, each analyzing 600 to 850 severe accidents involving trucks and semi-trailers, reported that Electronic Stability Control (ESC) and Adaptive Cruise Control (ACC) systems can prevent up to 30 % of rear-end and lane departure accidents [6]. Based on such studies, the European Commission estimates that the implementation of intelligent safety systems could reduce the number of fatalities in road accidents by 1,000 every year [4].

Other reasons for fleet owners to equip their vehicles with DAS – especially in economically challenging times – include potential attractive insurance discounts or a reduction in road tolls. The Association of the German Automotive Industry (VDA) and insurance companies are currently considering such proposals.

3 The Evolution of Safety Systems for Commercial Vehicles

Active safety systems were the first generation of systems that significantly contributed to a reduction of fatalities in road traffic. They help the driver to stabilize and control the vehicle and include Anti-Lock Braking Systems (ABS), Automatic Traction Control, Electronically Controlled Braking Systems (EBS) and ESC.

3.1 ABS – Anti-lock Braking System

Wabco pioneered ABS technology for trucks, trailers and buses with Daimler in 1981. ABS is a control unit that detects when any of the wheels is about to lock-up. The system acts on these signals and releases the service brakes on the particular wheel, ensuring that the wheel keeps rotating and maintains its grip on the road in emergency braking situations or in slippery road conditions. Such technology assists the driver in maintaining control of the vehicle and avoiding an accident. Furthermore, lateral forces can still be effective between the road surface and the wheels being braked – even at full brake application – to ensure the stability of a truck or trailer. ABS became standard for heavy commercial vehicles in the EU as of October 1991 and since 2001 it is also mandatory for light commercial vehicles.

In the late 1980s, ABS was extended to include Automatic Traction Control, in Europe commonly known as ASR (for the German expression Antriebsschlupfregelung). It significantly improves stability under acceleration and traction by means of propulsion limitation and differential brake intervention.

3.2 EBS – Electronically Controlled Braking System

In 1996, Wabco launched EBS for commercial vehicles. This system reduces the braking distance by transmitting the driver's actuation of the brake pedal into electron-

The Authors

Dr. Christian Wiehen is Wabco Chief Technology Officer in Brussels (Belgium).

Kurt Lehmann is Wabco Vice President, Product Engineering in Brussels (Belgium).

Jean-Christophe Figueroa is Wabco Vice President, Vehicle Dynamics and Control in Brussels (Belgium).

ic signals automatically providing and distributing the necessary pneumatic pressures to each axle. This way of signal transmission allows a faster and more direct response from the brake cylinders. The control of driving stability and steerability throughout the braking process is further ensured as ABS is also part of EBS.

3.3 ESC – Electronic Stability Control

ESC is an extension of EBS and was introduced in 2001 by Wabco. ESC uses ABS sensors to measure wheel speeds; a steering angle sensor to recognize the driver's steering intention; a lateral acceleration sensor, and a yaw rate sensor, which measures the actual vehicle movement around its vertical axis. These sensors communicate with EBS so that all data are analyzed to compare actual movement of the vehicle with the driver's intention while assessing if critical stability limits are to be exceeded in the next moments. If a dangerous situation is predicted, ESC intervenes by individually applying single wheel brakes. This helps correct a possible instability of the vehicle and prevents it from over- or under-steering. Furthermore, it also helps support the roll stability and maintaining the intended driving direction.

4 Driver Assistance Systems – Advanced Technologies for Commercial Vehicle Safety

Safety systems described so far in this article focus on the reaction of the vehicle to actions initiated by the driver. DAS further advances by also monitoring the surrounding environment, recognizing other traffic participants, and autonomously reacting if necessary. This evolution in safety systems is illustrated in **Figure 1**.

The European Commission highlights advanced DAS as a major investment for vehicle safety [5]. However, systems currently available on the market have been designed mainly as comfort or warning systems and include, for example, Adaptive Cruise Control, Collision Warning Systems (CWS) or Lane Departure Warning (LDW) systems. A new milestone is the industry's first autonomous emergency braking system: Wabco's OnGuardMax. It reacts not only to moving vehicles ahead (like ACC) but also to stopped vehicles. OnGuardMax will be available in 2011.

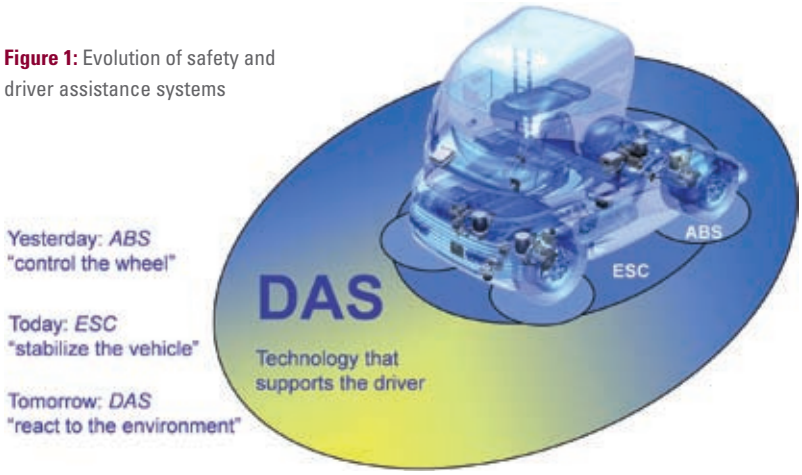

Figure 1: Evolution of safety and driver assistance systems

4.1 ACC – Adaptive Cruise Control

Adaptive Cruise Control is an extension of conventional cruise control systems for the highway; aside from controlling a certain speed, it automatically controls the distance to the vehicle ahead. Although developed for increasing the driver's comfort, it positively influences safety as it is able to decelerate the vehicle up to a certain level (typically -2.5 m/s²) by using endurance and foundation brakes. It also improves fuel efficiency as it allows for a more steady drive.

In the event that the distance to the vehicle ahead becomes potentially dangerous, for example, when the preceding vehicle decelerates, ACC first warns the driver and then adapts engine torque and uses endurance and foundation brakes to adjust the vehicle speed. At the same time, the driver can always deactivate or overrule the system – even if this turns out to be a wrong decision.

Once activated, ACC's headway sensor monitors the road ahead and also parts of the adjacent lanes. Integrated with yaw rate information, the system constantly identifies road curvature and predicts the vehicle's path. Doing so it can differentiate between vehicles in the same lane, which are relevant for distance control, and those in other lanes. ACC's far rate distance sensor has a detection capability up to 200 meters and a horizontal detection angle between 10 and 15 degrees. Radar (radio detection and ranging) and Lidar (light detection and ranging) sensors recognize objects such as vehicles and roadside objects by analyzing their reflected energy. Processing that information, the position of an object, its distance and relative speed can be measured. However, ACC systems can only react to moving vehicles or those vehicles previously detected as moving.

4.2 CWS – Collision Warning System

While ACC is only active when demanded by the driver, its far range sensor can also be used for a collision warning function, which is always active. Processing the distance and relative speed signals of the preceding vehicle in relation to the host vehicle's current speed and acceleration, CWS continuously monitors the relevant vehicle ahead and predicts appropriate assistance. Based on typical driver reaction times and braking capabilities, CWS is able to recognize a collision imminent situation. If the system detects that the driver will have to exert hard braking to avoid a crash, it will raise a visual and acoustic warning. When the driver reacts to that warning, either by braking or evasive steering maneuver, an accident can be avoided. As with ACC, CWS typically does not react to stopped vehicles.

4.3 LDW – Lane Departure Warning

Unintentional lane departures are one of the most frequent causes of accidents involving commercial vehicles. Technologies that help detect and warn a driver when he/she is going to unintentionally leave their current lane can help avoid half of this type of accident [3].

LDW systems use a front camera installed at the windshield to monitor the road ahead. Assisted by image processing, the camera identifies the lane markers on the road surface and assesses the delay time until the vehicles tires will

cross the lines. If the vehicle is tending to leave the current lane while the driver has not set the respective turning indicator, an acoustic signal will alarm the driver to revert to the center of the lane.

4.4 CMS – Collision Mitigation System

A further enhancement of ACC and CWS is a Collision Mitigation System (CMS). It will not only warn but also autonomously brake in collision imminent situations – even if the driver has not activated the ACC. Such a system uses the information of a far range distance sensor at the front of a truck and, as a result, it has the same detection limitations as ACC but cannot react to stopped vehicles.

Compared with ACC and CWS, CMS takes into account possible lateral movements of the host vehicle. The system predicts the time necessary for an evasive maneuver and warns the driver. When CMS concludes that the driver will not be able to prevent a rear-end collision by steering or full braking, it will autonomously apply the foundation brakes to decrease the amount of movement energy generated in a collision.

OnGuard is an ACC system with foundation brake application and CMS capabilities. It was introduced in 2008 to the North American market by Meritor Wabco, a joint venture of ArvinMeritor and Wabco. With this additional CMS function, OnGuard is able to realize a deceleration up to -3.5 m/s², which is nearly half of a full brake application.

5 Wabco's OnGuardMax

A new milestone in DAS is the latest development from Wabco: OnGuardMax. Based on OnGuard and ACC technologies, OnGuardMax can autonomously initiate an emergency braking. It is also the first DAS that reacts to moving and stopped vehicles alike. It ensures most effective deceleration and can bring the vehicle to a complete stop. First presented at IAA 2008, the major trade show held in Hanover, Germany, Wabco's newest DAS system will be available to truck and bus original equipment manufacturers from 2011.

5.1 Technological Approach

OnGuardMax is designed to react in typical road traffic situations; for example, at the end of a traffic jam. In a collision imminent situation, the system will warn the driver and if he/she remains passive, OnGuardMax will autonomously apply the foundations brakes – as does OnGuard – but with maximum possible deceleration.

The system combines data from a front camera (as used in LDW) and a far range distance sensor to gather reliable information about the traffic ahead. Wabco uses this data fusion approach for combining the data of both sensors to distinguish between relevant vehicles and other objects such as bridges or road signs which could trigger a false braking reaction.

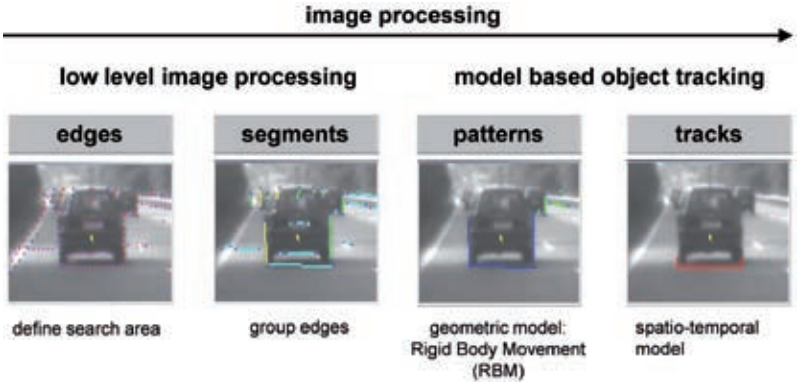

Figure 2: Principle of image processing of the front camera [7]

5.2 Functionality

OnGuardMax uses a combination of a windshield mounted camera and a Lidar sensor to monitor surroundings and provide data for a movement prediction for the host and preceding vehicles alike. Assisted by this prediction, the system verifies whether the driver will be able to prevent even touching the preceding vehicle.

To detect the distance, Wabco uses a Lidar sensor with a maximum detection range of 200 meters. Compared to a radar sensor, this laser sensor can more exactly measure lateral object features due to its twelve single beams. The camera with integrated image processing is able to search and identify vehicle-like shapes – also in the dark – as shown in **Figure 2**. Furthermore, to minimize the computing power in the camera module, the respective algorithms use input from the Lidar sensor to define regions of interest in the image.

The system combines the best data of both sensors: the camera's precision of lateral dimension and position combined with distance and relative speed provided by the distance sensor. In **Figure 3**, the interplay of video camera and distance sensor is illustrated. Using the combined sensor approach, it is able to measure not only distance and relative speed, but also the

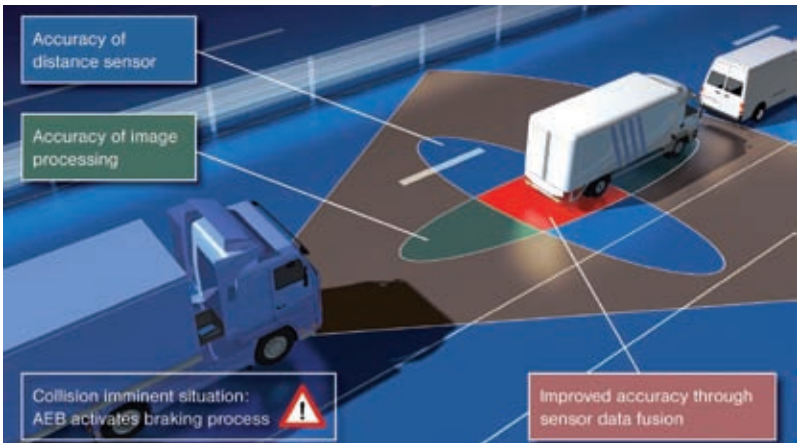

Figure 3: Data fusion of OnGuardMax

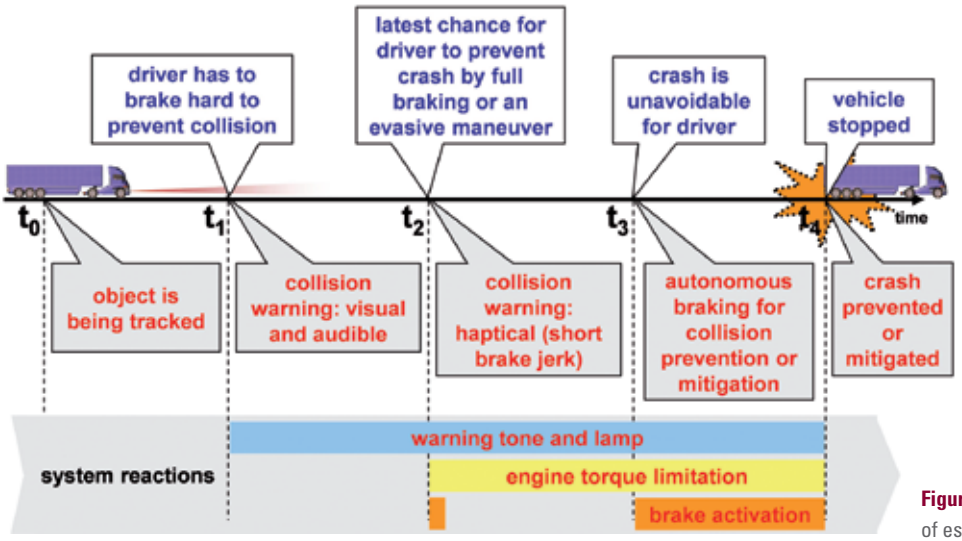

Figure 4: OnGuardMax steps of escalation

width of the preceding vehicle and its exact lateral offset relative to the host vehicle's center axis.

OnGuardMax has several steps of escalation before it autonomously activates its emergency braking as illustrated in **Figure 4**. When the host vehicle is approaching a preceding vehicle and the system senses a potential collision, warning tones and a visual alarm will alert the driver. At that moment, the driver would be able to prevent a collision by performing a hard braking maneuver. When more time has lapsed without appropriate intervention by the driver – in addition to the visual and acoustic warning – the system initiates a deceleration by limiting the engine torque and inducing a short braking jerk. As the wheel brakes are activated only for a moment, the driver can make use of the maximum lateral force potential to perform an evasive maneuver to avoid a collision. If the driver still does not react and a collision can no longer be avoided, OnGuardMax autonomously initiates the maximum possible braking. Depending on the specific situation, it is capable of avoiding a collision or at least mitigating its effects.

5.3 Limits and Further Potential

Currently, OnGuardMax is the only system for commercial vehicles that reacts to moving or stopped vehicles and can bring the truck to a complete stop. On dry road conditions, a collision can be fully avoided if the host vehicle is driving less than approximately 50 km/h faster than the vehicle ahead. In the event the host vehicle is driving faster, the system will mitigate the effects of the collision.

Further development potential for the system includes monitoring of the adjacent lanes to provide additional information and determining whether an evasive maneuver is feasible. As a result, OnGuardMax could initiate a deceleration or an emergency brake even earlier. Currently, the system is not able to measure the current level of road friction; it anticipates dry ground. Therefore, another potential advancement would be the detection of the actual road surface condition and how it would influence braking distance.

6 Future Trends in Driver Assistance Systems

While technologies mentioned in this article have already been introduced or will be introduced in due course, there remains a need for a continued investment in advanced technologies that often have already been introduced for passenger cars but need extended development for potential commercial vehicle versions. Future technologies such as DAS, blind spot detection systems, lane change or lane keeping support systems are expected to be ready for the commercial vehicle market in the next three to ten years.

Blind Spot Detection (BSD) systems focus on urban traffic, often a critical area for trucks. Due to the shape of a truck, there are large areas in front and on the sides that cannot be monitored properly by the driver. Although a large number of mirrors have been introduced in recent years, continuous monitoring of all areas is not guaranteed by a driver, especially when he/she is simultaneously performing driving maneuvers such as turning at a road intersection [8]. A BSD system would autonomously monitor blind spots and would detect and track pedestrians, cyclists and other vulnerable road users directly in front and at the passenger side of the truck, up to approximately four meters. In a collision imminent situation, the driver is alarmed by the system.

A further development of BSD will be Lane Change Assist (LCA) that also measures speed and distance of vehicles approaching from the rear of the truck. With these critical data, the system estimates the time when a trailing vehicle will enter the host truck's blind spot. When the driver is about to change lanes and operates the turn indicator, the LCA will warn the driver by an audible, visual or tactile alert if changing lanes is not safe at the moment.

Other than today's LDW systems that are designed solely to warn the driver if the truck is going to unintentionally leave its lane, a Lane Keeping Support (LKS) system could also intervene in the lateral dynamics of a commercial vehicle to avoid a potential dangerous situation. It would induce a lateral impulse to prevent the commercial vehicle from leaving its lane.

Such assistance can be done either by directly commanding a steering system or using individual wheel brake application as stability control (ESC) does.

7 Summary

Since the introduction of ABS in the early 1980s, commercial vehicle safety systems such as ESC have made a significant contribution to reduce not only fatalities in road traffic accidents involving commercial vehicles but also injuries and consequential cost. These systems as well as EBS, ACC, CWS and LDW have paved the road for one of the latest technology innovations in DAS: Wabco's OnGuardMax. The system incorporates existing DAS technologies while innovating further as it can detect moving or stopped vehicles ahead and can autonomously bring the vehicle to a complete stop. Building on this technology, further DAS advancements will be developed. Technological prospects include advanced systems that can monitor blind spots or systems that can improve today's DAS functionalities by gathering more information about the surrounding environment.

References

[1] European Commission: White Paper on European Transport Policy for 2010: Time to Decide. Brussels, 12.09.2001

[2] International Transport Forum: Transport Trends 2007 – Road Injuries. Table C3: Killed. http://www.internationaltransportforum.org/statistics/statistics.html. Access date: 23.02.2009

[3] Allianz, DEKRA, Mercedes Benz: Press release. "Safetyplus Truck" initiative: safety technology pays economic dividends. Hanover, 20.09.2006

[4] Rother, F.; Henrich, A.; Wettach, S.: Unfallvermeidung. Politik macht Druck bei Fahrer-Assistenzsystemen für Lkw. In: Wirtschaftswoche, 06.06.2008

[5] European Commission: Communication from the Commission to the Council and the European Parliament. Information and Communications Technologies for Safe and Intelligent Vehicles. Brussels, 15.09.2003

[6] Allianz: Wirkungspotentiale von Fahrerassistenzsystemen im Nutzfahrzeug. http://www.allianz-autowelt.de/automotive/azt-allianz-zentrum-technik/sicherheit/assistenzsysteme/index_fahrer-assistenz_nfz.html. Access date: 23.02.2009

[7] Leser, H.; Icke, S.: Rechts abbiegende Lkw und Radfahrer – Feldversuche zum Blickverhalten von Lkw-Fahrern. In: VDI-Berichte Nr. 1986, 2007

[8] Thiem, J.; Mühlenberg, M.: Datafusion of two Driver Assistance System Sensors, Advanced Microsystems for Automotive Applications. Berlin, 2005

IMPRINT

ATZ WORLDWIDE

www.ATZonline.com

07-08|2009 · July-August 2009 · Volume 111
Springer Automotive Media | GWV Fachverlage GmbH
P. O. Box 15 46 · 65173 Wiesbaden · Germany
Abraham-Lincoln-Straße 46 · 65189 Wiesbaden · Germany

Managing Directors Dr. Ralf Birkelbach, Albrecht Schirmacher
Senior Advertising Thomas Werner
Senior Production Ingo Eichel
Senior Sales Gabriel Göttlinger

EDITORS-IN-CHARGE

Dr.-Ing. E. h. Richard van Basshuysen
Wolfgang Siebenpfeiffer

EDITORIAL STAFF

Editor-in-Chief
Johannes Winterhagen (win)
Phone +49 611 7878-342 · Fax +49 611 7878-462
E-Mail: johannes.winterhagen@springer.com

Vice-Editor-in-Chief
Dipl.-Ing. Michael Reichenbach (rei)
Phone +49 611 7878-341 · Fax +49 611 7878-462
E-Mail: michael.reichenbach@springer.com

Chief-on-Duty
Kirsten Beckmann M. A. (kb)
Phone +49 611 7878-343 · Fax +49 611 7878-462
E-Mail: kirsten.beckmann@springer.com

Sections
Body, Safety
Dipl.-Ing. Ulrich Knorra (kno)
Phone +49 611 7878-314 · Fax +49 611 7878-462
E-Mail: ulrich.knorra@springer.com

Chassis
Roland Schedel (rs)
Phone +49 6128 85 37 58 · Fax +49 6128 85 37 59
E-Mail: ATZautotechnology@text-com.de

Electrics, Electronics
Markus Schöttle (scho)
Phone +49 611 7878-257 · Fax +49 611 7878-462
E-Mail: markus.schoettle@springer.com

Engine
Dipl.-Ing. (FH) Moritz-York von Hohenthal (mvh)
Tel. +49 611 7878-278 · +49 611 7878-462
E-Mail: moritz.von.hohenthal@springer.com

Heavy Duty Techniques
Ruben Danisch (rd)
Phone +49 611 7878-393 · Fax +49 611 7878-462
E-Mail: ruben.danisch@springer.com

Online
Dipl.-Ing. (FH) Caterina Schröder (cs)
Phone +49 611 7878-190 · Fax +49 611 7878-462
E-Mail: caterina.schroeder@springer.com

Production, Materials
Stefan Schlott (hlo)
Phone +49 8191 70845 · Fax +49 8191 66002
E-Mail: Redaktion_Schlott@gmx.net

Service, Event Calendar
Martina Schraad
Phone +49 212 64 235 16
E-Mail: martina.schraad@springer.com

Transmission, Research
Dipl.-Ing. Michael Reichenbach (rei)
Phone +49 611 7878-341 · Fax +49 611 7878-462
E-Mail: michael.reichenbach@springer.com

English Language Consultant
Paul Willin (pw)

Permanent Contributors
Richard Backhaus (rb), Christian Bartsch (cb), Prof. Dr.-Ing. Peter Boy (bo), Prof. Dr.-Ing. Stefan Breuer (sb), Jörg Christoffel (jc), Jürgen Grandel (gl), Prof. Dr.-Ing. Fred Schäfer (fs), Bettina Seehawer (bs)

Address
P.O. Box 15 46, 65173 Wiesbaden, Germany
E-Mail: redaktion@ATZonline.de

MARKETING | OFFPRINTS

Product Management Automotive Media
Sabrina Brokopp
Phone +49 611 7878-192 · Fax +49 611 7878-407
E-Mail: sabrina.brokopp@springer.com

Offprints
Martin Leopold
Phone +49 2642 9075-96 · Fax +49 2642 9075-97
E-Mail: leopold@medien-kontor.de

ADVERTISING | GWV MEDIA

Ad Manager
Britta Dolch
Phone +49 611 7878-323 · Fax +49 611 7878-140
E-Mail: britta.dolch@gwv-media.de

Key Account Manager
Elisabeth Maßfeller
Phone +49 611 7878-399 · Fax +49 611 7878-140
E-Mail: elisabeth.massfeller@gwv-media.de

Ad Sales Manager
Sabine Röck
Phone +49 611 7878-269 · Fax +49 611 7878-140
E-Mail: sabine.roeck@gwv-media.de

Ad Sales
Heinrich X. Prinz Reuß
Phone +49 611 7878-229 · Fax +49 611 7878-140
E-Mail: heinrich.reuss@gwv-media.de

Display Ad Manager
Susanne Bretschneider
Phone +49 611 7878-153 · Fax +49 611 7878-443
E-Mail: susanne.bretschneider@gwv-media.de

Ad Prices
Price List No. 52

SUBSCRIPTIONS

VVA-Zeitschriftenservice, Abt. D6 F6, ATZ
P. O. Box 77 77, 33310 Gütersloh, Germany
Renate Vies
Phone +49 5241 80-1692 · Fax +49 5241 80-9620
E-Mail: SpringerAutomotive@abo-service.info

SUBSCRIPTION CONDITIONS

The eMagazine appears 11 times a year at an annual subscription rate of 269 €. Special rate for students on proof of status in the form of current registration certificate 124 €. Special rate for VDI/ÖVK/VKS members on proof of status in the form of current member certificate 208 €. Special rate for studying VDI members on proof of status in the form of current registration and member certificate 89 €. The subscribtion can be cancelled in written form at any time with effect from the next available issue.

PRODUCTION | LAYOUT

Kerstin Gollarz
Phone +49 611 7878-173 · Fax +49 611 7878-464
E-Mail: kerstin.gollarz@gwv-fachverlage.de

HINTS FOR AUTHORS

All manuscripts should be sent directly to the editors. By submitting photographs and drawings the sender releases the publishers from claims by third parties. Only works not yet published in Germany or abroad can generally be accepted for publication. The manuscripts must not be offered for publication to other journals simultaneously. In accepting the manuscript the publisher acquires the right to produce royalty-free offprints. The journal and all articles and figures are protected by copyright. Any utilisation beyond the strict limits of the copyright law without permission of the publisher is illegal. This applies particularly to duplications, translations, microfilming and storage and processing in electronic systems.

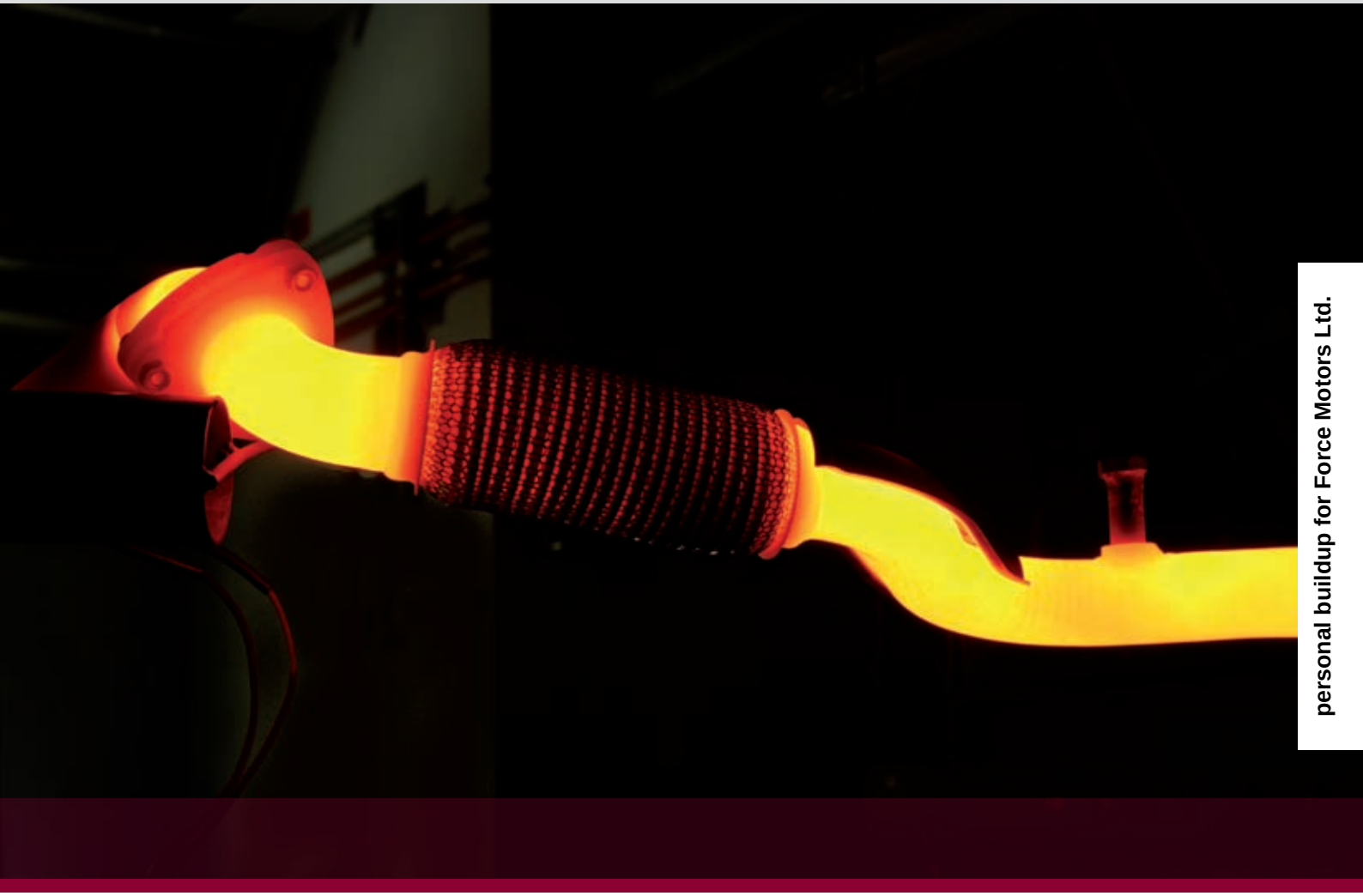

Structure-borne Noise Insulation of Turbocharger Noise in Exhaust Systems

Up to now, decoupling elements are primarily used to ensure the mechanical endurance of exhaust systems. Tenneco – Heinrich Gillet GmbH, in cooperation with the Acoustic Work Group at the University of Kaiserslautern, has developed a procedure to capture the acoustic decoupling effects of these elements up to 5 kHz, enabling an evaluation of their damping efficiency of the structure-borne noise created by the exhaust-gas turbocharger. A special vibro-acoustic test bench was developed and innovative concepts for structure-borne noise isolation were worked up.

1 Introduction

In line with the progressive trend toward concepts with turbocharging and downsizing for combustion engines the number of exhaust-gas turbochargers implemented also increases. Sources of acoustic interference previously unnoticed or masked by other sources of interference are becoming more relevant as the overall vehicle acoustics progressively improve and customer demands on comfort and convenience steadily increase. One of these undesirable sources of acoustic interference is the exhaust-gas turbocharger.

The exhaust-gas turbocharger emits two types of acoustic noise – by directly emitting airborne noise from its own part surface and by inducing structure-borne noise into adjacent components, from where the induced noise again radiates as airborne noise. The exhaust system is directly connected to the exhaust-gas turbocharger and the vibration created by the rotor dynamics is induced into the exhaust system structure, where it disperses as structure-borne noise and finally emits from the surface as airborne noise. Experiences at Tenneco have shown that the exhaust system emits typical turbocharger noise levels at frequencies of 500 Hz to 5 kHz [1]. The airborne noise emitted from the exhaust system surface excites the floor panel of the car and negatively affects the acoustic perception inside the car.

The surface characteristics of shell mufflers are especially susceptible to emitting structure-borne noise as airborne noise. Because the required space in underbodies on cars are getting progressively smaller this type of muffler is implemented more frequently, in comparison to round spun mufflers, which are much more resistant to structure-borne noise radiation [4].

Figure 1: A selection of decoupling elements used in testing

Passive elements are used to keep the structure-borne noise from expanding inside the exhaust line structure. Their behavior was examined as part of a cooperative project between Tenneco – Heinrich Gillet GmbH and the University of Kaiserslautern, which resulted in a company-own development effort of structure-borne noise decoupling elements. An innovative test bench was developed in cooperation with the Work Group for Acoustics at the faculty for fluid mechanics and fluid machinery at the University of Kaiserslautern. Furthermore, an experimental procedure was created to enable the specification and characterization of the exhaust-gas turbocharger. This makes it possible to identify critical vibrations very early and provide adequate solution concepts.

2 State of the Art

East-west inline engines are mostly implemented for combustion engine concepts with a low displacement volume and a small number of cylinders. Here the exhaust system must be equipped with a flexible decoupling device that isolates the concept-related engine movements, thus ensuring the durability of the exhaust system [6].

Standard flexible corrugated tube elements with an outside wire braiding can be used to accomplish this. The respective parts characteristics were previously only considered to be sufficient for frequencies up to 200 Hz. Continuous improvements focusing on acoustically relevant frequencies up to 5 kHz, considering the excitation exerted by the exhaust-gas turbocharger, represent a new challenge and offer an additional application option for acoustic decoupling to reduce the dispersion of structure-borne noise inside the exhaust system. Acoustic properties of a number of decoupling and thermal elements of different flexibility were tested as part of the cooperative project. **Figure 1** shows a selection of the standard elements examined.

The Authors

Dipl.-Ing. (FH) Tobias Pfeffer is Project Leader of the Advanced Engineering Project Turbocharger Decoupler at Tenneco – Heinrich Gillet GmbH in Edenkoben (Germany).

Dipl.-Ing. Hans-Jürgen Kammer is Research Assistant at the Institute of Fluid Dynamics and Fluid Machinery, Work Group Acoustics, at University of Kaiserslautern (Germany).

Dipl.-Ing. (FH) Marcel Womann is Supervisor of Advanced Engineering Department at Tenneco – Heinrich Gillet GmbH in Edenkoben (Germany).

Dr.-Ing. Manfred Fallen is Academic Director at the Institute of Fluid Mechanics and Fluid Machinery and Leader of the Work Group Acoustics at University of Kaiserslautern (Germany).

Prof. Dr.-Ing. Martin Böhle is Head of the Institute of Fluid Mechanics and Fluid Machinery at University of Kaiserslautern (Germany).

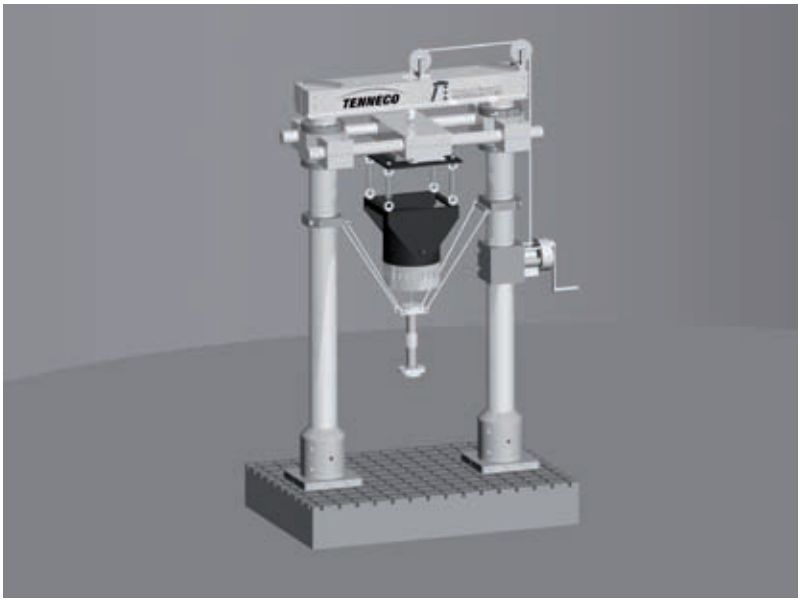

Figure 2: Test bench to measure structure-borne noise transfer properties of decoupling elements

3 Test Bench for Decoupling Elements

The cooperating partners set up a specially developed test bench to record the structure-borne noise transfer properties on the decoupling elements, which is shown in **Figure 2**. Using an indirect measuring procedure with defined terminating impedance the elements are depicted and tested at acoustically relevant frequencies up to 5 kHz.

Figure 3 shows a schematic of a decoupling element with terminating impedance and the respective variables at in- and output of the part. The measuring procedure characterizes the dynamic properties of the decoupling elements in a transfer matrix, considering both the longitudinal and lateral component characteristics.

For a detailed description of the measuring procedure, see [2] and [3]. Due to the fact that a number of tested decoupling elements shows significant nonlinear system behavior the transfer matrix elements are not only frequency- but also amplitude-dependent, which especially affects the frequencies below 500 Hz.

Therefore, reproducible and significant measuring results can only be obtained with a precise knowledge of the excitation vibration. Thus, it is advantageous to use an amplitude-controlled stepped sine testing procedure. Pre-stressing also affects the transfer behavior.

The correlation between the dynamic variables on in- and outlet of an oscillating decoupler is described by a stiffness matrix:

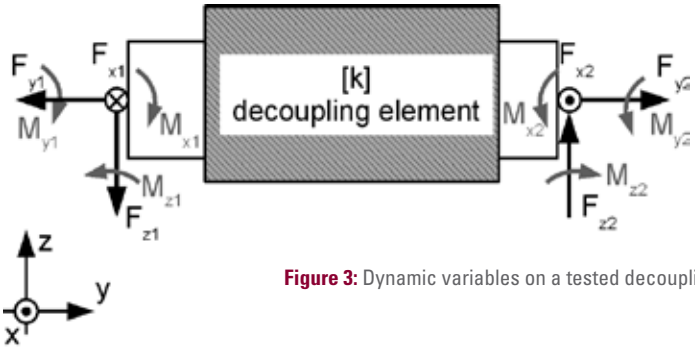

Figure 3: Dynamic variables on a tested decoupling element

$$\begin{pmatrix} F_1 \\ F_2 \end{pmatrix} = \begin{bmatrix} [k_{1,1}] & [k_{1,2}] \\ [k_{2,1}] & [k_{2,2}] \end{bmatrix} \begin{pmatrix} u_1 \\ u_2 \end{pmatrix} \quad \text{Eq. (1)}$$

Here, vectors

$$u_1 = (u_{x1}\ u_{y1}\ u_{z1}\ \gamma_{x1}\ \gamma_{y1}\ \gamma_{z1})^T \quad \text{Eq. (2)}$$

and

$$u_2 = (u_{x2}\ u_{y2}\ u_{z2}\ \gamma_{x2}\ \gamma_{y2}\ \gamma_{z2})^T \quad \text{Eq. (3)}$$

consist of vibrations displacements u and rotating angles γ, respective to the axes identified in the indices. The two vectors

$$F_1 = (F_{x1}\ F_{y1}\ F_{z1}\ M_{x1}\ M_{y1}\ M_{z1})^T \quad \text{Eq. (4)}$$

and

$$F_2 = (F_{x2}\ F_{y2}\ F_{z2}\ M_{x2}\ M_{y2}\ M_{z2})^T \quad \text{Eq. (5)}$$

contain force and momentum on in- and output. The stiffness matrix is made up of both the input stiffness $[k_{1,1}]$, $[k_{2,2}]$ and the transfer stiffness $[k_{1,2}]$, $[k_{2,1}]$ matrixes.

Under realistic conditions the hot exhaust-gas flows through the decoupling elements and heats them up. Depending on the application and the engine concept the surfaces of the decouplers heat up to 100 to 550 °C [7]. A heating sleeve is used to create this temperature on the test object to simulate realistic conditions.

4 Results

To evaluate structure-borne noise damping the dynamic transfer stiffness is considered, defined as the ratio between the excited vibration displacement on the part input and the force at the part output [3]. **Figure 4** shows a comparison of the axial transfer stiffness on different connection elements. The rigid connection is a 300 mm long exhaust-gas tube with a diameter of 50 mm and a wall thickness of 1.5 mm. The structure-borne noise decoupling element is a 21 mm long corrugated metal part and the flex element has a nominal length of 142 mm and an inside diameter of 50 mm. The construction is comparable to that of a corrugated tube element with outside wire braiding. Below 2 kHz the transfer stiffness on both decoupling elements is lower by a power of ten as compared to

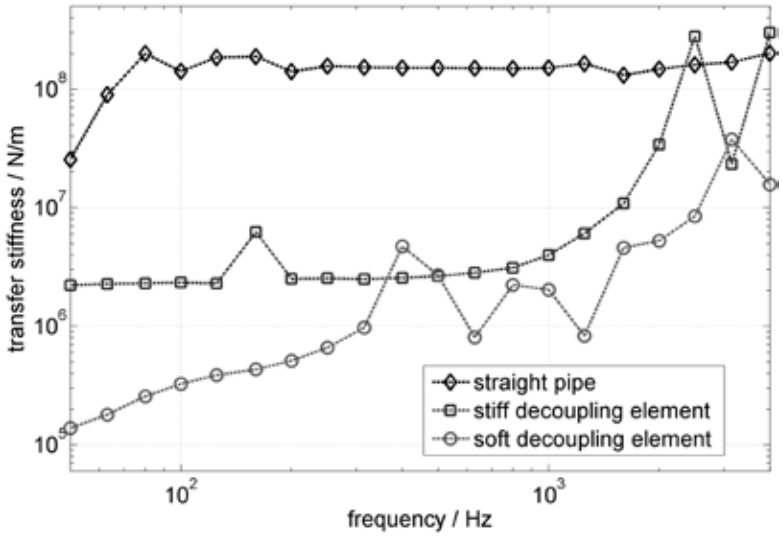

Figure 4: Comparison of transfer properties – axial transfer stiffness of different connection elements

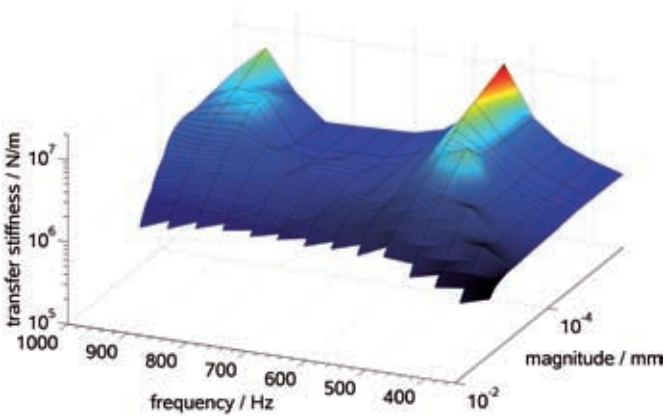

Figure 5: Transfer stiffness relative to frequency and magnitude

the rigid connection. Due to standing waves both the structure-borne noise decoupling element and the flex element become stiffer as frequencies increase.

The transfer properties on the flexible element show a non-linear behavior. There is a correlation between the transfer stiffness and both the excited frequency and excited vibration displacement. **Figure 5** depicts the transfer stiffness as a function of excited frequency and actual value of the vibrating displacement, based on a harmonic excitation. Flex elements do have a progressive stiffness characteristic, but due to the fact that testing takes place under pre-stressing the transfer stiffness decreases as the vibrating displacement increases. Under realistic conditions the effect of the amplitude decreases as the frequency increases, so that only the frequency-dependence of the transfer stiffness is notable above 1 kHz.

The length of the decoupling element represents a significant entity in the floor unit. **Figure 6** depicts the axial transfer stiffness of three different, identically constructed corrugated tube elements with a varying number of corrugations and consequently a different overall length. It turns out that the shortest element has the highest stiffness across most of the frequency range. But testing also showed that in regards to structure-borne noise damping it makes no sense to randomly extend the length of the element. Said length of the element should be such that no critical resonances are created in connection with the exhaust system that means the transfer stiffness should ideally be at a minimum in these areas.

Figure 7 compares the transfer stiffness of an unheated new corrugated tube to the transfer stiffness at a surface temperature of 600 °C. At a frequency range below 1 kHz the stiffness significantly increases in heated condition as compared to the stiffness at ambient temperature. However, no significant differences in part temperature are notable at frequencies above 1 kHz. The increase in transfer stiffness persists after the part has cooled down. At frequencies higher than 1 kHz identical behavior of the transfer stiffness can be observed after mechanical and thermal conditioning.

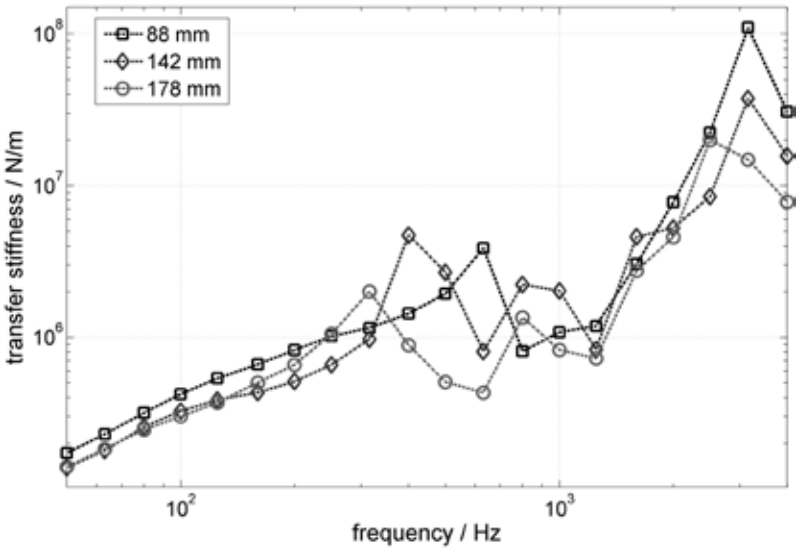

Figure 6: Impact of the flex element length

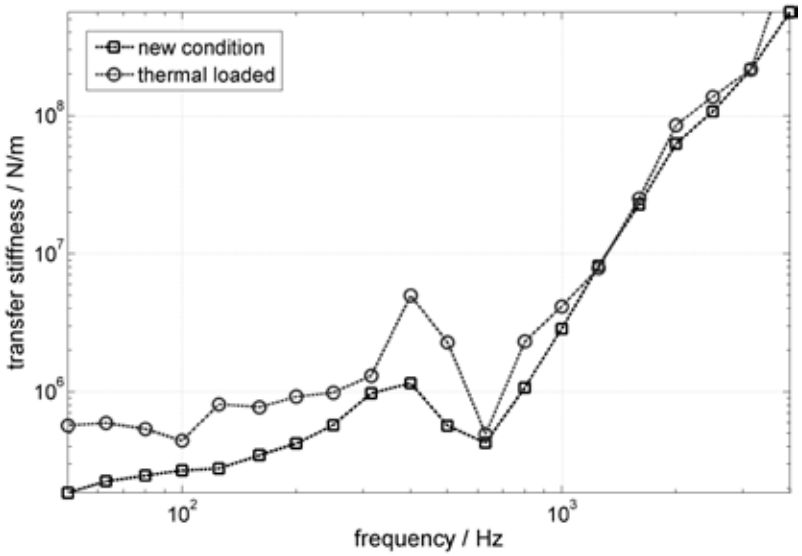

Figure 7: Thermal effects on transfer stiffness

5 Description of the Turbocharger as a Source of Structure-borne Noise

An experimental method is created to describe the exhaust-gas turbocharger as a source of structure-borne noise. It enables the identification of critical excitations and the consideration of problematic vibrations during the conceptual phase. Furthermore, it allows the implementation or selection of suitable decoupling parts during the early phase of development, before the exhaust system even exists.

The source description is based on the electrical engineering based power source modeling concept, also called the Thévenin equivalent. Mechanically applied, the sources of the structure-borne noise, combustion engine and exhaust-gas turbocharger, are modeled as an ideal power source with internal resistance. The model parameters are determined by inducing various mechanical impedances into the vibrating source. These terminating impedances primarily act like rigid masses across the entire relevant frequency range.

On the surface of these terminating impedances, accelerations are measured in all three spatial directions and split into their spectra via FFT, thus enabling a description of the frequency-dependent power excitation in all spatial directions. Several acceleration sensors are positioned to separate the translation and rotation accelerations. **Figure 8** shows on the left an equivalent circuit diagram of the structure-borne noise source, consisting of power source F_q and internal resistance Z_q with the load impedance Z_L applied. The source impedance consists of masses and linear-visco-elastic elements in good approximation. The respective operating point is the intersection of the source and load characteristic lines, as shown in Figure 8 on the right. Entities F and v depict the excitation force and velocity at the point of force application.

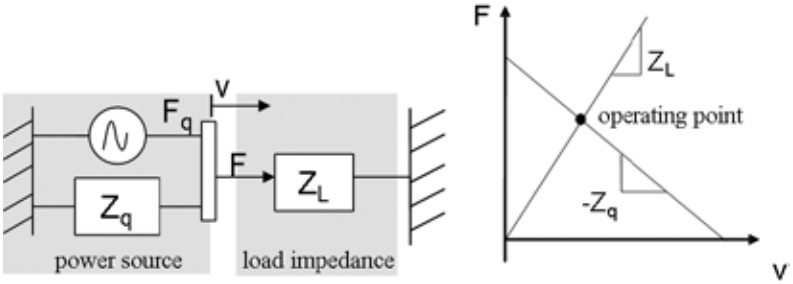

Figure 8: Equivalent circuit (left) and operating point (right) after the Thévenin equivalent

6 Integration in Existing Calculation Models

One of the main objectives of the test procedure introduced here is the integration of the decoupling element transfer characteristics and the turbocharger excitation spectra into the in-house CAE-process, to enable the calculation of the surface radiated noise on exhaust systems. The company Tenneco – Heinrich Gillet GmbH has been developing and using calculation processes that enable us to predict the surface radiated noise on exhaust systems and to optimize the surfaces for a number of years – see [4] and [5]. A missing link in this simulation process was the previously unknown mechanical transfer characteristics on decoupling elements within the acoustically relevant frequency ranges as well as the unknown excitation levels for the structure-borne noise phenomenon created by the exhaust-gas turbocharger.

The integration of measured results into this calculation process makes it possible to depict the entire exhaust system as part of the acoustic simulation process, thus enabling better and more precise predictions regarding the radiation of surface radiated noise. Furthermore, the acoustic transfer behavior of a decoupling element as part of the overall system can already be considered during the conceptual phase and be integrated into the selection process as an additional parts characteristic.

7 Alternate Structure-borne Noise Decoupling Concepts

Acoustic problems due to surface radiated noise are often discovered very late in the development phase of an exhaust system. At this time the hanger points on the exhaust systems are already defined and it takes extensive development efforts to integrate a decoupling element with increased flexibility into the ex-

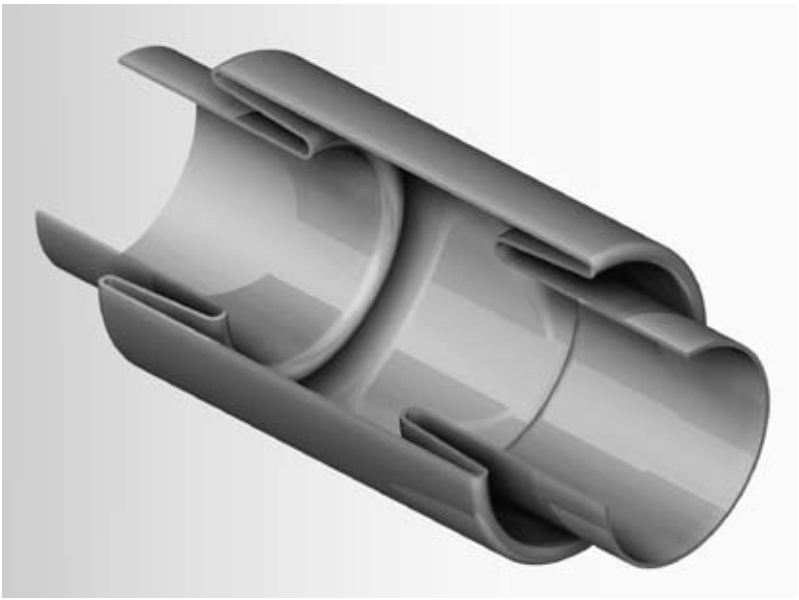

Figure 9: Section view of the double S-Shape decoupler, patent application filed

haust line. Extensive validation efforts are required to ensure the durability of the system. Therefore, it was a primary objective to develop an alternate part with as much stiffness as possible for integration into the exhaust system, requiring as few validation efforts as possible. It was also a base requirement that the part has a sufficient acoustic decoupling effect at frequencies of 500 Hz to 5 kHz and complies with the required fatigue limit specifications.

In the past acoustic problems were often solved by adding additional weight and vibration dampers. But solutions requiring an increase in weight and material efforts are no longer feasible today. The part developed by Tenneco – Heinrich Gillet GmbH and the University of Kaiserslautern is a compromise between maximum stiffness and acoustic decoupling at nearly the same weight and installation space as an exhaust tube. **Figure 9** shows a section view of a decoupling element with a double S-Shape. Since the part is a supporting part, no additional hanger points are required inside the car body.

The principle of the double S-Shape decoupler for one is based on adding an impedance mismatch into the structure of the exhaust line, causing incoming structure-borne noise waves to be reflected and secondly on the flexible geometry introduced into the structure of the exhaust line, thus causing a targeted change in the resonant behavior of the exhaust line. A parametric study examined the influence of the geometric parameters of the S-Shape on the part behavior, enabling an adaptation of the part to the respective application requirements.

8 Summary

An innovative test bench to examine the transfer behavior of flexible decoupling elements under varying conditions up to frequencies of 5 kHz is introduced by Tenneco – Heinrich Gillet GmbH in cooperation with the Acoustic Work Group at the University of Kaiserslautern. The calculation models of the transfer functions for decoupling elements and turbochargers are integrable into the CAE processes.

Furthermore, a procedure is described that characterizes the exhaust-gas turbocharger as a source for structure-borne noise and enables the detection of potential structure-borne noise problems in an early development phase. Finally, an alternate part called double S-Shape decoupler is introduced to passively prevent the dispersion of structure-borne noise inside the exhaust system, thus improving the NVH behavior on the overall vehicle without requiring significantly more space than a straight exhaust tube and without increasing the overall weight of the exhaust system.

References

[1] Brand, J.-F.; Fallen, M.; Kammer, H.-J.: Future Technologies against Turbocharger Noise Transferred to Exhaust Systems. SAE Paper, 2008-01-0891, USA, 2008

[2] Kammer, H.-J.; Fallen, M.; Brand, J.-F.: Übertragungsverhalten von Flex-Elementen in Abgasanlagen bei Frequenzen bis 5000 Hz. Proceeding, DAGA, Dresden, 2008

[3] Kammer, H.-J.; Fallen, M.; Pfeffer, T.; Brand, J.-F.: Experimentelle Ermittlung des akustischen Übertragungsverhaltens von Entkoppelelementen in Kfz-Abgasanlagen. VDI-Tagungsband 2052, Maschinenakustik, Böblingen, 2008

[4] Brand, J.-F.: Oberflächenschallabstrahlung von Abgasanlagen bei Straßenfahrzeugen. Fortschritt-Berichte VDI, Reihe 12, Nr. 648

[5] Garcia, P.; Wiemeler, D.; Brand, J.-F.: Oberflächenschallabstrahlung von Abgasanlagen – CAE-Methode und Entwicklungsprozess. In: MTZ 67 (2006), Nr. 11, S. 852-859

[6] Burkhardt, C.; Rösler, R.; Seeger, B.; Börner, F.; Herrmann, G.: Feldanalyse und Korrosionssimulation zur Werkstoffauswahl bei Entkoppelelementen. In: ATZ 110 (2008), Nr. 1, S. 54-61

The Mercedes-Benz **Experimental Safety Vehicle ESF 2009**

Between 1970 and 1974, Daimler-Benz AG, as it was then known, contributed 24 test vehicles to the Experimental Safety Vehicle (ESV) program. The program developed numerous systems for improving passive and active safety, which can be found today in virtually all new passenger cars. In ESF 2009, Mercedes-Benz aims to demonstrate the potential of the new design concepts made feasible by today's technology. This will also include systems, which are still not possible to implement in series production so as to stimulate discussion of the necessary technological developments.

1 Introduction and Motivation

The vehicles presented at the first ESV conference, **Figure 1**, already showed that active and passive safety were topics, which should not be treated separately. This integrated safety approach, based on the technology of the day, offered glimpses of the type of improvements in vehicle safety that was to come. Today, most of the systems that were considered revolutionary at that time can be found in the series production vehicles of virtually every manufacturer. No further experimental safety vehicles have been built anywhere in the world, or presented at the ESV conference, since 1974.

In constructing a new experimental safety vehicle, the intention of Mercedes-Benz is to again promote discussion of the whole subject of vehicle safety.

The hope is to present feasible new solutions based on today's technologies and illustrate the potential they offer. Systems whose production breakpoint is not yet possible from a present-day perspective have been consciously included to elicit discussion of the basic requirements and technological advances that will be required.

2 Descriptions of the Main Topics

The scope of this paper does not permit a comprehensive exposition of the 30 topics from six different areas. Selected systems have therefore been presented in more detail as being representative for each of the topic areas. The following areas were included in the ESF 2009, grouped according to the integrated safety approach [1], i.e. ranging from accident prevention and protection for road users, to the measures that can be taken after an accident.

2.1 Systems to Increase Awareness

One area that offers considerable potential for reducing accident statistics is improved awareness of the traffic situation by the driver and other road users.

The "Spotlight" topic offers a solution for making other road users more visible and differentiating between them. This technology points directly to where the hazard lies among the surrounding traffic. The technical solution in the ESF 2009 gives an example of how one's own vehicle can be seen more easily by other road users, particularly from the side. This was achieved by using passive reflective measures.

Figure 1: The ESV 13 in 1972

The Authors

Ulrich Mellinghoff is Head of Mercedes-Benz Cars, Development Safety, NVH and Testing at Daimler AG in Stuttgart (Germany).

Prof. Dr. Thomas Breitling is Head of the Center for Active Safety, Vehicle Dynamics and Energy management at Daimler AG in Stuttgart (Germany).

Prof. Dr. Rodolfo Schöneburg is Head of the Center for Passive Safety, Durability and Vehicle Functions at Daimler AG in Stuttgart (Germany).

Hans-Georg Metzler is Head of the Center for Driver Assistance Systems and Chassis at Daimler AG in Stuttgart (Germany).

Both topics are discussed in detail below. The topic of Intelligent Night View for active night vision recognition and for accentuating the visibility of pedestrians and animals is also examined.

2.2 Vehicle Communication

Vehicle communication systems for accident prevention or rescue will make an important contribution on the way to achieving safer driving. Communication between vehicles offers crucial added value, especially in situations that could be adequately defused with the help of an early warning system, or where an existing autonomous vehicle sensor system, e.g. where visibility is restricted, cannot offer any added value. However, at this point, a single-manufacturer solution cannot help us achieve our goal. Instead, what is needed is a successful collaboration between a large number of manufacturers with the aim of developing uniform standards and a model for rapid market penetration of the technologies involved. For that reason, this important topic has also been included in the vehicle.

2.3 Driver Assistance Systems

Systems to prevent and reduce the severity of accidents represent an important basis for future developments to improve vehicle safety. Building on improved and extended vehicle sensing systems (radar and stereo cameras), new assistance functions will become possible that will help the driver, e.g. in critical situations at intersections.

The assistance systems in the ESF 2009 address the topics of improving longitudinal and lateral guidance, as well as general awareness:

- The blind spot assistance system can not only trigger a warning, but also help avoid a potential collision with a vehicle in the blind spot by braking individual wheels.
- The extended Lane Assistant also comprises an alarm level, and, if it recognizes the danger of a critical departure from the lane, intervenes by applying independent wheel braking to correct the steering course. At a later stage of development, corrective steering intervention can also occur if objects with which the vehicle is likely to collide are identified.
- Traffic sign assistance system to display the currently applicable speed limit.

2.4 Virtual Protection Zone

Several manufacturers have recently introduced systems to help the driver in situations with a high risk of rear-end collisions. With its introduction of the Pre-Safe brake in 2006, and the enhanced version with an emergency braking function in 2009, Mercedes-Benz has brought to the market the final stage of development for the present of a system designed to reduce the risks posed by tailbacks. The Pre-Safe brake system combines acoustic and visual warnings, adaptive brake assistance, and autonomous partial and emergency braking to offer an all-round package that helps to avoid an accident, or to reduce kinetic energy before a possible collision. Preventive occupant protection functions are also activated. Using the phase immediately prior to a collision to provide occupant protection can have the effect of further significantly reducing the consequences of an accident for those involved. This effectively extends passive safety, the so-called „New Passive Safety“ [2] to the moments immediately before the accident. The braking bag in the ESF 2009 represents a further development stage. This will be explained in more detail in a later section.

2.5 Initial Impetus / Innovative Occupant Protection Systems

To date, the development of occupant protection systems has focused on extending the protective space, and on adaptability. Extended fitting of airbags down into the subcompact range, and refinement of the seatbelt with automatic tightening and force limiter have greatly reduced the forces to which occupants are subjected in accident situations. Over the last few years, however, we have witnessed an asymptotic trend in the reduction of forces under the specified load conditions. If we consider conventional restraint systems, even experts believe that the possibilities for further development in the future are slim.

Nevertheless, if we consider the pre-accident phase, links can be created between reversible and conventional occupant protection systems that, in combination, open up further possibilities. One example of this is the initial impetus Pre-Pulse occupant side protection system, which will be presented in a later section.

A further area where occupant protection can be improved is in the rear seat row, which has different requirements from the front seat row. On the one hand, children are often transported in this area, so that occupant protection systems must meet the requirements for this occupant group. Similarly, the requirements for a chauffeur limousine, as in the present luxury vehicle segment, are quite different as regards occupant protection. The solutions presented for child safety and the belt bag should prove enhancements to the range of protective equipment, and will be described in more detail as part of the vehicle presentation.

On the question of resolving the conflicting objectives of structural safety, body rigidity and lightweight construction, the topic “Pre-Safe-Structure” in the ESF 2009 will be addressed and presented separately in a later section.

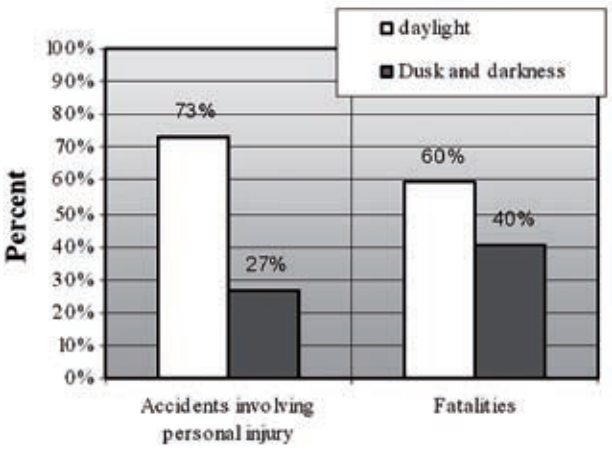

Figure 2: Frequency of accidents in different light conditions in Germany in 2007

3 Technical Descriptions of Selected Systems

3.1 Side Reflect – Improvement in Side Visibility at Night

Dusk and darkness pose an enormous risk potential. Over one quarter of all accidents occur under these lighting conditions. Additionally, the severity of injuries increases during these times. Some 40 % of accidents involving fatalities occur at night [3], **Figure 2**.

The (active) lighting techniques have been steadily improved over the last few years. However, there are still many situations presenting an increased risk potential, such as an unlit vehicle that has been left at the side of a country road, or vehicles crossing an intersection without warning.

The objective of Side Reflect is to enhance the side visibility of the vehicle in order to reduce this accident risk at night. The lateral reflective properties are enhanced, **Figure 3**. One element consisted of reflective strips on the tires (as has been standard on cycle tires for a number of years).

An additional component that was presented by way of example in the ESF 2009 was door seals with reflective properties. Here, the external area of the door seal rubber was coated with a special film that integrates seamlessly into the vehicle design. These reflective door seals emphasize the vehicle contour for enhanced nighttime visibility.

3.2 LED Pixel Headlamps for Hazard Light

Night vision systems are a great help for drivers. With night view assist, an „electronic main beam“ allows drivers to still see their own lane and the right-hand side of the road without the risk of being dazzled even if there is oncoming traffic. Advances in camera technology and image processing now allow systems to recognize potential dangers on and immediately adjacent to the roadway.

These can be specially highlighted on a suitable display to warn drivers. The preferred solution would be for drivers to receive an alert about a potential hazard directly in the traffic area, without wasting time looking at a display. This function will be referred to as “Spotlight” below.

Figure 3: Improvements to lateral visibility through side reflect

The ESF 2009 demonstrates a fixed headlamp with electronically controllable light distribution since the spotlight function, **Figure 4**, needs to react within fractions of a second. There are essentially two ways of designing non-mechanical systems: one is to use a video projector [4] or similar; the other uses electronically addressable LED arrays [5]. The second variant has been implemented in the ESF 2009. An array of this kind basically consists of a number of individual LED chips arranged in rows and columns. Approximately 40 to 100 LED pixels are needed to create a vehicle headlamp (depending on the desired resolution and the maximum area to be illuminated). The ESF 2009 has 96 pixels arranged in four rows, with a different number of pixels per row. Each of the 96 pixels can be dimmed in 256 steps, and can be switched on within a few milliseconds.

As well as the “Spotlight,” it is possible to use this LED array to implement adaptive light functions, such as active curve illumination and partial high beam. As well as image analysis, a variety of options for alerting the driver was tested in the ESV, none of which should dazzle other road users. Pedestrians could, for example, be illuminated up to waistline height; projecting a „light pointer“ onto the road surface was another possible solution.

While most of the technical problems have been solved, further study is still needed here, together with amendments to the legal provisions.

3.3 Virtual Protection Zone Braking Bag

The current E-Class model year 2009 features the last development stage for the time being of an automatic emergency brake system. The emergency braking

Figure 4: The spotlight function

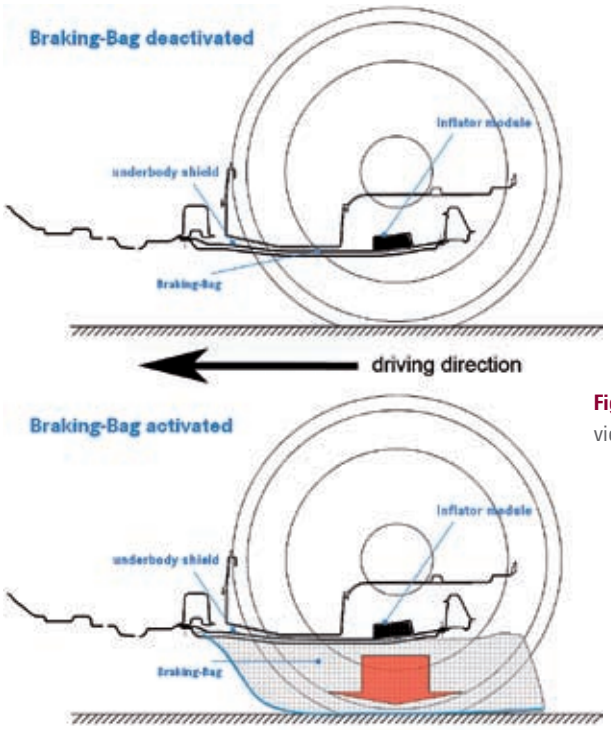

Figure 5: Cut-away view of the braking bag

function, already implemented by Mercedes-Benz in series production vehicles in the event of unavoidable collisions in thickening tailback traffic, reduces the subsequent collision speed by approximately an additional 6 to 8 km/h. Approximately 0.6 s before the collision the function imposes emergency braking on the already partially braked vehicle. A further escalation stage is needed to raise the deceleration energy above that of the wheel brake since the vehicle has already been decelerated to the slippage limit.

In this context, Mercedes-Benz has developed the concept of the braking bags. An airbag containing a driver's airbag gas generator was added to the front underbody paneling of a standard S-Class vehicle. This paneling has a double-wall design, so that the airbag can be installed spread out between both body panels. Once activated, the airbag expands, supporting itself on the top side of the front integral support member, **Figure 5**. The underside is fitted with a friction lining designed to achieve optimum deceleration. It is mounted in front on the vehicle cross member, so as to transfer the frictional forces generated by bracing the vehicle on the roadway.

If the braking bag is activated as the vehicle in front is approached ever more closely, i.e. approximately 2.6 s before the moment of collision after an initial warning has been issued, approximately 1.6 s before the moment of collision after partial braking has been initiated, and at approximately 0.6 s before the collision after emergency braking has been initiated, then the result is a rapid and temporary increase in deceleration lasting approximately 75 to 100ms, with a deceleration rate of 20 m/s², **Figure 6**.

The increase in deceleration is primarily influenced by an elevation in the center of gravity of the vehicle as it performs the emergency braking maneuver. When the airbag expands, it momentarily raises the vehicle by approximately 80 mm. During this brief period, the thrust exerted on the friction lining of the braking bag is increased by the factor of the mass acceleration and the overall vehicle mass.

This increased thrust leads to a briefly increased rate of deceleration, **Figure 7**, than can be generated with a normal wheel brake. In this context, it is important that the precise collision point is predicted as exactly as possible, since the process is reversed after a certain period, leading to a load reduction that has a negative impact on the deceleration force.

The following effects can also be observed. As a result of the vehicle's upward movement, brake dive movement is further compensated for, thus improving the geometric compatibility of the braking vehicle. The deformation structures adjust to the original design configuration.

Also observed, as a consequence of the vehicle being raised, was the adjustment of the seat structure to the inert mass of the occupants. The distance measured in tests was approximately 20 mm, which means that the compression of the elastic seat foam and the convergence between the seat ramp and the

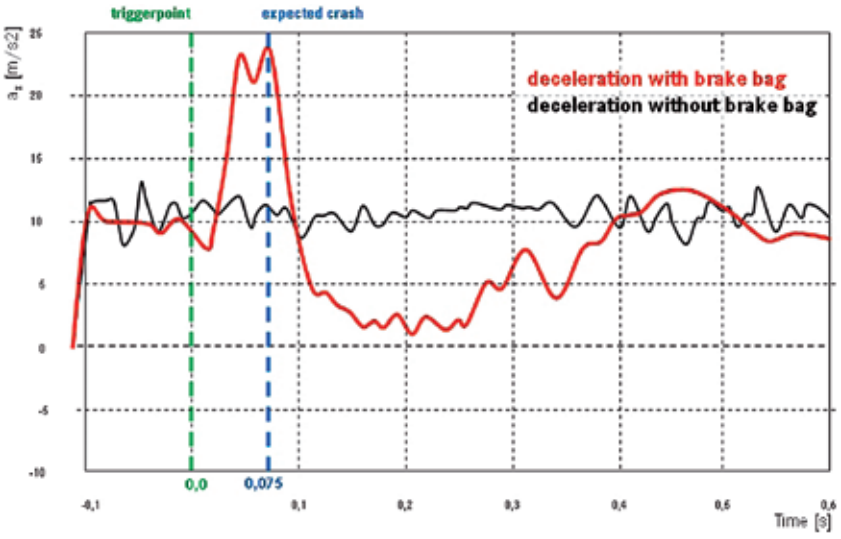

Figure 6: Deceleration pattern after initiation of the braking bag

bodies of the occupants result in improved contact between them in the subsequent crash.

This applies in equal measure to with the contact between the occupant and the already tensioned seatbelt in the Pre-Safe phase. In the moments preceding the accident, the occupant is held in position by a reversible tensioning, in preparation for the subsequent emergency braking.

The emergency braking then generates an increase to approximately 400 to 600 N on the belt through the inertia force imparted. The deceleration caused by the braking bag of approximately 20 m/s2 further enhances this seatbelt pretensioning to approximately 800 to 1,200 N, thus helping to optimize deceleration contact even before the pyrotechnic belt tensioner is triggered.

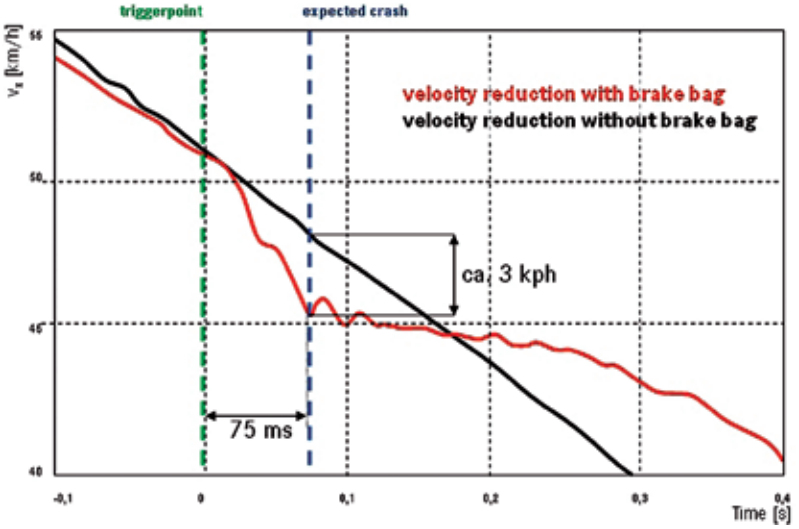

Figure 7: Reduction in speed after initiation of the braking bag

3.4 Initial Impetus Occupant Safety System

Standard restraint systems can be described as merely reactive occupant safety systems. For example, a build-up of force and the associated energy conversion within the belt system occurs only after the occupant has traveled the necessary distance after a specific period by being thrust forward in a frontal impact. However, at this point, valuable deformation space has been used only for the vehicle deceleration, but not to decelerate the occupants. The way the airbag operates is similar to the functioning of the belt described above. Only after sufficient internal pressure has developed from precompression of the bag does deceleration (or acceleration in the case of a side impact) occur, and thus to energy being brought to bear on the occupant.

The crucial lever for reducing the load values in a side impact is the distance between the occupant and the door. The greater this distance, the lower the speed at which the door accelerates the occupant through the occupant protection system. At the same time, this distance is limited by the possible vehicle size and the comfort dimensions. The contact speed of the intruding door is primarily influenced by measures adopted for the body shell and the door. Here, too, there are restrictions imposed by limits on vehicle weight and equipment packaging. Measures undertaken to date to increase side-impact protection have mainly been implemented in the vehicle itself, i.e. influencing the occupants has not been considered so far. An initial impetus occupant safety system, as presented in the ESF 2009, taking the example of a side impact, uses the early information on the unavoidable collision to bring some initial preparatory energy to bear on the occupant. The instant the accident occurs, these so-called Pre-Safe-Pulse systems accelerate the occupant in the direction taken by the impact energy, **Figure 8**, thus reducing the energy differential between the vehicle and the occupant at this early stage. The energy is not just brought to bear when an impact occurs, but instead the total energy is distributed between a smaller initial impact, and a reduced main impact.

This can be simply explained using the example of a side impact: in order to generate the pre-pulse effect on the occupant, the seat was fitted with the dynamic ride components of the multi-contour seat. This features air cushions in the "cheeks" of the driver and front seat passenger backrests, thus improving lateral support on bends by inflating.

The size and inflation characteristics of these cushions were modified so that they could propel the occupant towards the center of the vehicle by suddenly inflating. This process is reversible and can be repeated.

The movement towards the center of the vehicle increases the distance between the occupant and the door.

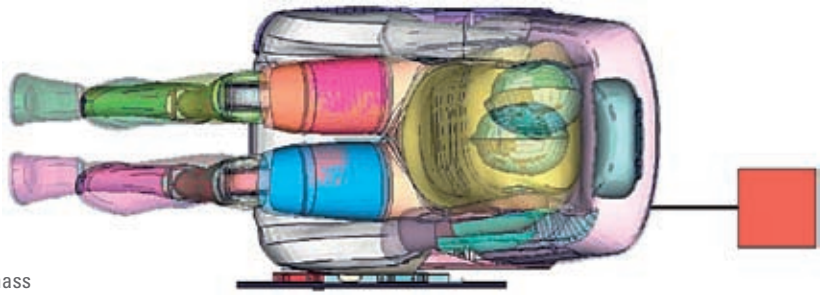

Figure 8: Deflection of the occupant's mass

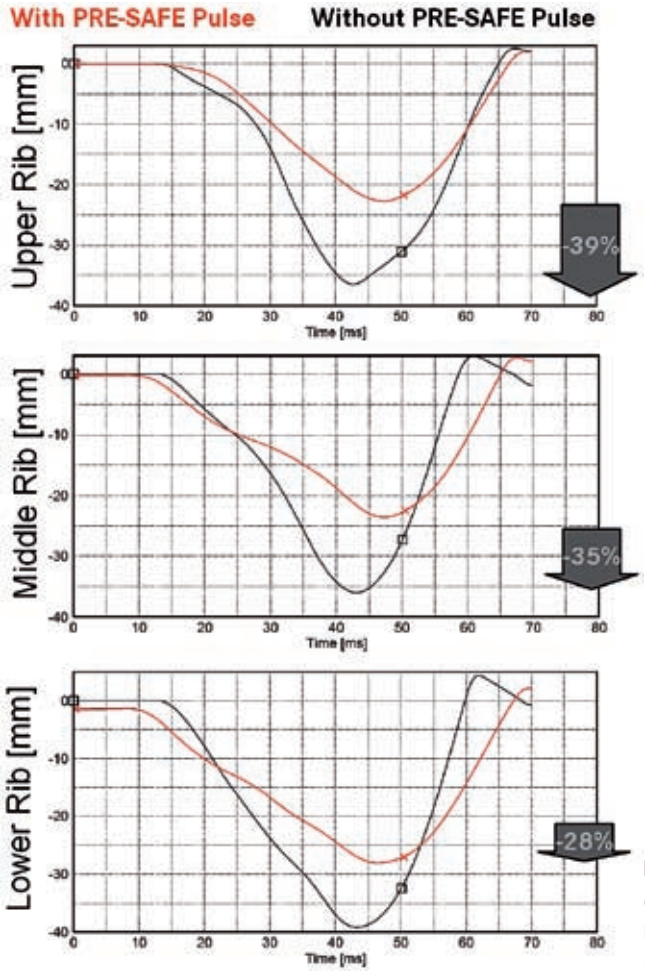

Figure 9: Rib deflection in the FMVSS 214 load case (new)

The side bag can now be safely deployed. The moment of contact between the door and the occupant held by the restraint system now occurs later, i.e. at a lower intrusion speed.

Additionally, the occupant is already moving at a certain velocity in the same direction as the impact, and this velocity no longer needs to be imparted through contact with the side bag and the door. Simulation tests showed an average 30 % reduction in rib intrusion, **Figure 9**.

3.5 Pre-safe-Structure

The crash properties of vehicle structures such as bodyshell and basic door components can be adapted to behave intelligently towards the imminent accident. Subjecting these structures instantaneously to high internal pressure is one possible approach which has been investigated as part of this concentrated research and development work.

The development approaches essentially emerge from two basic principles:

1. Changing the deformation properties through subjection to pressure while retaining the original component geometry. The maximum pressure level must, of course, be carefully tailored to the material, the joining technology and the original component geometry.
2. Changing the deformation properties by enlarging the component's cross section. When subjected to pressure, the cross section will increase instantaneously from a small, packaging-optimized cross section to a larger cross section with a considerably greater resistance to deformation, **Figure 10**.

Depending on the circumstances, either a brief application of pressure to produce the desired geometry change will be sufficient or pressure will need to be applied for longer to ensure that the required high internal pressure is maintained for the whole period during which the component is deformed.

Pressure application and deformation of the components ceases after approximately 10 ms to 20 ms. The changes to the vehicle as the crash unfolds generally occur within at most 100 ms. Dense structural components can maintain the pressure at a very constant level during this time.

Theoretical and experimental studies have been carried out on a variety of vehicle structures. Components have been evaluated under both axial as well as torsional stresses.

In the case of longitudinal member structures, it was demonstrated that the force level could be raised by 20 kN to 40 kN and that the length of time over which the crash unfolded in the vehicle could theoretically be shortened by 10 mm to 100 mm.

The design for the crash-active door impact member envisaged meeting the FMVSS214 structural requirements without the member being activated; **Figure 11**.

During in-crash activation, the average force level varied, depending on the position of the gas generator, between 7.5 kN and 12 kN. Compared with the standard components, a weight reduction of approximately 500 g per component was demonstrated.

By a carefully timed pre-initiation of the door components it is possible to further increase the average force level by up to 50 %.

Crash-active structures in the lateral vehicle structure offer the same high safety level as series production components at a reduced structure weight. In addition, depending on the component geometry, simulation testing provided evidence of considerably reduced intrusion velocities.

Figure 10: Average height increase of a side impact member

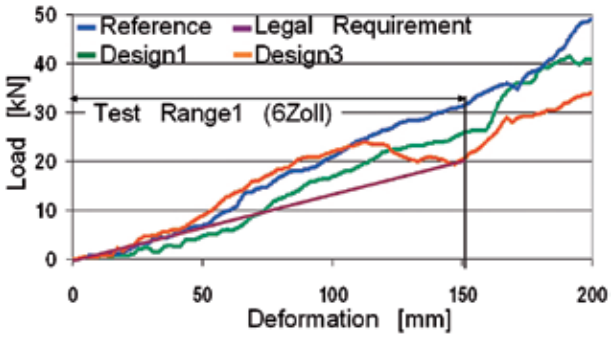

Figure 11: FMVSS214 pole crash

4 Summary

The purpose of the ESF 2009 is to illustrate new approaches aimed at improving vehicle safety. Some new, as yet unpublished approaches were selected for this. A solid foundation comes from using information on the traffic environment that is as precise and reliable as possible. Recording information using sensor beams and the networking of vehicles with the help of new communication technologies should yield further support measures in the future that will help avoid or reduce the severity of accidents.

Further milestones on the way to our vision of accident-free driving will be achieved by using innovative light technologies to ensure awareness of other road users, and also by improving the discernibility of the vehicle itself, particularly from the side.

Along the way, exploiting information about an imminent, unavoidable collision offers further potential for the safety of vehicle occupants and other road users. An important component in this area is the use of the initial impetus mechanism to distribute the collision energy over several impulses.

Further studies into the area between the occupants to protect them from injuring each other and the adaptability of the size and absorption capacity of the airbag have not been discussed in this paper, but both play an important role in accident protection in the ESV.

Intelligent vehicle structures, which can adjust their rigidity and deformation properties to the crash as it occurs, offer long-term potential for optimizing structural solutions combined with notable packaging and weight benefits. Subjecting vehicle structures to internal pressure are a possible approach to a solution.

The ESF 2009 offers an in-depth look at current advance design projects relating to vehicle safety at Mercedes-Benz. To an extent, it therefore also represents a risk for the company. However, it is important that experts should have the chance to discuss important new, and, in certain cases, unconventional ways of improving safety, and then develop them systematically.

The features of the ESF 2009 are intended to provide just such an opportunity.

References

[1] Schöneburg R., Breitling T.: Enhancement of Active and Passive Safety by future Pre-Safe® Systems, 2005 ESV Conference, Washington DC Paper 05-0080

[2] Schöneburg R.: Die "Neue Passive Sicherheit" – Steigerung der Insassensicherheit durch Nutzung der Vorunfallphase (The „New Passive Safety" – Increasing occupant safety by exploiting the pre-accident phase), VDA – 11th technical congress, Wolfsburg, 2009

[3] www.destatis.de Federal Statistical Office, Germany

[4] M. Enders: Pixel Light, Proc. Int. Symposium on Progress in Automobile Lighting, Darmstadt 2001, pp. 234-239

[5] M. Griesinger, H. Hoffmann, M. Holz, J. Moisel, T. Schaal, E. Zeeb: Multifunctional Use of Semiconductor Based Car Lighting Systems: Potentials and Challenges, Proc. Int. Symposium on Automotive Lighting, Darmstadt 2005, pp. 73-81

The Centrifugal Pendulum-type Absorber

Application, Performance and Limits of Speed-adaptive Absorbers

Providing driving pleasure while reducing fuel consumption and CO_2 emissions means, on the one hand, combustion engines that generate high torque at low speeds and, on the other, transmission concepts with a large spread. For these developments to exploit their full potential, the comfort objectives at low speeds must also be achieved. In this case, the performance capability of torsional vibration dampers like dual mass flywheels plays an important role. As a speed-adaptive absorber, the centrifugal pendulum-type absorber developed by LuK is an ideal means of providing the isolation necessary in new drive systems.

1 Introduction

Further development of a drive train is limited by the subsystem with the lowest performance. This can be the internal combustion engine itself or any of the attached power-transmitting components. The limitation may be the result of lacking robustness or strength, or even failure to satisfy comfort criteria. In this regard, the importance of reducing the vibration caused by the rotational irregularity of the internal combustion engine has increased significantly over the past 20 years. Although relatively low engine torques meant that there were no major requirements in this area until the early 1990s, the situation changed dramatically with the introduction of new combustion methods in combination with turbocharging of diesel engines. As a result of these technologies, maximum possible specific engine torques have now been tripled. This evolutionary development would not have been possible without new vibration-reducing measures.

The dual mass flywheel (DMF) introduced by LuK in 1985 represented an effective long-term solution with exceptional characteristics for effective vibration reduction in the drive train, **Figure 1**. Systematic further development and intensive use of virtual simulation techniques has helped to compensate the ever more demanding requirements that have since arisen and thus achieve comfort objectives.

Pressure to reduce fuel consumption and CO_2 emissions has been growing for some years. Massive efforts to increase overall efficiency are giving rise to new engine and transmission concepts. In the case of the internal combustion engine, this means further increases in cylinder pressures (turbo-charging), a reduction in the number of cylinders and higher torques at ever lower speeds. All of these developments greatly increase the torsional vibrations introduced in the drive train.

The increase in cylinder pressures leads directly to an increase in excitation and, with identical engine displacement, to less isolation by the damper, since its torque capacity must be adjusted accordingly, **Figure 2**. With identical torque, a reduction in the number of cylinders leads both to greater irregularity and lower excitation frequency. With identical engine speed, the torsional vibration of the clutch shaft increases as a result. These effects are illustrated in the following example: If a three-cylinder engine provides the same maximum engine torque as a four-cylinder engine and the maximum torque is already available at 1400 instead of at 2000 rpm, the irregularity at the clutch shaft quadruples when the damper technology remains the same.

The overall situation regarding vibration reduction is aggravated further by the greater sensitivity of the drive train as a consequence of loss reduction and lightweight construction as well as higher customer expectations when purchasing a new car. Because of the reasons mentioned above, vibration-reducing damper systems represent an increasingly important key technology in modern engine concepts. Existing damper concepts are reaching their limits, thus necessitating the consideration of alternative operating principles to satisfy future requirements.

The Authors

Dipl.-Ing.
Matthias Zink
is Head of the Clutch Systems Division at LuK GmbH & Co. oHG in Bühl (Germany).

Dipl.-Ing.
Markus Hausner
is responsible for Overall Clutch System Development at LuK GmbH & Co. oHG in Bühl (Germany).

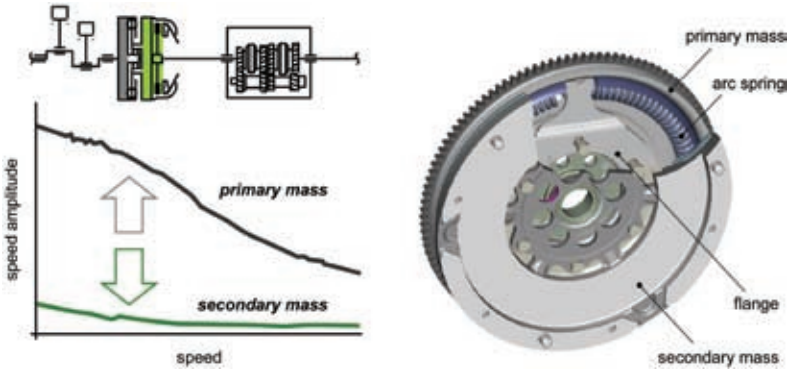

Figure 1: Dual mass flywheel – long-term solution to vibration isolation

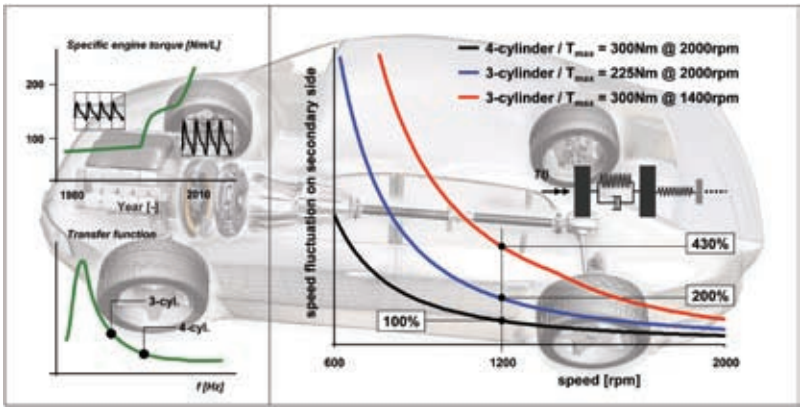

Figure 2: Increasing requirements for vibration reduction

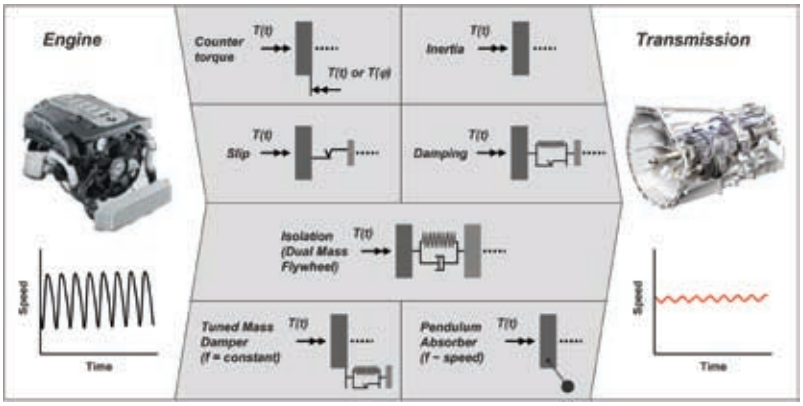

Figure 3: Possibilities for reducing vibration (symbolic)

2 Physical Principles for Vibration Reduction – Potential and Limits

There are a number of possible physical principles for combating interfering vibrations. With regard to physical effects, a satisfactory result can theoretically be achieved with any number of approaches. The potential and limits are the result of criteria such as constructive implementation, installation space, additional weight and costs, **Figure 3**.

The conventional combination of a single mass flywheel and torsion-damped clutch disc, for example, reaches its limits relatively quickly, due to the potential inertia and damping capacity. Nevertheless, this option still has enough potential for the low and medium torque ranges.

In conjunction with slip, almost perfect isolation could be achieved, but there are significant additional costs associated with the manual transmission as a result of the required controllers and actuators. Moreover, such a system must usually be combined with a DMF, as the required slip speeds would otherwise lead to greater fuel consumption and wear. Systems for generating an opposing torque to the oscillating torque of the internal combustion engine always require a controller and actuator unit to adjust the amplitude and phasing.

LuK considers the speed-adaptive absorber to be a lasting solution for further vibration reduction and has been investigating and developing it actively for some time. The world's first system has been used successfully with a production six-cylinder engine since mid-2008.

The tried-and-tested DMF continues to be used as the basis, since its isolating characteristics significantly reduce amplitudes on the secondary side. The speed-adaptive absorber now operates on the secondary side and must only reduce the residual irregularity. Compared to use on the primary side or in combination with a single mass flywheel, this arrangement offers significant benefits in terms of masses and space required. Because of the already significantly reduced vibration on the secondary side of a dual mass flywheel, outstanding results can be achieved with relatively low absorber masses.

3 Speed-adaptive Absorber

The speed-adaptive absorber operates on the principle of a mathematical pendulum (thread pendulum). For small deflections, the natural frequency for a given gravitational acceleration is determined only by the length of the thread and is independent of other variables such as the moving mass, **Figure 4**.

In the centrifugal pendulum-type absorber, gravitational force is replaced by centrifugal force. The centrifugal force itself is proportional to the angular velocity squared, as a result of which the natural frequency of the pendulum is ultimately proportional to the speed. The desired absorber arrangement is now defined by the length ratio R/L. The ignition frequency of a four-stroke four-cylinder engine, for example, results in a length ratio R/L of 4. For the opposing torque of the absorber follows: $M = -mdR\Omega^2\sin\varphi$.

Theoretically, such an absorber can completely eliminate the main excitation order; with suitably large pendulum masses, this can virtually be put into practice. However, in the case if realistically achievable pendulum masses, the effectiveness of the absorber is limited by the vibration angle of the pendulum. Furthermore, tolerances and variations during construction must be taken into account to avoid entering the excitation range of the absorber during operation. The challenge is to approach the limits of the ideal absorber as closely as possible, while also ensuring reliable operation under all conditions. To achieve optimum utilization of the limited vibration angle available, the path of the pendulum can be corrected. With a classic pendulum – a thread pendulum for instance – the mass moves along a circular path and the absorbing action decreases as the vibration angle increases. By deviating from the circular path, the performance of the centrifugal pendulum-type absorber can be increased significantly.

Established simulation methods with high levels of predictive accuracy are necessary to exhaust the full potential of the absorber in all aspects, such as operational reliability, inherent noise and ab-

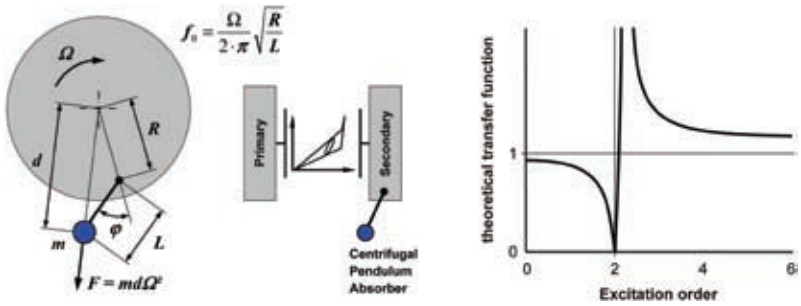

Figure 4: Physical principle of a centrifugal pendulum-type absorber

sorbing capability. For this purpose, LuK employs special simulation tools that have been developed in-house and used successfully for years in the development and design of absorbers. In the case of the centrifugal pendulum-type absorber, optimum utilization of the installation space is achieved with the aid of simulation techniques. The paths are designed in such a way as to maximize the achievement of comfort and strength objectives at all operating points and under all operating conditions. In this case, driving at varying engine speeds (for example accelerating under full load), along with related evaluation criteria such as rattling and humming, certainly represent the most important driving situation. However, all other operating points such as start/stop, idling and start-up are also investigated and evaluated. With regard to strength and evaluating the possible striking of the pendulum mass, driving from low speeds all the way up to resonance frequency is of central importance. This is also reproduced using simulation techniques and taken into systematic consideration when designing the centrifugal pendulum-type absorber.

By way of example, **Figure 5** shows a simulation model for the operating point „drive" along with the simulation results obtained. Despite highly developed simulation techniques, measurements cannot be dispensed with entirely. The basic models must be compared with vehicle measurements (left in Figure 5) in order to obtain sufficiently accurate results in subsequent virtual investigations and variations. In the example (centre of Figure 5), the isolation properties are investigated according to the order of alignment. In this case, the evaluation criteria are isolation and vibration angle reserve. Selected variants are also investigated with regard to misuse (right in Figure 5) to ensure adequate durability.

Figure 6 shows the design of a dual mass flywheel with a centrifugal pendulum-type absorber. The pendulum masses are attached to both sides of the flange, which is riveted to the secondary side. In this example, four pendulum masses with a total weight of about 1 kg are attached. Two tracks each are machined into the flange and pendulum masses. Rollers allowing the pendulum to oscillate opposite the flange are located between the pendulum- and flange-side tracks.

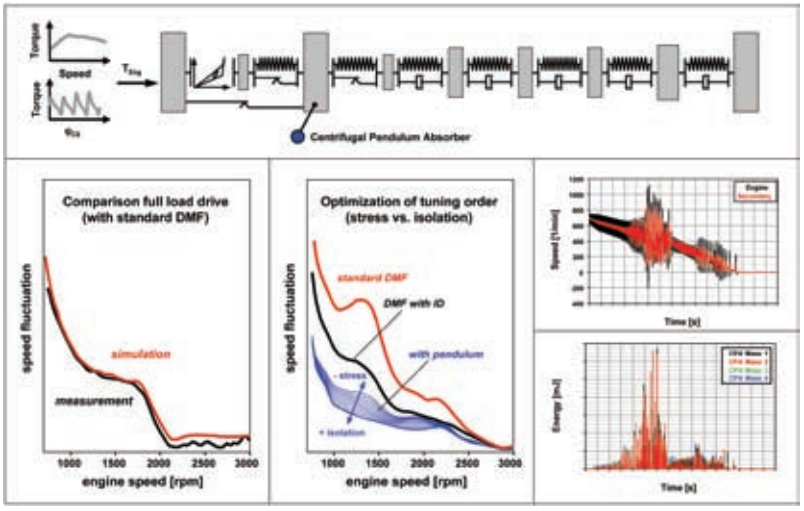

Figure 5: Simulation technique for designing and optimizing the centrifugal pendulum-type absorber

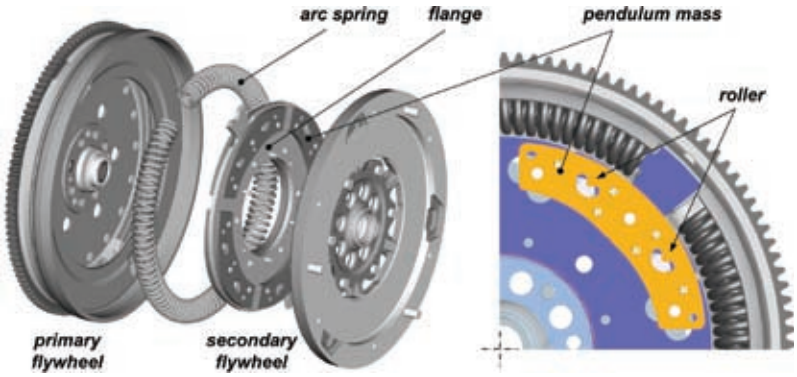

Figure 6: Design of a DMF with a centrifugal pendulum-type absorber

This arrangement is called bifilar suspension, since in contrast to a thread pendulum (monofilar) two attachment points are provided. In normal operation, the motion of the individual pendulum masses is synchronized. To prevent the pendulum masses from striking one another when starting and stopping the engine, this is taken into consideration during the design.

4 Variants and Areas of Application

The basic variant consists of a dual mass flywheel without an inner damper. As already depicted in Figure 6, the pendulum masses are located on the flange below the arc springs. This enables a construction requiring no extra space. However, the additional integration of an inner damper is not possible. Nevertheless, this variant already offers significant benefits over the standard DMF with inner damper. Only at higher speeds (>3000 rpm), do the pendulum masses lose their effectiveness due to friction. Isolation is then comparable to that provided by a DMF without a centrifugal pendulum-type absorber.

If the additional benefits of an inner damper are required, there would be no space on the flange for the pendulum masses. However, a centrifugal pendulum-type absorber can still be added to such a dual mass flywheel. There are basically two ways of accomplishing this. In the first approach, the pendulum masses are arranged next to the arc springs at a greater radial distance. In this case, the DMF has a greater axial length than the basic version. However, because of the larger radius, the same absorbing action can be achieved with a smaller total pendulum mass. This arrangement provides

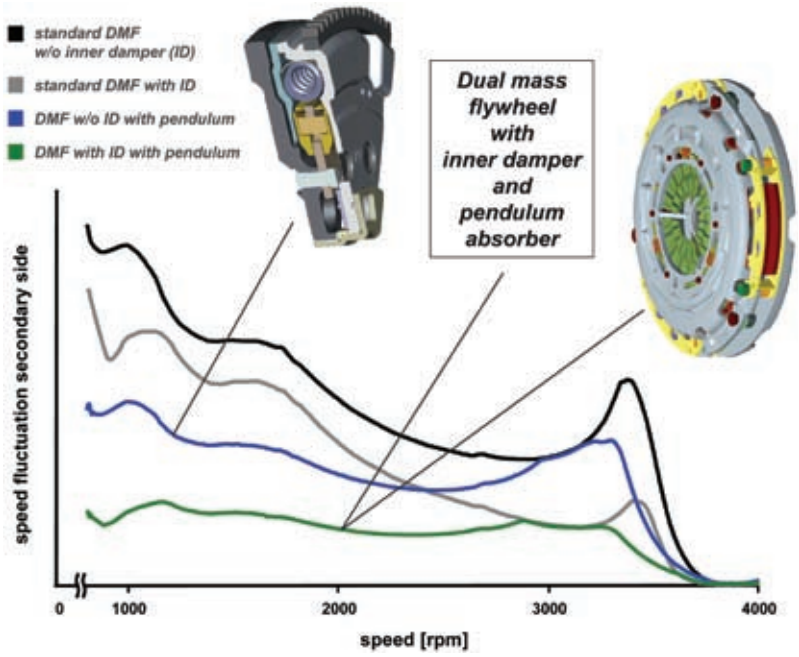

Figure 7: Design variants of centrifugal pendulum-type absorbers

significantly more isolation than a standard DMF with an inner damper. In the lower speed range, the vibration amplitudes on the secondary side can be reduced by up to 60 %, yielding new standards in terms of noise levels.

A further approach involves placement on the cover of the clutch pressure plate. The potential is comparable to that of the DMF variant with pendulum masses arranged next to the arc springs, **Figure 7**. The benefit is a more favourable installation space for the clutch/damper unit.

Regardless of the arrangement variant selected, the damping system must always be designed as a complete package. Only in this way is it possible to ensure that the centrifugal pendulum-type absorber functions properly at all operating points and achieves a long service life with excellent reliability.

In the above, the discussion focused primarily on the centrifugal pendulum-type absorbers in combination with a manual transmission. The reason for this is that development was initially pursued for manual transmissions and commercialized for an application with the most demanding requirements. However, the principle of the centrifugal pendulum-type absorber can also be employed with all other transmission concepts.

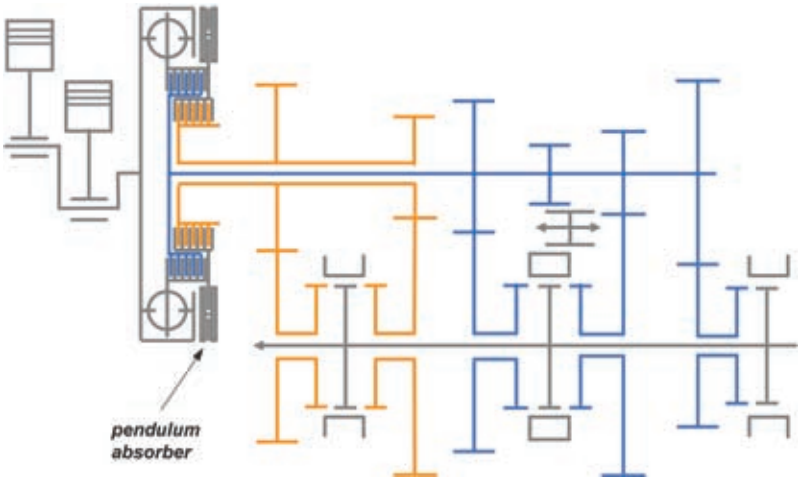

Figure 8: Centrifugal pendulum-type absorber for a wet dual clutch transmission (schematic)

In the case of the forward-looking dual clutch transmissions, requirements with regard to permissible vibration amplitudes at the transmission input are even more challenging than those posed by a manual transmission, for several reasons. Based on the operating principle, the sensitivity to torsional vibrations is higher, since one half of the transmission is not involved in the power flow. Dual clutch transmissions already have up to seven gears as well as a high spread, so that the gear providing optimum fuel consumption can always be selected automatically. To exploit this potential fully, the objective is to drive at low engine speeds. However, a prerequisite for this is that the comfort criteria are satisfied, specifically in this lower speed range, which is particularly susceptible to vibration impulses. As a result, potential reductions in fuel consumption are determined largely by the damper system employed and its performance. Overall, a centrifugal pendulum-type absorber provides ideal prerequisites for optimizing fuel consumption and thus CO_2 emissions.

In dual clutch transmissions, there are two different types of clutch systems: wet or dry. A centrifugal pendulum-type absorber can be designed for both variants. In a dry system, the secondary mass needed for a DMF is already present in the form of the dual clutch unit to which a pendulum can be added. In contrast, the clutches in a wet system have a low moment of inertia, **Figure 8**. To achieve the functionality of a DMF, an additional mass must be incorporated. The use of a centrifugal pendulum-type absorber can significantly reduce the additional moment of inertia while achieving the same isolation; this reduces the required installation space and fuel consumption, while also improves driving dynamics.

With today's converter systems, high-torque operation at a low speed is possible only with the lock-up clutch open or in slip mode. However, this reduces efficiency and makes the objectives of reduced fuel consumption and CO_2 emis-

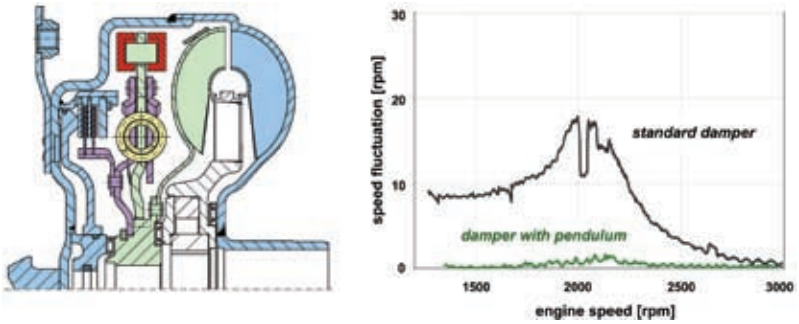

Figure 9: Centrifugal pendulum-type absorber for a torque converter

sions harder to achieve. Therefore, the full potential of new engine technologies can only be exploited with better damping concepts. In this regard, the centrifugal pendulum-type absorber also provides forward-looking potential. In contrast to manual and dual clutch transmissions, the centrifugal clutch operates in an oil bath when used with a converter, resulting in special criteria with regard to pendulum alignment. The centrifugal pendulum-type absorber is placed on the turbine side. When the lock-up clutch is closed, a damping spring system provides basic isolation. The residual irregularity is then absorbed almost completely by the centrifugal pendulum-type absorber. The result is impressive, as the comparison measurement presented in **Figure 9** shows when driving under full load. Compared to a conventional damper, the maximum speed fluctuations at the differential input are reduced by more than 70 %.

5 Summary

New combustion engines providing high torque at low speeds pose new challenges for damper technology. The tried-and-tested dual mass flywheel has reached the limits of what is physically feasible given the space available. The centrifugal pendulum-type absorber developed by LuK represents a solution with which the system limits can be expanded considerably. Depending on the design, isolation can be improved by 60 % and more over that provided by a standard dual mass flywheel.

Moreover, it does not matter whether a manual, dual clutch or automatic transmission is involved. The dual mass flywheel with a centrifugal pendulum-type absorber exhibits outstanding isolation, allowing new generations of engines to achieve their full potential without adversely affecting comfort, fuel consumption or CO_2 emissions.

References

[1] Müller, Bruno: LuK-Drehmomentwandler – Strategiefähige Wandler für neue Automatikgetriebe. VDI-Bericht Nr. 2029, S. 567 – 577, Düsseldorf, 2008

[2] Keller, Winfried; Wastl, Werner: Neue Methoden und Konzepte zur Drehungleichförmigkeits-Reduzierung. VDI-Bericht Nr. 2029, S. 595 – 606, Düsseldorf, 2008

[3] Seebacher, Roland; Fidlin, Alexander: Simulationstechnik am Beispiel des ZMS. Vortrag, LuK Kolloquium 2006, Bühl

[4] Balashov, Dmitry; Burkovski, Lidia; Ferderer, Frank; Fidlin, Alexander; Kremer, Maria; Pennec, Bertrand; Seebacher, Roland: Simulation bei Drehschwingungsdämpfern. In: ATZ 108 (2006), Nr. 12, S. 1038-1045

Relative Movement Analysis for a Rapid and Focused Vibration Analysis

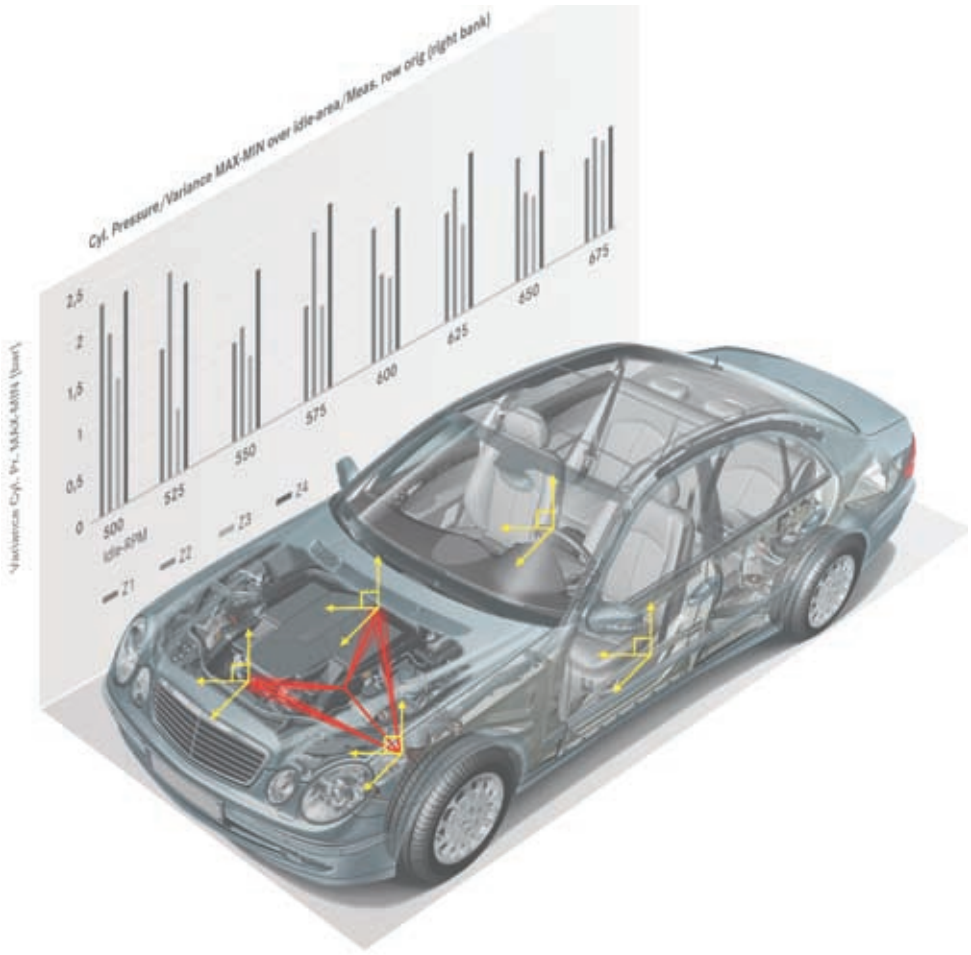

MBtech Powertrain GmbH, a company of the MBtech Group, has developed an efficient method called relative movement analysis (RMA) which is used in this example for optimization of the idling behavior and characteristics of a sedan with a V8 gasoline engine. This method enables engineers to rapidly and efficiently analyze the cause and effect chain, in this case, between the crankcase movements and steering wheel- and seat-vibrations. In the example presented, the RMA is utilized to optimize this vehicle's engine mounting.

1 Introduction

The high current technological standard of automobiles is, among other things, a result of the continuously increasing activities in the field of engine development. Traditional development goals such as the compliance with new legal regulations, or the mechanical endurance testing safeguards represent „must be" quality characteristics. However, as customers regard the "must be" criteria as a matter of fact, they no longer represent an additional purchase appeal.

As a result, it is becoming increasingly important to analyze and fulfill additional „add on" criteria in order to increase customer satisfaction. These "add-on" criteria make a decisive contribution to customer satisfaction by offering true and subjective added value when purchasing a vehicle. In addition to the classical Noise Vibration Harshness (NVH) optimization, the associated comfort application is becoming increasingly important. In this regard vehicles differ strongly for the customer – thus percep-

tible and/or audible advantages over competing products can be achieved. The customers' expectations are not only fulfilled but rather exceeded, and their satisfaction with the vehicle increases.

The following article describes a new calculation method (relative movement analysis; RMA) developed by MBtech which enables the overview and global interaction of several measurement points by means of a vibration analysis. In contrast to an examination of individual points, this method based on a global model for the vibrating object offers calculated numerical values rapidly and with relatively few measurement points in order to describe either the relative movement between different components or the relative distortion of the object itself. This calculation of real values gives additionally comparisonal basis for the stress development in the component itself and its relative movements compared to neighboring components. In addition, the correlations of the results through RMA were compared with those from combustion pressure and the rotational vibration.

The RMA enables the vectoral calculation of three dimensional amplitudes for multiple measurement points simultaneously. Thus in a short time the engineers calculate the maximum paths of movement of the measurement points in relation to a static unloaded situation, as well as the deformation of a body or relative movement against neighbor components. Furthermore, using a limousine-class car as an example, the MBtech measured parallel the combustion pressure while simultaneously recorded and evaluated the torsional vibrations of the crankshaft.

2 Relative Movement Analysis Method

2.1 Measurement Environment

In this study the well-known vibration analysis programs were utilized with the aid of 3-axis acceleration sensors. The combustion pressure was measured in usual way with measuring spark plug with integrated pressure sensor for the right cylinder bank of V8 engine. Also parallel a torsional vibration analysis on the basis of the engine speed signal was measured. The advantage for the used system lies in the fact that all of the measurements can be recorded simultaneously on the same time axis – which means that the MBtech engineers performed the combustion, torsional vibration and operating vibration analyses in parallel.

Figure 1 displays the position of the measurement sensors and the defined measurement points on the vehicle. At the same time a virtual triangle is created between the defined measurement points. The measurements were performed at varying idling speeds. Between the measurement series the transmission mounting and the front engine mounting were replaced.

2.2 Relative Movement Analysis (RMA)

The block movements are recorded with water-cooled three-axis acceleration sensors attached to the engine block, body, seat-rails and steering wheel.

Animation and measured amplitudes enable the new RMA-method to create a three dimensional calculation of the block movements for the first time over several points simultaneously.

One forms a triangular system via three measurement points (the coordinates are determined in advance either from a drawing or via measurements) and calculates the height of the triangle, **Figure 2**. The height of the triangle during zero load situation is compared with the height at the maximum stress-amplitude. During the individual resonance states per section the new position of the three corner points can be calculated as a vector for every maximum amplitude as also the new height of the particular triangle [see Figure 2]. The maxima for the difference between the height of triangle at a maximum amplitude (H`) and the height at zero load (H) corresponds to max. value of RMA at this particular load point. These values are equivalent to maximum movement/stress of the component at certain load points.

In comparison to the individual point/direction observation the RMA offers the advantage of being able to display the complete moving body on the basis of multiple measurement points simultaneously. As a result, the path of motion for each measurement points and the resulting stress situation in the component and the effect on neighbored components are clear as amplitudes and can be compared better to contrast the variety of different load states.

3 Evaluations of Different Analysis Methods

In the beginning, the pure application methodology as e.g. increased idle-rews did not increase idle-comfort. For this reason several analysis-methods were used in order to get better understanding for cause effect chain.

The Authors

Dipl.-Ing.
Reino Eskelinen
is Project Manager NVH Calibration at MBtech Powertrain GmbH in Sindelfingen (Germany).

Dipl.-Ing.
Andreas Biemelt
is Manager Combustion Development SI Engine at MBtech Powertrain GmbH in Sindelfingen (Germany).

Dr.-Ing.
Stephan Krämer
is Director Combustion Development and Calibration at MBtech Powertrain GmbH in Sindelfingen (Germany).

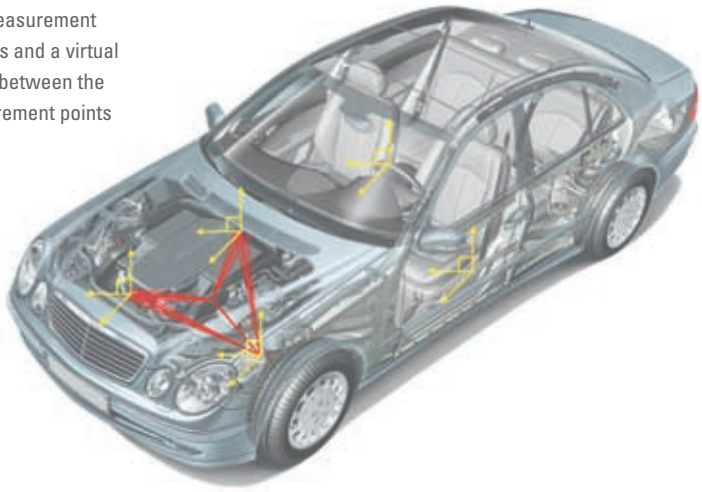

Figure 1: the measurement sensor positions and a virtual triangle drawn between the defined measurement points

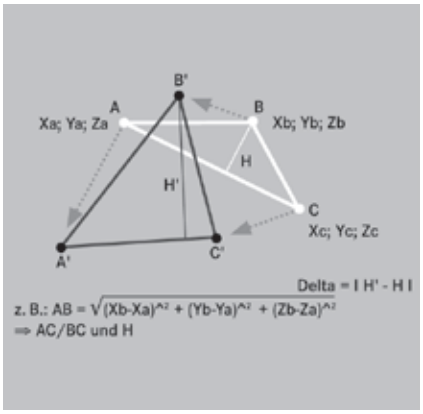

Figure 2: Calculation method for the triangle and height

3.1 The Cylinder Pressure Indexing

The cylinder pressure was recorded in four cylinders for every idling speed and then statistically evaluated. The engine running smoothness was illustrated at different engine speeds as a scatter plot of the combustion pressure, **Figure 3**. A relatively large spread of the individual cylinder pressures for each chamber and between the cylinders is visible. This effect was reduced by an increasing engine idle-speed.

3.2 Evaluation of the Torsional Vibration

For further diagnose of the engine smoothness during the combustion process, the MBtech also performed a torsional vibration analysis against the engine speed signal. This displays the shock effect of the change of turning acceleration (°CA/s³), **Figure 4**.

The torsional analysis provides the same positive trend of engine-speed roughness with increasing idle revolutions as combustion analysis.

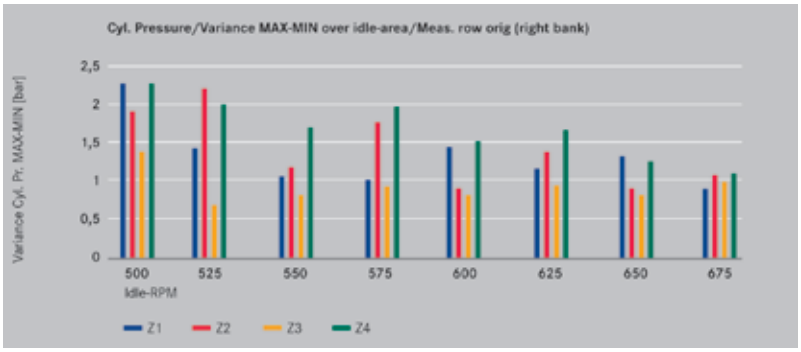

Figure 3: Variation of the individual cylinder pressures at different idling speeds

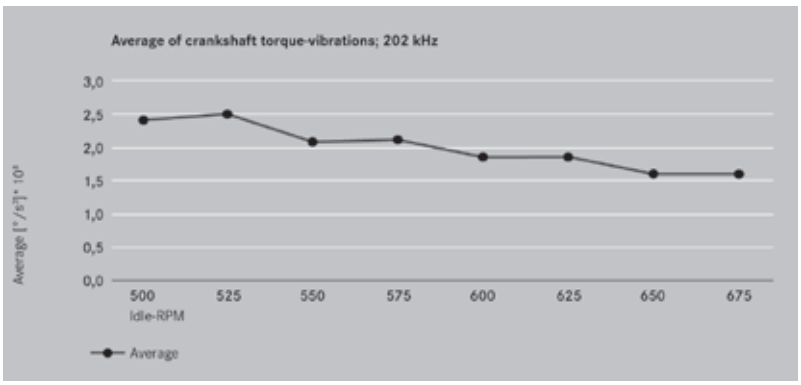

Figure 4: Mean of the derivate for torsional speed of the crankshaft at different idling speeds (Average of 100 cycles)

3.3 Results of Relative Movement Analysis (RMA)

In order to avoid undesired, noticeable steering wheel- and seat-rail-vibrations, the effects of earlier analyses concentrated solely on the front engine mounting. In the hope of controlling the situation adjustable front engine mountings were tried. However, replacing the front mounting – on the basis of these previous investigations – did not deliver any significant improvements.

Through this RMA calculation method MBtech was able to prove, which of the engine mountings is responsible for the undesired vibration in the components.

First the engineers compared two vehicles with the same original front engine mounting but a different rear transmission mounting. They calculated the correlation of the block movements front/rear with the vibration of the seat-rails and the steering wheel.

Through RMA it succeeded to show, which mounting correlated with seat-rail and steering wheel vibrations. A soft rear engine mounting causes a tumbling motion in the transmission which then leads to larger vectoral movements in the steering wheel and seat-rail.

Figure 5 reflects the effect between the rear block movement (transmission) rela-

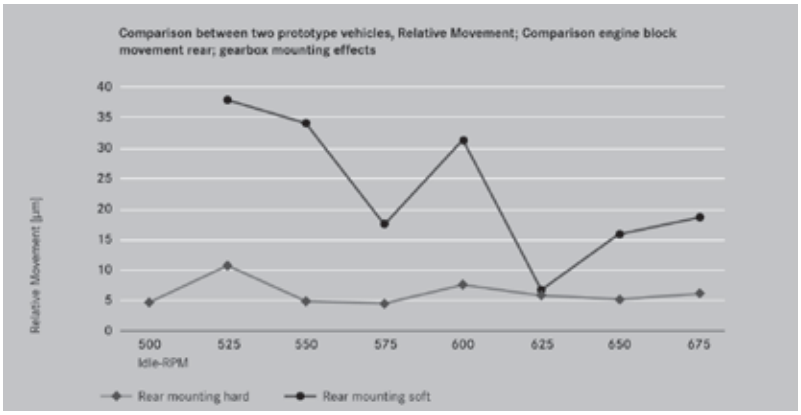

Figure 5: Relative movement of the engine block rear

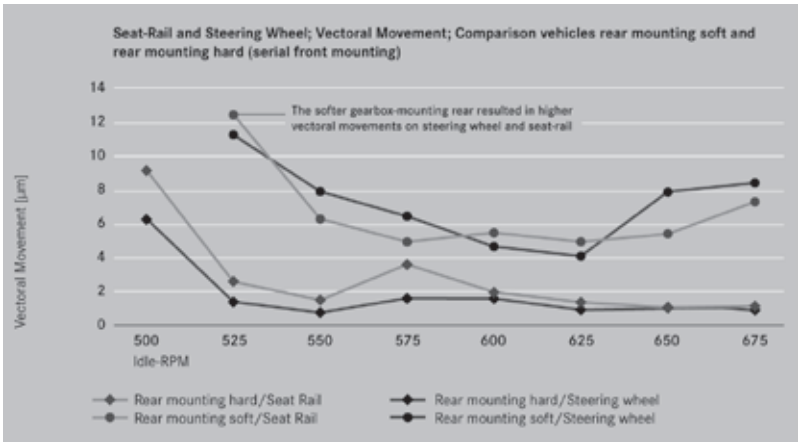

Figure 6: Relative vectoral movement of the seat-rail and steering wheel: displayed the correlation with the rear engine mounting, the movements of the steering wheel and seat-rail

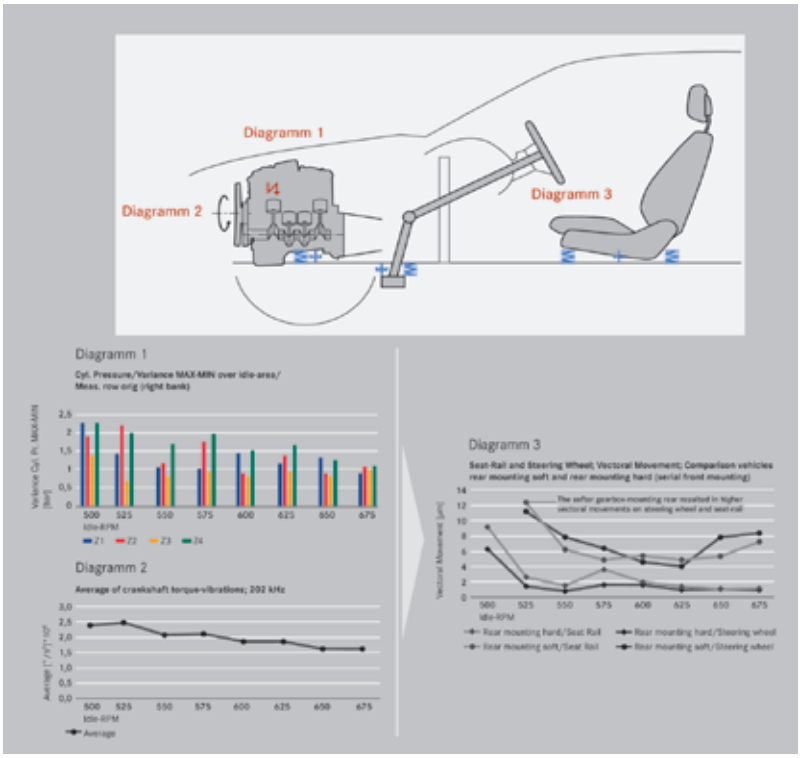

Figure 7: The left side displays the variations of the cylinder pressures and torsional change of the angular acceleration against engine speed – the diagram on the right illustrates the vectoral movements of the seat-rail and steering wheel for harder and softer rear mounting

tive to the chassis. The difference between a harder and a softer rear mounting (the front mountings remained in this case identical) is evident. In the case of the softer transmission mounting the increased relative movement is clearly recognizable (see Figure 5: "Rear mounting soft").

Figure 6 shows the effect of this movement according to rear mounting hardness to the seat-rail and steering wheel: A greater movement of the rear part of the block is clearly transferred to the seat-rail and the steering wheel.

The cause for discomfort on seat-rail and steering wheel was the movement of the rear block-part through the softness of the transmission mounting. In comparison, the differences in front block movements were relatively small. Thus the interaction between the rear part of the block and the movements of the seat-rail and the steering wheel was clearly proven.

Changing the rigidity of the rear mounting resulted in less movement of the seat-rail and steering wheel (see Figure 6). The front mounting could not be efficiently adapted until the rear mounting had been optimized.

3.4 Correlation between the Analysis Methods

Combining the different analyses delivered meaningful results for improving the vibration behavior at higher idling speeds for example. The diagrams in **Figure 7** describe the connection between combustion and torsional vibration with the vectoral movements of the steering wheel and seat-rail.

This study shows that pure increase of idle as shown only by the cylinder-pressure and torisional vibration analysis is not enough in order to derivate better idle-comfort. Only after additional analysis throught RMA we can see the optimum point at 625/min.

4 Optimizing the Front Engine Mounting

The effect of the front engine mounting based on the vibration behavior of the engine becomes visible only after correcting the rigidity of the rear engine mounting.

In the process it became apparent that the customer requirements regarding the comfort with the original mounting could not be achieved. Therefore further investigations with different rigidities of the static front engine mounting were realized.

Figure 8 and **Figure 9** show the effect of two front mounting variants (Serial against Variant A) as vectoral movement on seat-rail and steering wheel. The effect of optimized frontal engine mounting on seat-rail is considerably perceptible in case of an idle-speed area up to 600 1/min. At higher idle-speed range the effect was less perceptible. On steering wheel however, the influence of the engine mounting is recognizable only up to 525 1/min. After this optimization of engine-mounting system with the help of RMA, the idle-comfort became again almost independent of idle-rew which again opened new possibilities for applicational an NVH needs.

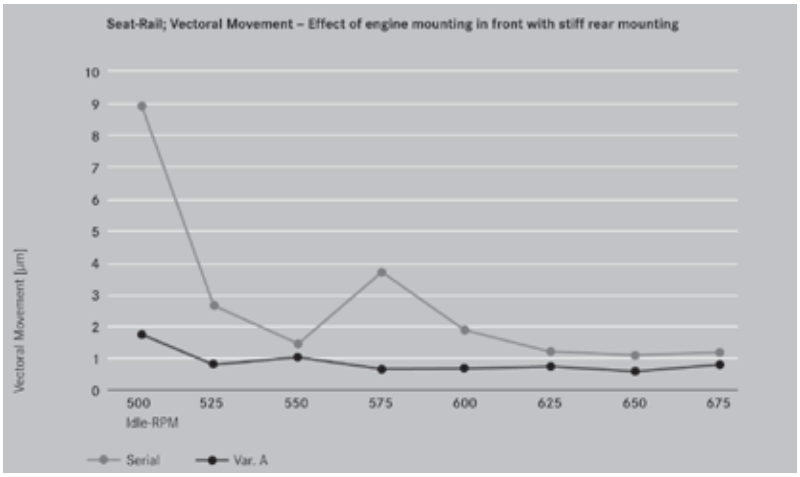

Figure 8: Vectoral movement of the seat-rail with different front engine mountings

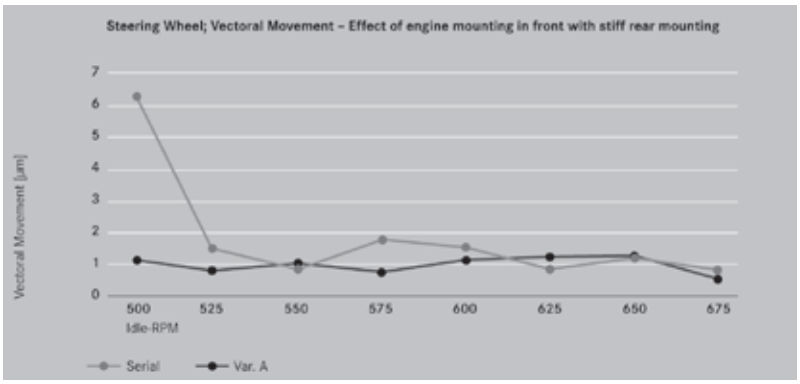

Figure 9: Vectoral movement of the steering wheel with different front engine mountings

5 Summary

The relative movement analysis (RMA) is a new method for analyzing vibrations. Additionally in this case combustion pressure and torsional vibration analyses were combined with motion measurements for the engine block and steering wheel and seat-rail.

The presented RMA is a simple as well as an effective calculation method.

Based on defined triangles, distributed among the engine block parts and the body, the RMA provides an essential contribution to NVH optimization.

Furthermore the rapid comparison method enables the analysis of dominant engine block movements. This served to clearly identify the effects of different engine mountings and engine speeds on the movements of the seat-rail and steering wheel.

The subjective impressions of selected test persons further supported the study's results.

It was also shown, that the different individual analysis methods (combustion pressure, torsional vibrations and RMA) each alone did not reflect the subjectively perceptible best solution. Only the weighted focus on all the methods leads to the best compromise and an optimal solution.

In general the newly developed RMA method can be used where components move relatively to each other. Thus, the RMA could also be employed to determine the largest stress on the component itself in different resonance states – for example in order to begin an endurance test run as a resonance test in highest stress point.

Numerous different components can be analyzed: Beginning with the crankcase, for example, diverse mounting components onward to EGR pipes and complete exhaust systems.

RMA and FE modelling could also be combined in order to enable initial comparison results in the form of a direct stress evaluation. In the meanwhile the MBtech increases the speed of calculation by combining the vibration analysis with additionally used mathlab programs. ■

Peer Review ATZ|MTZ

Peer Review Process for Research Articles in ATZ and MTZ

Steering Committee

Prof. Dr.-Ing. Stefan Gies	RWTH Aachen	Institut für Kraftfahrwesen Aachen
Prof. Dipl.-Des. Wolfgang Kraus	HAW Hamburg	Department Fahrzeugtechnik und Flugzeugbau
Prof. Dr.-Ing. Ferit Küçükay	Technische Universität Braunschweig	Institut für Fahrzeugtechnik
Prof. Dr.-Ing. Stefan Pischinger	RWTH Aachen	Lehrstuhl für Verbrennungskraftmaschinen
Prof. Dr.-Ing. Hans-Christian Reuss	Universität Stuttgart	Institut für Verbrennungsmotoren und Kraftfahrwesen
Prof. Dr.-Ing. Ulrich Spicher	Universität Karlsruhe	Institut für Kolbenmaschinen
Prof. Dr.-Ing. Hans Zellbeck	Technische Universität Dresden	Lehrstuhl für Verbrennungsmotoren

Advisory Board

Prof. Dr.-Ing. Klaus Augsburg	**Dr.-Ing. Markus Lienkamp**
Prof. Dr.-Ing. Bernard Bäker	**Prof. Dr. rer. nat. habil. Ulrich Maas**
Prof. Dr.-Ing. Michael Bargende	**Prof. Dr.-Ing. Martin Meywerk**
Dr.-Ing. Christoph Bollig	**Prof. Dr.-Ing. Werner Mischke**
Prof. Dr. sc. techn. Konstantinos Boulouchos	**Prof. Dr.-Ing. Klaus D. Müller-Glaser**
Prof. Dr.-Ing. Ralph Bruder	**Dr. techn. Reinhard Mundl**
Dr. Gerhard Bruner	**Dr.-Ing. Lothar Patberg**
Prof. Dr. rer. nat. Heiner Bubb	**Prof. Dr.-Ing. Peter Pelz**
Prof. Dr. rer. nat. habil. Olaf Deutschmann	**Prof. Dr. techn. Ernst Pucher**
Dr. techn. Arno Eichberger	**Dr. Jochen Rauh**
Prof. Dr. techn. Helmut Eichlseder	**Prof. Dr.-Ing. Konrad Reif**
Dr.-Ing. Gerald Eifler	**Dr.-Ing. Swen Schaub**
Prof. Dr.-Ing. Wolfgang Eifler	**Prof. Dr. sc. nat. Christoph Schierz**
Prof. Dr. rer. nat. Frank Gauterin	**Prof. Dr. rer. nat. Christof Schulz**
Prof. Dr. techn. Bernhard Geringer	**Prof. Dr. rer. nat. Andy Schürr**
Prof. Dr.-Ing. Uwe Grebe	**Prof. Dr.-Ing. Ulrich Seiffert**
Prof. Dr.-Ing. Horst Harndorf	**Prof. Dr.-Ing. Hermann J. Stadtfeld**
Prof. Dr. techn. Wolfgang Hirschberg	**Prof. Dr. techn. Hermann Steffan**
Univ.-Doz. Dr. techn. Peter Hofmann	**Dr.-Ing. Wolfgang Steiger**
Prof. Dr.-Ing. Günter Hohenberg	**Prof. Dr.-Ing. Peter Steinberg**
Prof. Dr.-Ing. Bernd-Robert Höhn	**Prof. Dr.-Ing. Christoph Stiller**
Prof. Dr. rer. nat. Peter Holstein	**Dr.-Ing. Peter Stommel**
Prof. Dr.-Ing. habil. Werner Hufenbach	**Prof. Dr.-Ing. Wolfgang Thiemann**
Prof. Dr.-Ing. Roland Kasper	**Prof. Dr.-Ing. Helmut Tschöke**
Prof. Dr.-Ing. Tran Quoc Khanh	**Dr.-Ing. Pim van der Jagt**
Dr. Philip Köhn	**Prof. Dr.-Ing. Georg Wachtmeister**
Prof. Dr.-Ing. Ulrich Konigorski	**Prof. Dr.-Ing. Henning Wallentowitz**
Dr. Oliver Kröcher	**Prof. Dr.-Ing. Jochen Wiedemann**
Dr. Christian Krüger	**Prof. Dr. techn. Andreas Wimmer**
Univ.-Ass. Dr. techn. Thomas Lauer	**Prof Dr. rer. nat. Hermann Winner**
Prof. Dr. rer. nat. Uli Lemmer	**Prof. Dr. med. habil. Hartmut Witte**
Dr. Malte Lewerenz	**Dr. rer. nat. Bodo Wolf**

Seal of Approval – this seal is awarded to articles in ATZ/MTZ that have successfully completed the peer review process

Scientific articles in ATZ Automobiltechnische Zeitschrift and MTZ Motortechnische Zeitschrift are subject to a proofing method, the so-called peer review process. Articles accepted by the editors are reviewed by experts from research and industry before publication. For the reader, the peer review process further enhances the quality of ATZ and MTZ as leading scientific journals in the field of vehicle and engine technology on a national and international level. For authors, it provides a scientifically recognised publication platform.

Therefore, since the second quarter of 2008, ATZ and MTZ have the status of refereed publications. The German association "WKM Wissenschaftliche Gesellschaft für Kraftfahrzeug- und Motorentechnik" supports the magazines in the introduction and execution of the peer review process. The WKM has also applied to the German Research Foundation (DFG) for the magazines to be included in the "Impact Factor" (IF) list.

In the ATZ/MTZ Peer Review Process, once the editorial staff has received an article, it is reviewed by two experts from the Advisory Board. If these experts do not reach a unanimous agreement, a member of the Steering Committee acts as an arbitrator. Following the experts' recommended corrections and subsequent editing by the author, the article is accepted. *rei*

ATZ Peer Review

The Seal of Approval for scientific articles in ATZ.
Reviewed by experts from research and industry.

Received .....
Reviewed .....
Accepted .....

Experimental and Numerical Investigation of Air Dam Aeroacoustics

Different vehicle manufacturers mount an air dam on the vehicle undercarriage just in front of the wheels. For better understanding of the noise generation mechanisms and flow induced vibrations directly at their source region, the acoustical effects in the interior of the vehicle will be correlated by the University of Applied Sciences Duesseldorf and BMW with the pressure fluctuations of the exterior of the vehicle. Steady state CFD calculations in the area of the rotating front wheel will be carried out for the positioning of the surface microphones and for a better understanding of the flow topology.

1 Influence on the Interior Acoustics

In addition to design, safety and handling characteristics of automobiles, the acoustic perception of the car occupants is becoming of even greater importance. New experimental and simulation methods already play a role during the conceptual phase of a vehicle design. It is for this reason that BMW's acoustic wind tunnel is equipped with additional measurement methods for the undercarriage, **Figure 1** [1].

Wind tunnel experiments on their own are not sufficient in order to understand the influence of engine, roll and wind noise. Wind tunnel experiments only draw conclusions on the acoustics of the air flow, other noise sources stay unconsidered. An additional possibility for gathering all relevant car-related noise would be road testing in realistic conditions. In the present paper, acoustical effects in the interior of the vehicle in order will be correlated with the pressure fluctuations of the exterior of the vehicle to understand the noise generation mechanism and flow induced vibrations in their source region. A special attention will be drawn on the influence of the air dams, Figure 1. They are located on the undercarriage in front of each wheel respective each wheel housing, **Figure 2**.

2 Aerodynamic Processes at Wheel and Wheel Housing

The investigation of aeroacoustic processes at the wheels and in the wheel housings gained importance as recently as in the last 15 years. The high degree of cavities, edged connection rods and turned sheets in this area result into highly uneven and cleft surfaces which not only cause a remarkable flow drag, but also represent a exceedingly source for flow noise. According to [4] wheels, wheel housings and undercarriage at a passenger car with a drag coefficient of c_D = 0.3 are responsible for over half of the aerodynamic drag.

To avoid or to reduce the direct flow against the wheels and to achieve better flow around the wheel, the air dam was fitted on the part of BMW and other automobile manufacturers. The construction at the experimental vehicle covers the complete span of the front wheel housing. At the rear wheel housing, the air dam is approximately only 200 mm long which equates to the width of the wheel.

In the front part of the wheel housing around the rotating wheel, **Figure 3**, the flow sucks upwards and hits the boundary layer flow close to the body on the edge of the car body. At this location an unrolling longitudinal vortex is expected, which probably is disturbed by the emergent air of the wheelhouse area and flow separation occurs.

3 Measurement Instrumentation and Conditions

For Wagners thesis [3] Brüel & Kjær has kindly provided the detection of dynamic pressure fluctuations with surface microphones of the types 4949 and 4949B, **Figure 4**. Despite the small dimensions (Ø 20 mm, height 2.5 mm) they are,

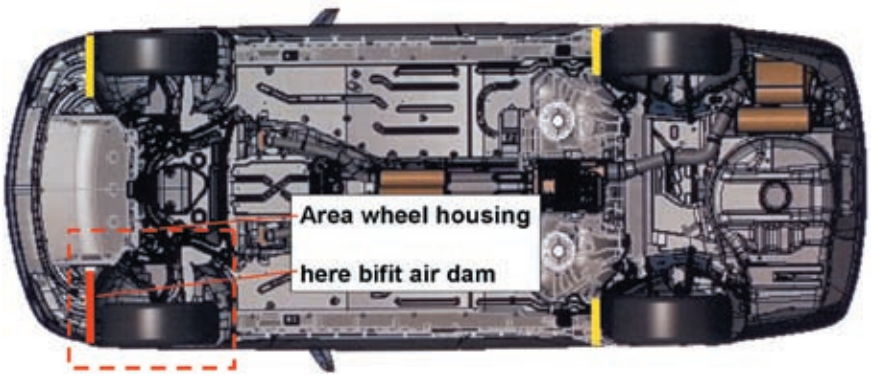

Figure 1: Vehicle undercarriage with the position of the air dam in front of the front wheel [2]

The Authors

Prof. Dr.-Ing. Frank Kameier is Professor of Fluid Mechanics and Acoustics at the University of Applied Sciences Duesseldorf (Germany).

Thomas Wagner MScEng was Research Assistant at the University of Applied Sciences Duesseldorf and is now Research Assistant at the Technical University Kaiserslautern (Germany).

Igor Horvat MScEng is Research Assistant at the University of Applied Sciences Duesseldorf (Germany).

Dipl.-Ing. Frank Ullrich is responsible for Aeroacoustics and the Acoustic Wind Tunnel of the BMW Group in Munich (Germany).

ATZ Peer Review
The Seal of Approval for scientific articles in ATZ.
Reviewed by experts from research and industry.

Received ..... March 02, 2009
Reviewed ..... March 16, 2009
Accepted ..... March 31, 2009

Figure 2: Bifid air dam of the model BMW E92 [3]

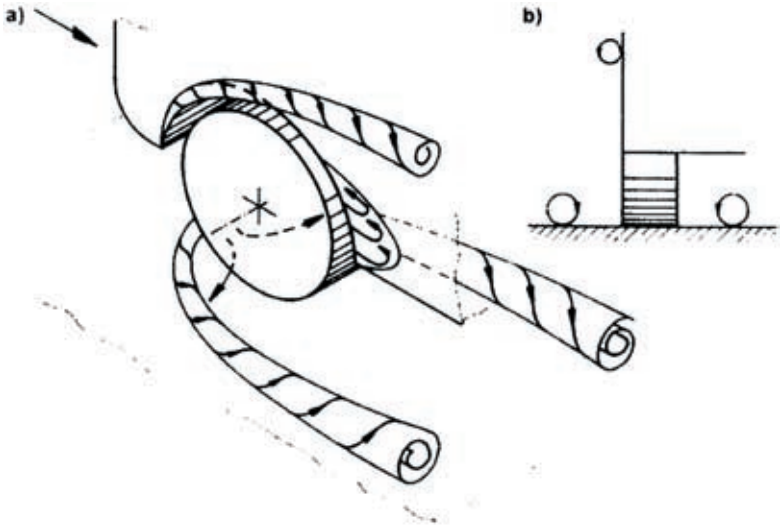

Figure 3: Schematic view of the longitudinal vortex in the area of the wheel housing with rotating wheel and with moving street – view from the side (a) and from behind (b) [5]

Figure 4: Surface microphone (left) and its positions on the vehicle (right, air dam not mounted), compare with Figure 8

based on a titanium casing, very sustainable against wet (corrosion) and oily environments. The acoustic sensitivity and the dynamic range are approximately equal to traditional ¼" condenser measurement microphones. Figure 4 shows the approximately selected positions of the surface microphones. Parallel to the measurements, further numerical calculations of the simplified vehicle section were continued.

At all measurements the surface microphones were provided with a little covering, protecting the membrane from dirt particles, as well as with a mounting pad. This to the outer diameter flattening ring causes a better flow around the microphone. The so called self-noise, which is measured by the microphone itself, is generated by vortex separation which causes pressure fluctuations at the microphone body. This self-noise can be minimized by the shaping of the microphone. On the other hand, a structure-borne sound isolation between wall and surface microphone can be achieved with this indirect placement [6]. For acquisition of all relevant aeroacoustic data, a mobile data acquisition unit MK II and the software PAK of MüllerBBM VibroAkustik Systeme GmbH were used.

For road testing an E92, 320d Coupé experimental vehicle was provided by BMW Group. For reproducible measurement results the motorway A59 between Düsseldorf and Leverkusen was used. This route offers good test conditions , due to its new and homogenous road surface as well as its low traffic volume.

In forefront of the measurements, a simplified sketch of the wheel housing was used in CFD calculations with Ansys 11 to find the best measurement positions for the surface microphones. Within the steady state CFD calculations by using a shear stress transport (SST) model it was paid attention on the boundary conditions of the relative movement between vehicle and road as well as on the rotation of the wheel. Thereby only a small part of the vehicle was design-engineered and meshed for the simulation. This enables focusing the mesh on the main area of influence and an efficient calculation.

To verify the boundary layers and the numerical simulation under conditions close to reality the boundary conditions, the calculation area and the velocity distributions are shown in **Figure 5**.

4 Measurement Results of the Pressure Fluctuations

Figure 6 shows a comparison of the sound pressure spectra of the vehicle interior at a velocity of 150 km/h with and without an air dam. Harmonic tonal frequency components of the rotational wheel speed occur only without the air dam. Without the air dam, even more tonal frequency components are clearly transferred in the interior of the vehicle. Differences at low frequencies in the signals of the surface microphones mounted in the wheel housing occur between the spectra with and without air dam, **Figure 7**.

5 Correlation of the Wall Pressure Fluctuations

By using a correlation analysis it is possible to differ between acoustic pressure fluctuations with the speed of sound, as their propagation velocity and aerodynamic pressure fluctuations which are not obligatory relevant for noise. Important for the interpretation of the phase characteristics in accordance to [7] is the microphone placement in the wheel housing, Figure 4.

With the knowledge of the distance Δx between the microphone positions, it is possible to calculate the speed of propagation of the pressure fluctuation from the phase angle of the cross-spectrum. With a sufficient level of the coherence of two adjacent pressure transducers, the linear phase shift at constant speed of propagation (non dispersive propagation process) can be allocated. In **Figure 8** the coherence and the phase angle of the microphone signals on position 2 to the reference channel above the wheel housing 4 is shown (blue: measurement with air dam, red: measurement without air dam).

The calculation of the time delay results by means of the phase slope [8]. The time delay yields from:

$$t_{verz} = \frac{\Delta\varphi}{\omega} = \frac{\frac{\Delta\varphi°}{360°} \cdot 2\pi}{\Delta f \cdot 2\pi} \qquad \text{Eq. (1)}$$

With t_{verz} and the distance of the microphones the velocity $v = \Delta x/t_{verz}$ results. The speeds of propagation from the phase of the characteristics shown in Figure 8 represents between 500 and 800 Hz with $\Delta\varphi$ = 180°, Δf = 300 Hz and Δx = 0.52 m approximately v = 324 m/s (the speed of sound at 5 °C is 334.5 m/s) and between 1700 and 1800 Hz with $\Delta\varphi$ = 360°, Δf = 60 Hz and Δx = 0.52 m approximately v = 31 m/s (driven speed: approximately 42 m/s).

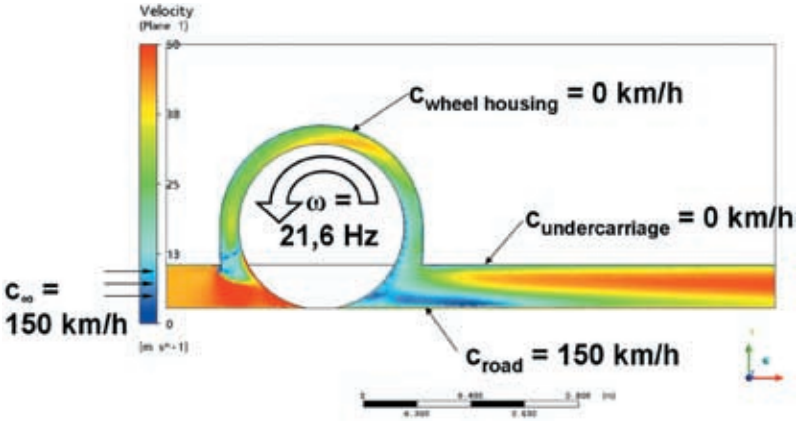

Figure 5: Boundary conditions of the CFD calculation

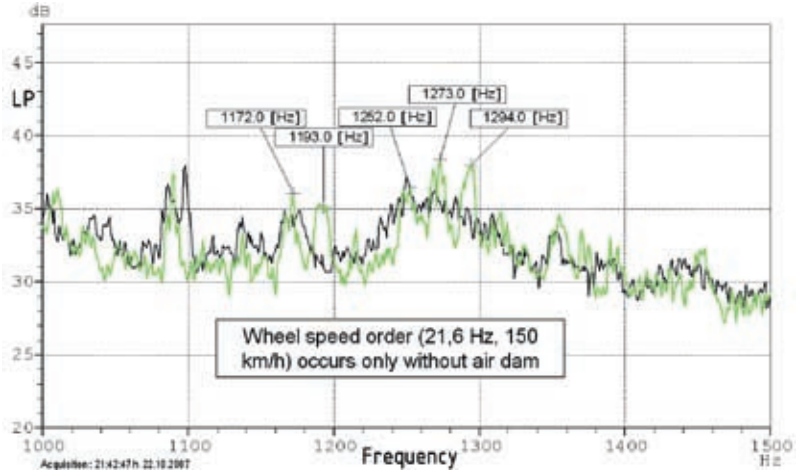

Figure 6: Sound pressure levels in the vehicle interior with (black) and without (green) air dams, road drive, v = 150 km/h

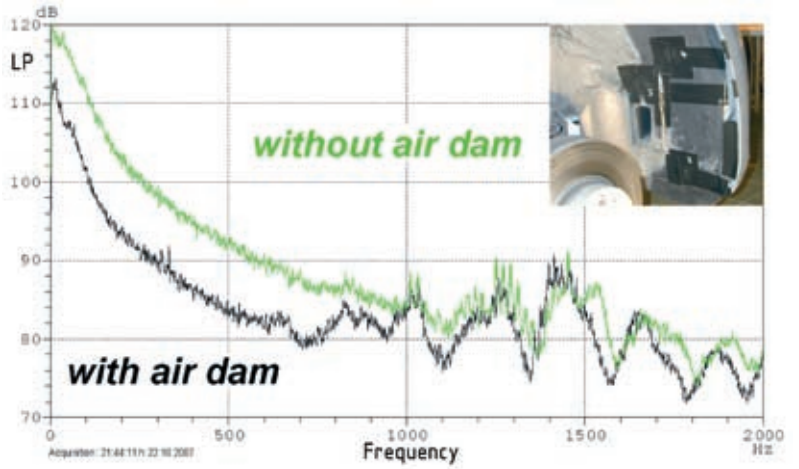

Figure 7: Wall pressure fluctuation levels in the wheel housing with (black) and without (green) air dams, test drive, v = 150 km/h

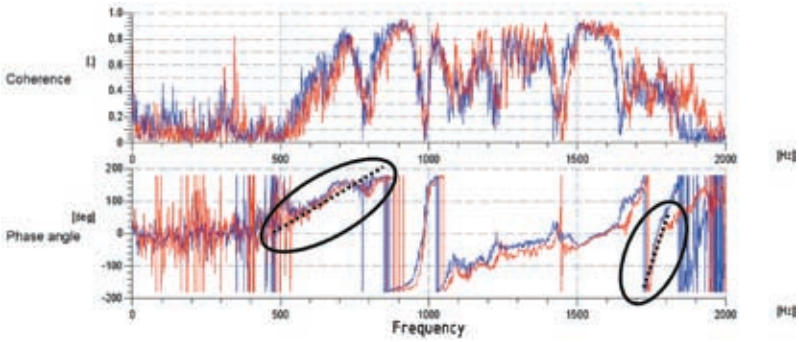

Figure 8: Coherence and the phase angle of the cross-spectrum of the wall pressure fluctuations position 2 towards position 4 (compare with Figure 4); with (blue) and without (red) air dam measurements

Hence the speed of propagation is well-defined between high values near the speed of sound and lower levels in the range of the travelling speed of the vehicle. On the one hand, a steep slope of the phase angle indicates a slow speed of propagation, in comparison to the speed of sound. It will be generated by the flow itself respectively by turbulent pressure fluctuations.

On the other hand, a minor slope indicates that it concerns with noise propagation in terms of acoustic pressure fluctuations. In addition the propagation direction can be detected by means of a positive or negative slope: With a positive slope the sound arrives with a certain delay at the second microphone. The propagation occurs from the rear to the front – opposite to the outer flow around the vehicle – and therefore is dominated by the rotating wheel. It is not possible to measure this phenomenon in a wind tunnel with a non-rotating wheel. The velocity of the vortex rope matches the slip with 74 % compared to the circumferential speed of the wheel.

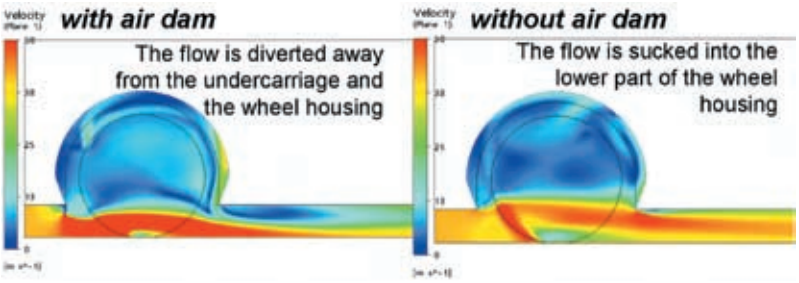

Figure 9: Velocity distribution wit and without air dam of the simplified wheel housing model

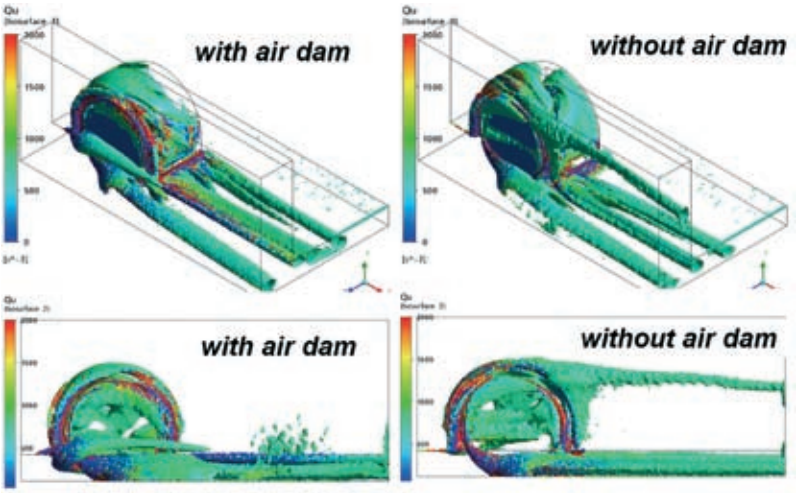

Figure 10: By Q-criterion calculated vortex pattern with and without air dam

6 Presentation of Vortex Structures with the Q-Criterion

Figure 9 shows the extensive velocity distribution around the rotating wheel both with and without air dam. In order to compare vortex pattern from the numerical CFD calculation with the topology of the flow in accordance to the schematic sketch of Figure 3, an extensive vector analytical computation of the flow velocity gradients is necessary.

In order to visualise vortices, the Q criterion in accordance to [9] was implemented in the Ansys CFD post processing, so that coherent vortex structures of the velocity gradients are visible [10]. Generally, a shear strain is specified as a gradient of the velocity:

$$\text{grad } \underline{u} = \begin{pmatrix} \frac{\partial u}{\partial x} & \frac{\partial v}{\partial x} & \frac{\partial w}{\partial x} \\ \frac{\partial u}{\partial y} & \frac{\partial v}{\partial y} & \frac{\partial w}{\partial y} \\ \frac{\partial u}{\partial z} & \frac{\partial v}{\partial z} & \frac{\partial w}{\partial z} \end{pmatrix} = \frac{\partial u_i}{\partial x_j} \qquad \text{Eq. (2)}$$

This gradient can be converted with following formulas:

$$\underline{\underline{S}} = \frac{1}{2} \cdot (\text{grad } \underline{u} + \text{grad } {}^{T}\underline{u}) \text{ and}$$
$$\underline{\underline{\Omega}} = \frac{1}{2} \cdot (\text{grad } \underline{u} - \text{grad } {}^{T}\underline{u}) \qquad \text{Eq. (3)}$$

to the symmetric shear rate tensor $\underline{\underline{S}}$ and the antimetric vorticity tensor $\underline{\underline{\Omega}}$:

$$\text{grad } \underline{u} = \underline{\underline{S}} + \underline{\underline{\Omega}} \qquad \text{Eq. (4)}$$

The Q criterion is derived out of both of these tensors:

$$Q = \frac{1}{2} \cdot \left(\left| \underline{\underline{\Omega}}^2 \right| - \left| \underline{\underline{S}}^2 \right| \right) > 0 \qquad \text{Eq. (5)}$$

$$Q = \frac{1}{2} \cdot \left[\left(\frac{\partial u}{\partial x} \right)^2 + \left(\frac{\partial v}{\partial y} \right)^2 + \left(\frac{\partial w}{\partial z} \right)^2 \right] -$$
$$\left[\frac{\partial v}{\partial x} \frac{\partial u}{\partial y} + \frac{\partial w}{\partial x} \frac{\partial u}{\partial z} + \frac{\partial v}{\partial z} \frac{\partial w}{\partial y} \right] \qquad \text{Eq. (6)}$$

Figure 10 shows the vortex patterns calculated with the Q criterion. In addition to the schematic illustration of Hucho [5],

which shows the vortex system without an air dam in Figure 3, Figure 10 displays the vortex system with an air dam. With an air dam, the vortex is pushed from the upper side of the wheel down to the driving surface and produces here fore less pressure fluctuations at the carriage of the vehicle. This has a positive effect on the acoustics.

Whilst the flow topology with and without the air dam is almost the same in the area of the undercarriage, there are obvious differences at the exterior behind the wheel housing. At this area a longitudinal vortex develops with a demounted air dam. At the shown simulation this vortex is not present. Probably in consequence of the diverted air flow by the air dam, which makes sure that only a small flow rate is conducted through the gap between the wheel and the carriage at the wheel housing.

7 Summary

Within an experimental and numerical investigation by the University of Applied Sciences Duesseldorf and BMW the acoustic effect of the air dam of a BMW 3-Series vehicle was investigated. Both realistic drive tests on public roads as well as numerical calculations in the area of the front rotating wheel were performed. One of the major aspects were on the one hand the correlation of the pressure fluctuations at the exterior and the wheel housing with noise inside the car and on the other hand the illustration of the flow field with CFD calculations. To show the influence of the flow velocity and to gain better understanding of the noises and the flow induced vibration directly at the source, the vehicle was equipped with seven surface microphones at the exterior and two measurement microphones in the interior. The drive tests were performed at various velocities with and without a mounted air dam.

At the spectra between 450 and 600 Hz as well as between 1200 and 1400 Hz without an air dam, an increased level of 3 to 5 dB was measured. The frequency components appear in a distance of 21 Hz (matching with the wheel speed order), which were not-existant with a mounted air dam. The reason for these frequency components is the incident air flow of the tire profile. The mount of the air dam just in front of the wheel housing makes sure that the air flow is deflected away from the wheel and the undercarriage. Through this air flow deflection, different pressure distributions result especially at the wheel housing, causing a lower sound pressure level for a frequency range below 1000 Hz. A completely different situation is present at the measurement points directly in front and behind the air dam. The air dam represents a fluid dynamical barrier, where the air flow dams up and at which leading edge the wake vortices separate. These separations probably represent the reason for the higher pressure fluctuations at this area. On the basis of the spectograms shown by Wagner [3] you can draw the conclusion, that not only rotation speed dependent activities, but also structural acoustic effects in the wheel housing are responsible for the noise generation mechanisms. Distinct differences between the measurements with and without air dam, at least for the area of the wheel housing, are evident.

The observation of the correlation analysis provides for neighbouring measurement points coherences which partially raise to 0.9 for a frequency range between 700 and 1700 Hz. With the slope of the phase angle, conclusions can be drawn on the kind of sound propagation. The measured pressure fluctuations are composed by turbulent (caused by the air flow) and acoustic pressure fluctuations. Due to the determined slip of 74 % of the driving speed and the propagation direction the measured pressure fluctuations can be allocated to the rotating wheel. Measurements in the acoustic wind tunnel with a non-rotating wheel cannot cover these effects.

With the aid of the simulation tool Ansys CFX the flow topology around the unrolling wheel was pictured. The air dam makes sure that the air flow is deflected. The stagnation point is displaced to a position further away from the wheel just in front of the air dam. Herewith, a direct flow against the wheel is avoided. The effect can be shown on the basis of flow lines. Beside the velocity distribution the visualisation of vortex pattern with the appropriate allocation of velocity gradients is expedient. The results show clear analogies to the theory of Hucho [5]. At both vehicle configurations horseshoe vortices can be found. At the simulations without an air dam a longitudinal vortex develops on the exterior behind the wheel housing. Under circumstances this longitudinal vortex provides additional fluid structure interactions, which can influence the sound in the vehicles interior negatively.

References

[1] Kaltenhauser, A.; Kolb, S.; Ullrich, F.; Polansky, L.: Neue Modulwaage im Akustikwindkanal von BMW. In: ATZ 108 (2006), Nr. 12, S. 1026–1037

[2] Ullrich, F.: Aeroakustik: Neue Potenziale für die Innengeräuschoptimierung. Haus der Technik Essen, 4. Tagung Aeroakustik, Wildau, 2006

[3] Wagner, Th.: Experimentelle und numerische Untersuchung zur Strömungsakustik der Staulippe eines 3er BMWs. Master Thesis, Fachhochschule Düsseldorf, 2008

[4] Garrone, A.; Masoero, M.: Car Underside, Upperbody and Engine Cooling System Interactions and their Contribution to Aerodynamic Drag. SAE-Paper 860212, Warrendale, Pa., USA, 1986

[5] Hucho, W. (Hrsg.): Aerodynamik des Automobils. 5. Auflage, Vieweg-Verlag, Wiesbaden, 2005

[6] N. N.: Product Data Sheet, Automotive Surface Microphones – Types 4949 and 4949B. ATZ/MTZ-Konferenz Akustik – Akustik zukünftiger Fahrzeug- und Antriebskonzepte, Stuttgart, Mai 2006, http://www.bksv.com/doc/bp2055.pdf

[7] Bendat, J. S.; Piersol, A. G.: Engineering Applications of Correlation and Spectral Analysis. New York, USA, 1993

[8] Kameier, F.: Experimentelle Untersuchung zur Entstehung und Minderung des Blattspitzen-Wirbellärms axialer Strömungsmaschinen. Dissertation, TU Berlin, VDI-Fortschritt-Berichte, Reihe 7, Nr. 243, VDI-Verlag, Düsseldorf, 1994

[9] Spille-Kohoff, A.: Das Q-Kriterium. CFX Berlin Software GmbH, interner Bericht, Berlin, Juni 2006

[10] Fröhlich, J.: Large-Eddy-Simulation turbulenter Strömungen. Teubner-Verlag, Wiesbaden, 2006

personal buildup for Force Motors Ltd.

Methods of Evaluating and Developing Pedal and Brake Characteristics

The qualities of a particular car that are experienced by the driver in direct interaction with the car have come to be significant distinguishing features. The brake system is particularly important in this respect because it belongs to the essence of driving and of keeping the vehicle under control. An overview is given in this paper of methodology developed at the Ilmenau University of Technology for comprehensive, objective and definitive investigation of the interaction taking place between the driver and the vehicle during braking.

1 Introduction

The human machine interfaces (HMI) of braking systems of modern cars should be laid out in such a way that they are not only safe in objective terms but can also be used intuitively with ease. Manufacturers often insist on "typical" brake pedal feel for a brand to raise recognition of the vehicle type through the haptic features "felt" by the customer.

In the development process for the interface characteristics, the judgment as to whether the product is ripe for production, is, even today, still based on the experience and the subjective impressions of a small staff team. Though research relating the HMI in objective terms to the subjective impression goes back some time, the outcomes have, till now, found little acceptance among industrial users, being, at most, tacked on as an extra. Up-to-date overviews are to be found in [4] and [11].

This paper indicates the outcomes of critical appraisal of the state of the art to date. One result is that new or at least greatly improved methods and devices have been found, with validity and performance well above the previous ones. Another is that an interdisciplinary research team made up of automotive engineers and medical scientists has created and coordinated measurement techniques regarding the physiology of various drivers during the braking procedure, using these in extensive and thoroughgoing investigations. As far as the authors know, this is the first time that the research has taken the physiological characteristics of the driver into account. These results already support the developer with the means of achieving greater objectivity, better systems and increased efficiency. They are also providing the researcher with methodology whose performance is proven and a level of reliable knowledge which can be raised systematically. Because new types of drive technology have now become established in the automotive field, electrical components are gaining in significance. The possibility of energy recuperation will eventually mean that friction brakes wholly reliant on conventional mechanics will become a thing of the past. Given these facts, it is not surprising that interest in objective description of the human-machine connection can now be perceived to be stirring within the car industry.

There are four basic methodological foci for human machine interfaces, **Figure 1**:

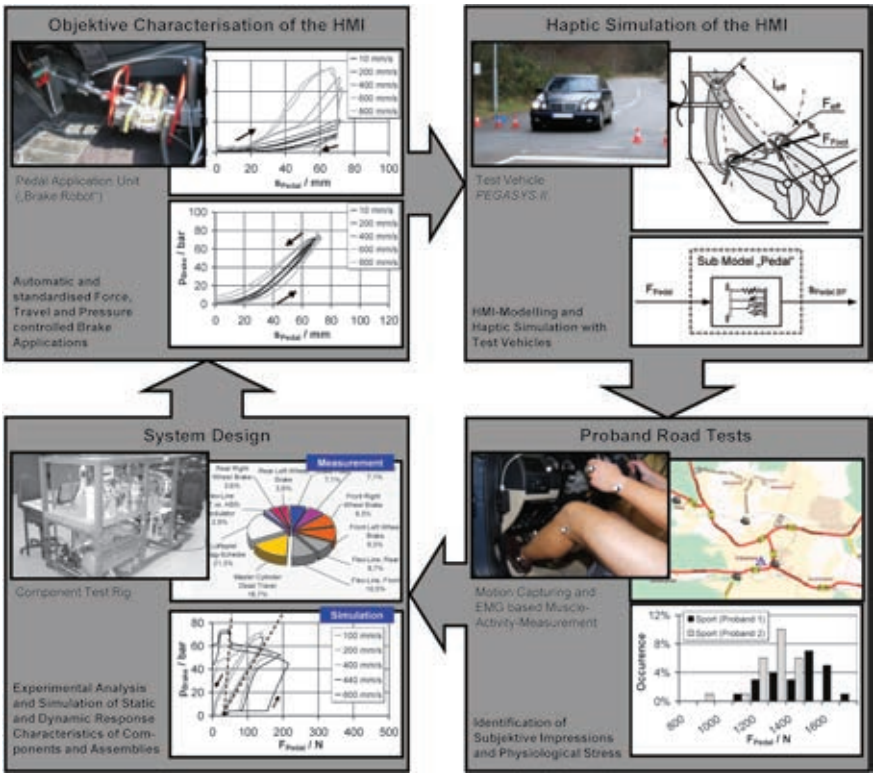

Figure 1: Methods for evaluation and development – basic methodological foci

The Authors

Dipl.-Ing. Jan Sendler is Researcher for Automotive Engineering at Ilmenau University of Technology (Germany).

Dr.-Ing. Ralf Trutschel was Researcher for Automotive Engineering at Ilmenau University of Technology and is Team Leader at Getrag in Untergruppenbach (Germany).

Prof. Dr.-Ing. Klaus Augsburg is Head Automotive Engineering at Ilmenau University of Technology (Germany).

Dr. med. Nikolaus Peter Schumann is Senior Researcher for Trauma, Hand and Reconstructive Surgery in the University Hospital at Friedrich Schiller University Jena (Germany).

Prof. Dr. med. Hans Christoph Scholle is Head of Motor Research, Pathophysiology and Biomechanics of Trauma, Hand and Reconstructive Surgery, University Hospital, at Friedrich Schiller University Jena (Germany).

ATZ Peer Review
The Seal of Approval for scientific articles in ATZ.
Reviewed by experts from research and industry.

Received ..... March 3, 2009
Reviewed ..... March 10, 2009
Accepted ..... April 29, 2009

1. Experimental, objective characterisation of the HMI: A pedal actuation unit was developed for the HMI analysis experiments. Numerous measurements have provided a basis for definitive models, by which the HMI characteristics could be described.
2. New technology for the purposes of haptic simulation of the HMI: Research vehicles have been developed, so that effective and definitive on-road tests under highly realistic conditions could be carried out, exploiting the vehicles' purpose-built technology for authentic model-based haptic simulation of the entire HMI – including the brake pedal. The unrestricted programmability has additionally permitted innovative investigation of the haptic feedback.
3. Proband road tests / customer clinics: Here, the subject of investigation has been the objective characteristics of the HMI and the subjective perceptions of the braking driver. These investigations have produced answers to such questions as those concerning the pedal use and braking behaviour of the ordinary driver, the limits of pedal sensibility and the subjective effect of HMI features. Further investigations, focussing on the human physiological and psychological aspects of the braking procedure have followed the original research.
4. Experimental analysis and numerical simulation / system design: For the layout of brakes and their associated components to be fit for purpose, the HMI characteristics must be analysed in relation to the design features they reflect. To this end, a vacuum-assisted brake system belonging to a mid-size saloon has been taken as an example, and the detailed analysis of its design, experimentally investigated, was transferred into a behaviour model.

The paper concludes by presenting guidelines for braking and pedal feel characteristics, which are associated with optimum comfort for mid-size saloons derived from investigations across the whole range.

2 Servo-hydraulic Pedal Actuation Unit

Reproducibility is barely possible for drivers' use of the pedal in on-road tests, and that use lacks variety and precise measurability. The use of an automated servo-hydraulic pedal actuation unit ("brake robot", **Figure 2**) removes these limitations. The brake robot will give an objective indication of the pedal behaviour for a wide variety of pedal actuation patterns. Thus it enables the HMI to be comprehensively characterised, Figure 2 and **Figure 3**.

By applying a uniform definition of pedal travel and of pedal force, and producing standardized pedal actuation patterns, effective evaluation and direct comparability have been achieved to serve as "benchmarks". Because of the high power density and the dynamic range, the brake robot has proved particularly valuable in the carrying out of standard tests in which the driver is subject to high physiological demands.

3 Model-based Description of Braking and Pedal Characteristics

For the objective description of the HMI characteristics, a physical and mathematical model is applied. When used in conjunction with the parameters and the characteristic curves, it provides a definitive description of the features of the sort of braking in normal traffic which predominates in everyday driving.

The pedal features are represented by a model ("pedal" sub-model, **Figure 4**) made up of a spring, a damper dependent on direction (in accordance with Stokes' law), and a Coulomb friction element. Two elements serve to depict the braking characteristics ("brake" sub-model, Figure 4). The more-or-less static relationship between the pedal travel and the brake pressure is described by a

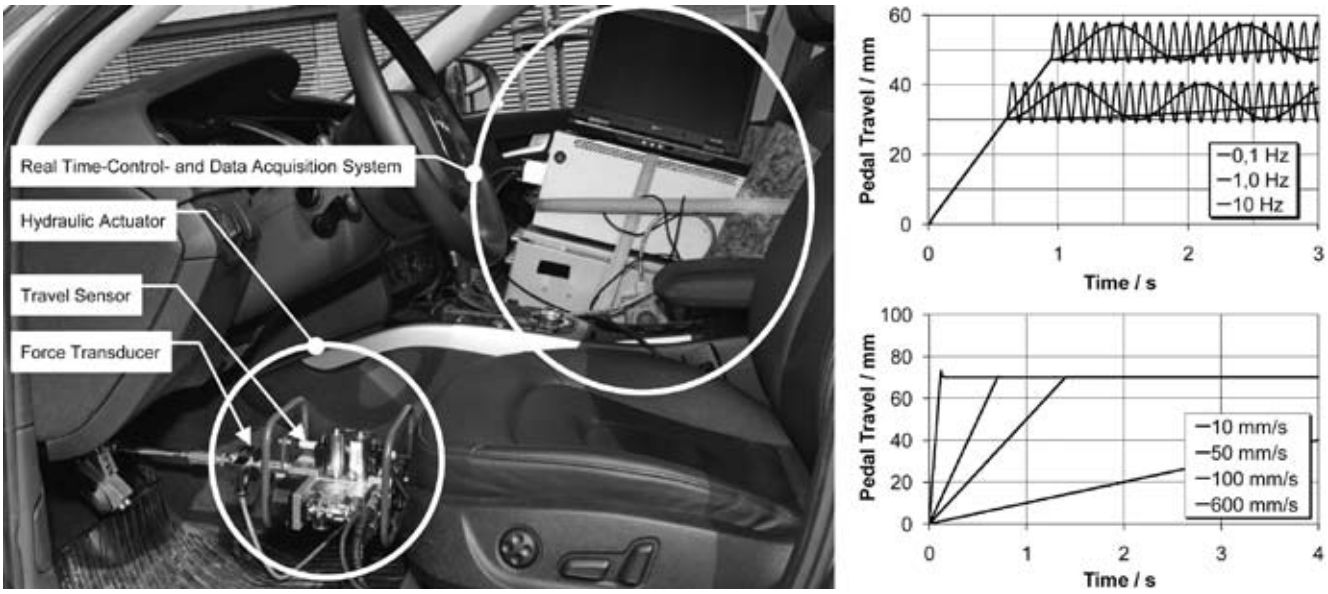

Figure 2: Vehicle with pedal actuation unit installed (left); examples of measurement results (right)

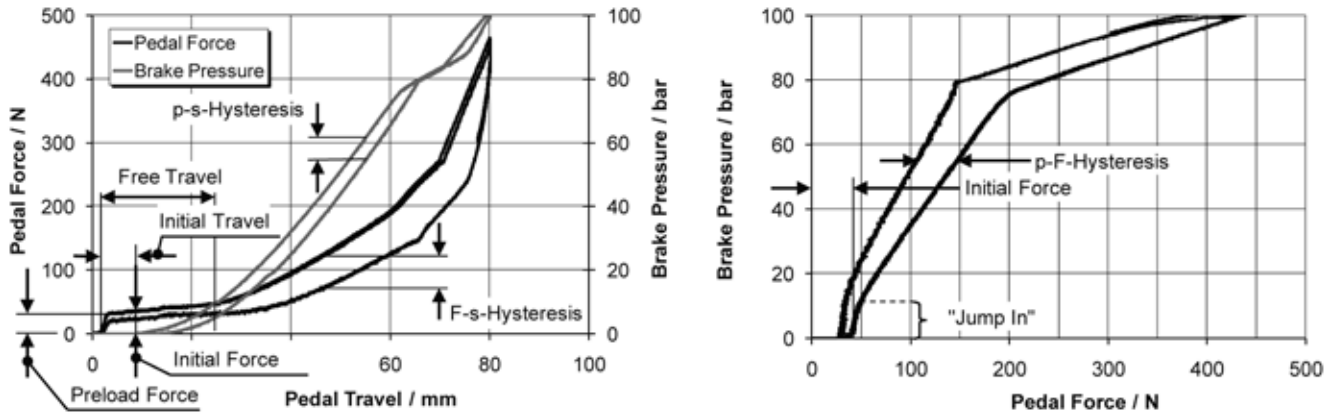

Figure 3: Pedal travel, pedal force and brake pressure – selected nominal values

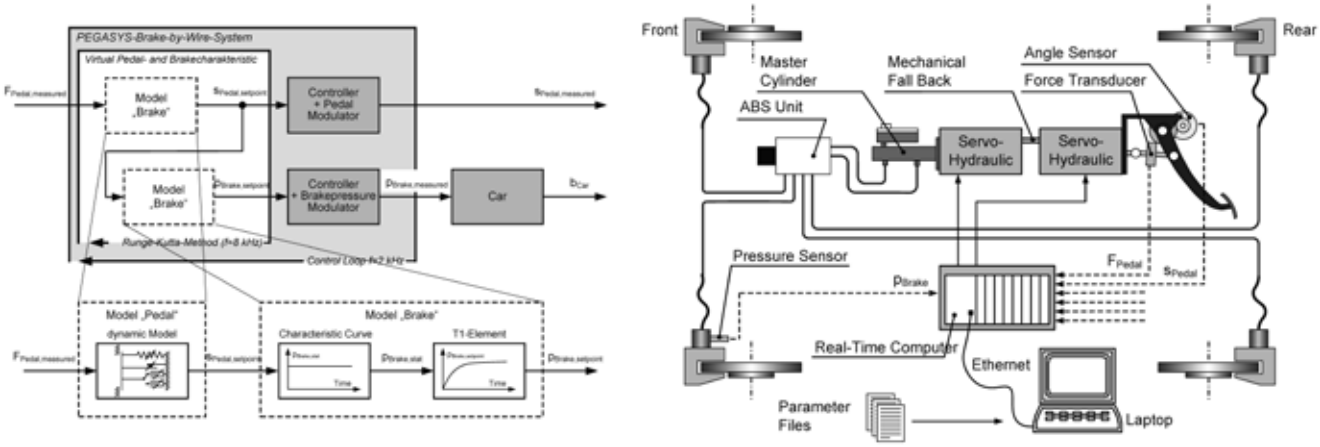

Figure 4: Brake-by-wire system with active brake pedal allowing haptic simulation of HMI: functional architecture of system and model-based description of the pedal and braking features (left); schematic representation (right) [11]

characteristic curve and the action over time is shown by a first-order element for delay.

An extended model also describes pressure-travel-hysteresis [11]. At the same time, these models provide the basis for the active haptic simulation described in the paper.

4 Research Vehicles for Variation of the Brake Pedal Feel

To exclude intrusive secondary influences on the outcome of the evaluation, it is necessary to use test vehicles in which the HMI parameters can be varied. On the other hand, it is a basic requirement of the on-road tests that the haptic simulation should be authentic. This technology to meet the need has been developed by the Department of Automotive Engineering at Ilmenau University of Technology and up to now has been installed in two adapted mid-size saloons and an N2-type commercial vehicle (system Pegasys, Pedal-Gefühl-Analyse-System). The pedal actuator is a hydraulic system reflecting the pedal travel; the brake pressure modulator is an additional hydraulic module to activate the brake master cylinder. The brake pressure and pedal travel follow the set values with virtually no delay and they mirror brake and pedal features (whether real or synthetic) in an absolutely authentic manner, with a free choice of parameters. There are additional functions which permit HMI characteristics to be reflected in dependence on speed; or wide-ranging haptic ABS-like feedback: these can be periodic patterns or individual events, and can be responses to triggers of various magnitudes.

The change between two types of data input takes place almost instantly and is also possible while the vehicle is driven. As it can be used on public roads, braking behaviour can be researched under very realistic conditions.

Investigations have been carried out with Pegasys vehicles to provide the answers to a number of questions. The starting point was the characterisation (with statistical confidence) of braking under normal traffic conditions and the related pedal use and brake action.

As an example, a noticeable feature of the results is that the distribution of occurrence of the vehicle deceleration episodes for the same stretch of road and normal conditions is independent of the pedal and braking characteristics obtaining at the time, **Figure 5** (top). To slow down to a given speed is obviously the primary aim. The distribution of occurrence for the pedal travel, Figure 5 (bottom), varies similarly, as does that for the pedal forces.

5 System Analysis and System Simulation for Passenger Car Braking Systems

In order to transfer the specifications for the characteristics of the interface into actual product features, they have to be related to the relevant components and parts. In the case of conventional cars, these will be almost exclusively mechanical components. The designs of the future for different types of drive or chassis with electrically triggered braking or a link to a generator will involve the use of electrical components. By way of example, first the vacuum-assisted brake system belonging to a mid-size saloon has been subjected to detailed experimental and theoretical analysis of its design. The testing area was extended for the purpose by the addition of dedicated testing and measuring equipment.

This has resulted in a model of physical behaviour, which renders both static and dynamic interface features and permits the influential parameters to be identified and traced back to the component level. It should be noted that the creation of the model structure and the setting of parameters must be carried out with great care, as different configurations of the assemblies will affect the static and dynamic behaviour of the HMI to varying degrees, **Figure 6**, [12].

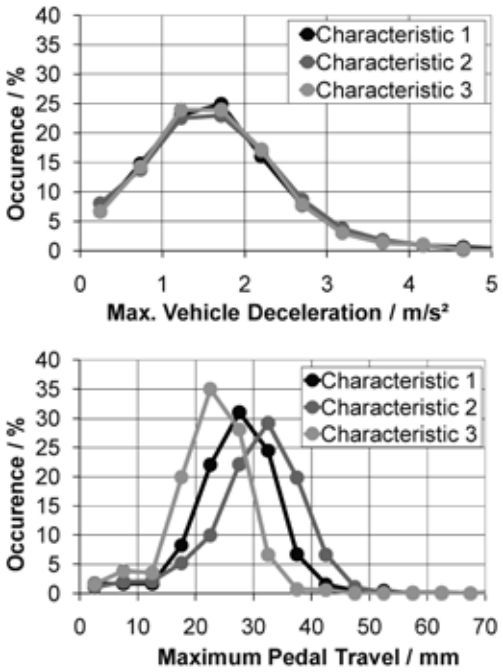

Figure 5: Statistics of maximum vehicle deceleration (top) and maximum pedal travel (bottom) in town traffic of Ilmenau [8]

6 Analysis of the Physiology of Braking

The evaluation of braking and pedal characteristics is influenced not only by objective parameters originating in the vehicle but also by some parameters that relate to the driver's immediate surroundings (for example seating ergonomics), the driver's individual physiological characteristics (for example his or her constitution and movement control) and his or her psychology (expectations, habituation effects...). To establish the relationship between the subjective judgment and the individual driver characteristics, both the ergonomics and physiology have been examined. Investigating muscle activation and strain opens up certain possibilities, among them the identification of how various parameters influence the driver's habits.

To capture muscle activity data, use was made of multi-channel surface electromyography [7]. An electromyogram (EMG) will reflect the electrophysiological activation taking place in muscles. These are not activated as an entire unit but as fixed groups of muscular fibres, called motor units. What is recorded is the sum of the action potentials of these motor units, or, where appropriate, their interference pattern [3, 5]. In surface electromyography, the EMG activity recorded is taking place fairly near the body surface [6].

6.1 Actual Braking Task as Factor

Figure 7 shows the EMG activity in selected muscles of the right leg for various braking manoeuvres. It is noticeable that the proportion of action belonging to the flexor of the foot, musculus tibialis anterior, represented by the white bar, is very much dependent on which braking manoeuvre is being performed. This muscle is hardly taxed at all during a "full brak-

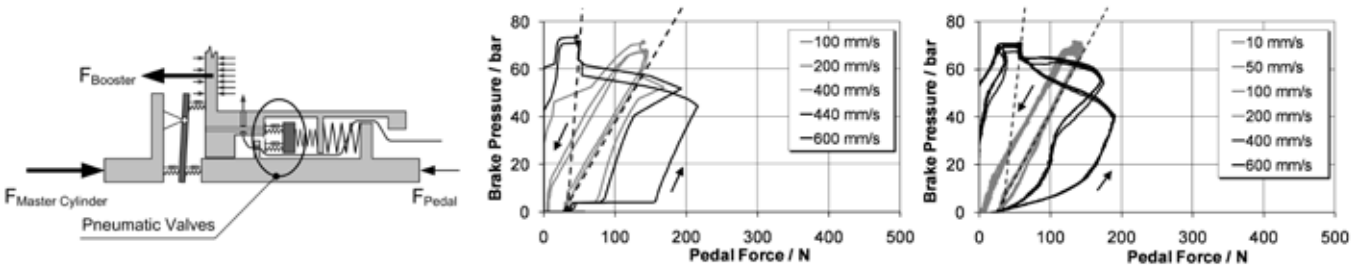

Figure 6: Brake booster force regulator – mechanical model (left); simulation and measurement of a brake assist feature (centre and right)

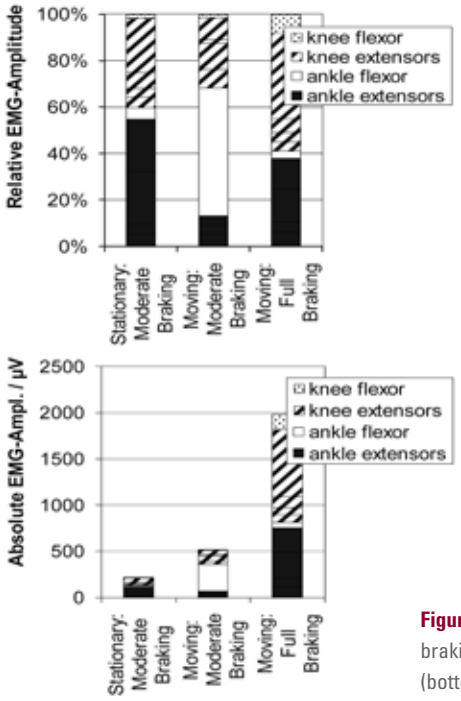

Figure 7: EMG muscle activity during braking process – relative (top) and absolute (bottom) mean EMG amplitude

ing", which does not primarily involve modulation of the deceleration, but it plays both absolutely and relatively a much larger part in "moderate braking".

Contracting the soleus and gastrocnemius muscles stretches the foot, and is what, in combination with some stretching of the knee and hip joints (or at least some stabilisation on their part), actually makes the brake pedal work. Any increase in the muscle force is controled by the central nervous system and realised by an increase of the firing rate of the motor units already working, and/or by the recruitment of further motor units, usually greater in size [2]. Regulation of either position or force can also take place by the interaction of agonist, synergists and antagonists.

The flexor, musculus tibialis anterior, is the antagonist to the two extensor muscles. The work necessary to regulate deceleration, as in moderate braking, actually manifests itself in the greater proportion of activity required of the flexor as it acts to stabilise the movement in the ankle joint [10].

The effect described is a clear indication that ergonomic investigations in unreal situations such as driving simulators should include vehicle feedback generated so as to be as realistic as possible.

6.2 Driver as Factor

Different test drivers will perceive one and the same set of pedal characteristics in different ways, depending on the physical condition of their muscles. The mean amplitude measured by EMG for a muscle is in an almost linear relation to the force applied. However, the figure itself and the linear ratio are different for each muscle and for each individual. With two test drivers as different examples, the principle is made clear: driver no. 1 is a tri-athlete fully in training and driver No. 2 someone whose sporting activities are occasional and whose body weight is below average.

In this case the investigations took place during braking tests based on the AMS-test used by the magazine "Auto, Motor und Sport", which is comparable with the full braking in Section 6.1 above. Driver no. 1 applied a mean activation force that was higher than that of driver no. 2, **Figure 8** (left). Despite this, the EMG amplitudes shown for driver no. 2 are considerably higher, Figure 8 (centre and right). This driver activates his muscles more strongly. Driver no. 1 clearly requires less muscular activity to achieve the same braking action and yet at the same time apply more actual pedal activating force.

Because driver no. 1 is in regular training, he has optimal muscular coordination. As the muscle fibres are probably enlarged (muscle hypertrophy), the motor units stimulated by the nerve fibres can produce more force while at the same time maintaining the level of activation for longer [9].

In consequence, for on-road tests, which are intended as an analysis of the human machine interface, test participants should be additionally evaluated on the basis of physical condition among the other factors. In the series of experiments here presented, physical condition was analysed individually for certain muscles, on the basis of the relation

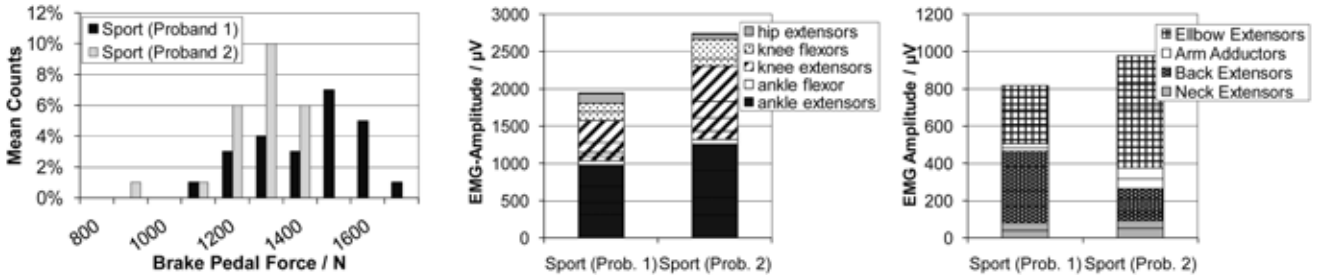

Figure 8: Distribution of mean pedal activation forces during braking in AMS test (left); EMG muscle activity during braking in AMS test (centre and right) (mean EMG amplitude; calculated as mean from ten braking episodes)

Table: Recommended layout (*Vehicle deceleration b in m/s²; pedal force F in N)

Criterion	Recommended Layout / Dimensions
Preload force	12 ... 18 N; at slow vehicle speeds (for example town traffic) low values are preferred
Developing of force on pedal vs. distance travel	Should consist a level and a progressively increasing section and should tend towards "soft" braking
Static force hysteresis	±5 N; increasing asymptotically with increasing force on pedal
Dynamic force hysteresis	Damping coefficient can remain constant; should only be set at a value, which will not significantly increase the total force hysteresis during comfort braking; good results were obtained with a linear damping coefficient of 0.045 N/(mm/s)
Developing of brake pressure vs. pedal travel	Rising gently in the lower pressure range; start of the steeper pressure curve should be in the flat section of the force on pedal vs. distance travel graph; mean braking effect on activating and releasing pedal to lie between approximately db/dF = 0.090 and 0.095 m/s²/N*
Initial travel (distance travel by pedal when brake pressure first arises)	At very low vehicle speeds (for example during parking): very short
Developing of vehicle deceleration vs. force on pedal	High braking effect (big ratio db/dF)*

between defined loads and the maximum voluntary muscle contraction. Given this background, any decisions on product development, which have been made on the basis of an individual person's judgement, should be viewed critically. Interfaces which are variable or will adapt in terms of force to be applied could well be of advantage.

7 Conclusion

This paper of Ilmenau University of Technology has presented new approaches, both methodological and technical, which are valuable from both the scientific and practical points of view. The fact that they have already met with approval in industry confirms how attractive the methodology is and how definitive the results. Admittedly, at present the interdisciplinary research to take physiological aspects into account is still at the fundamental stage. However, it holds promise for future investigations of human and machine interaction and construction of driver models, among other things.

The next stage of research will concentrate on driver physiology, psychology and ergonomics and will aim to enhance the general validity of the approaches, by raising the number of test drivers sampled and by selecting a variety of driving and/or traffic situations. Recommendations on layout of pedal and braking features, obtained primarily from tests on mid-size saloon cars are summarised in the **Table** [11].

References

[1] Augsburg, K.; Sendler, J.: Eine komplexe Methode zur Bewertung des Bremspedalgefühls. In: Becker, K.; et al.: Subjektive Fahreindrücke sichtbar machen III. Haus der Tech-nik, Fachbuch Band 56, Expert-Verlag, Renningen, 2006, S. 17-49

[2] Henneman, E.: The Size-principle: a Deterministic Output Emerges From a Set of Probabilistic Connections. In: J Exp Biol 115 (1985), pp 105-112

[3] Kleine, B. U.; Schumann, N. P.; Bradl, I.; Grieshaber, R.; Scholle, H. Ch.: Surface EMG of Shoulder and Back Muscles and Posture Analysis in Secretaries Typing at Visual Display Units. In: Int. Arch. Occup. Environ Health 72 (1999), pp 387-394

[4] Sailer, U.: Aussagen zum Pedalgefühl im rechnergestützten Auslegungsprozess und in der Applikation von Pkw-Bremsanlagen. Vortrag, brems.tech, München, 2002

[5] Scholle, H. Ch.; Schumann, N. P.; Anders, Ch.; Bradl, U.: Topographical Aspects of Myoelectrical Activation – a Possibility to Evaluate Seating? In: Mital, A.; Krueger, H.; Kumar, S.; Menozzi, M.; Fernandez, J. E. (Eds.): Advances in Occupational Ergonomics and Safety I. Vol. 1, International Society for Occupational Ergonomics and Safety, Cincinnati (Ohio, USA), 1996, pp 529-533

[6] Schumann, N. P.: Grundlagen der Elektromyographie – Registrierung, Analyse und Bewertung des EMG-Signals bei Muskelermüdung. In: Grieshaber, R.; Schneider, W.; Scholle, H. Ch. (Hrsg.): 9. Erfurter Tage. Prävention von arbeitsbedingten Gesundheitsgefahren und Erkrankungen. monade agentur für kommunikation GmbH, Leipzig, 2003, S. 265-283

[7] Schumann, N. P.; Sendler, J.; Grassme, R.; Fetter, R.; Augsburg, K.; Scholle, H. Ch.: Die muskuläre Beanspruchung bei Bremsmanövern im PKW. In: Grieshaber, R.; Stadeler, M.; Scholle, H.C. (Hrsg.): 14. Erfurter Tage. Prävention von arbeitsbedingten Gesundheitsgefahren und Erkrankungen. Verlag Dr. Bussert & Stadeler, Jena, 2008, S. 447-457

[8] Sendler, J.; Augsburg, K.; Fetter, R.; Auler, F.: Analysis of the Habituation Behaviour of Average Drivers Regarding the Brake Pedal Characteristic. Lecture, brake.tech, Munich, 2006

[9] Sendler, J.; Augsburg, K.; Scholle, H. Ch.; Schumann, N. P.: Analyse der physiologischen Aspekte des Betätigungsverhaltens beim Bremsen. Vortrag, brake.tech, München, 2008

[10] Sendler, J.; Augsburg, K.; Schumann, N. P.; Trutschel, R.; Scholle, H. C.: A Novel Method for Objectifying the Physiological Stress of the Car Driver While Braking. F2008-02-040. FISITA 2008 World Automotive Congress, Munich, Germany, 2008

[11] Trutschel, R.: Analytische und experimentelle Untersuchung der Mensch-Maschine-Schnittstellen von Pkw-Bremsanlagen. Dissertation, Technische Universität Ilmenau, 2007

[12] Trutschel, R.; Augsburg, K.: Efficient Experimental Analysis Tools for Objective Analysis of the Brake Pedal Feel Characteristic. Lecture, 22nd SAE Brake Colloquium & Ex-hibition, Anaheim/CA, USA, 2004